



**Matthias Ladurner, BSc**

# **Determination of the Electrical Conductivity of Biological Fluids using Glucose Sensors**

## **MASTER THESIS**

### **Supervisors:**

Dipl.-Ing. Dr.techn. Lukas Schaupp

(Medical University of Graz)



Dipl.-Ing. Dr.techn. Roland Schaller-Ammann

(JOANNEUM RESEARCH Forschungsgesellschaft mbH)



### **Evaluator:**

Ao.Univ.-Prof. Dipl.-Ing. Dr.techn. Hermann Scharfetter

Institut für Medizintechnik

Kronesgasse 5/II

8010 Graz

Head: Univ.-Prof. Dipl.-Ing. Dr.techn. Rudolf Stollberger

Graz, July 2013

## **STATUTORY DECLARATION**

I declare that I have authored this thesis independently, that I have not used other than the declared sources/ resources and that I have explicitly marked all material which has been quoted either literally or by content from the used sources.

.....

Place, Date

.....

Signature

## **EIDESSTATTLICHE ERKLÄRUNG**

Ich erkläre an Eides statt, dass ich die vorliegende Arbeit selbstständig verfasst, andere als die angegebenen Quellen/ Hilfsmittel nicht benutzt, und die den benutzten Quellen wörtliche und inhaltlich entnommene Stellen als solche kenntlich gemacht habe.

.....

Ort, Datum

.....

Unterschrift

# TABLE OF CONTENTS

STATUTORY DECLARATION	2
EIDESSTÄTLICHE ERKLÄRUNG	2
TABLE OF CONTENTS	3
LIST OF ABBREVIATIONS	5
ABSTRACT	6
ZUSAMMENFASSUNG	7
1 INTRODUCTION	8
1.1 Background	8
1.2 Objectives	14
2 RESEARCH DESIGN, METHODS AND RESULTS	15
2.1 Glucose Oxidase Sensor – Dexcom STS7	15
2.1.1 Sensor Principles/ Biochemical Background	15
2.1.2 Two and Three-Electrode Systems	17
2.1.3 Glucose Oxidase	17
2.1.4 Membrane	18
2.2 Flow Through Cell	19
2.3 Ionic Reference Technique	20
2.4 Analytical Methods	21
2.4.1 Offline Glucose Measurement – Super GL2	21
2.4.2 Conductivity Measurement – TraceDec	21
2.4.3 Glucose/ Conductivity Sensing – Gamry	22
2.4.3.1 Chrono-amperometry	22
2.4.3.2 Single Frequency Electrochemical Impedance Spectroscopy (EIS)	24
2.4.3.3 Sub-harmonic Sampling	24
2.4.3.4 Gamry’s Sequence Wizard	25
2.5 Data Acquisition and Analysis	26
2.5.1 Statistical Methods	26
2.6 In Vitro Investigations	27
2.6.1 Determination of the Polarization Potential using Cyclic Voltammetry	27

2.6.2	Temperature Dependency	28
2.6.3	Simultaneous Measurement Approach	30
2.6.3.1	Estimation of the optimal Parameters	30
2.6.3.2	Simultaneous Measurement of Glucose and Conductivity using the Optimal Parameters	33
2.6.4	Intermittent Measurement Approach	35
2.6.4.1	Estimation of the Optimal Parameters	35
2.6.4.2	Intermittent Measurement of Glucose and Conductivity using the Optimal Parameters	38
2.6.5	Test of the Final System inclusive ivMD	42
2.7	In Vivo Investigations	47
2.7.1	Primary Objective	47
2.7.2	Setup and Methods	47
2.7.2.1	Location of Catheters	47
2.7.2.2	Setup of the ivMD system	48
2.7.2.3	Risk Management Process	48
2.7.2.4	Safety Check	49
2.7.3	Clinical Study	50
2.7.3.1	Protocol	50
2.7.3.2	Subjects	51
2.7.3.3	Blood Sampling Procedure	51
2.7.3.4	Dialysate Sampling Procedure	52
2.7.4	Flow	52
2.7.5	Recovery	54
2.7.6	Filtering of Sensor Current	55
2.7.7	Regression Analysis of Glucose Data	57
2.7.8	Analysis of Conductivity Data	60
3	DISCUSSION	62
4	CONCLUSION AND OUTLOOK	67
5	ACKNOWLEDGMENTS	69
6	REFERENCES	70
7	APPENDIX	74

## LIST OF ABBREVIATIONS

AC	Alternative Current
AGES	Austrian Agency of Health and Food Safety
BG	Blood Glucose
BMI	Body Mass Index
CE	Counter Electrode
CGM	Continuous Glucose Monitoring
CL	Clamp Level
CRF	Case Report Form
CV	Coefficient of Variation
EIS	Electrochemical Impedance Spectroscopy
EU-CLAMP	Eu-glycaemic Clinical Application for Metabolic Profiling
FMEA	Failure Mode and Effect Analysis
FTA	Fault Tree Analysis
GIR	Glucose Infusion Rate
Gox	Glucose Oxidase
GUI	Graphical User Interface
ID	Inner Diameter
IDDM	Insulin Dependent Diabetes Mellitus
IRT	Ionic Reference Technique
ISF	Interstitial Fluid
iv	Intravenous
MARD	Mean Absolute Relative Difference
MD	Microdialysis
NIDDM	Non-Insulin Dependent Diabetes Mellitus
OD	Outer Diameter
SNR	Signal to Noise Ratio
WE	Working Electrode

## ABSTRACT

**Objective:** New insulin analogues used to treat patients with diabetes must be tested in clinical clamp studies. Automated clamp devices could reduce the costs of these labour-intensive manual clamps. Intravenous microdialysis (ivMD) has become an attractive approach for continuous glucose monitoring (CGM); however, fluctuations in recovery limit its usefulness. It has been shown in previous studies that such fluctuations in glucose recovery can be partly compensated by using the Ionic Reference Technique (IRT). Our objective was to investigate whether CGM using ivMD can be improved by measuring the conductivity online, over the sensor electrodes, enabling the IRT.

**Methods:** The CGM comprises the CMA64 ivMD, Dexcom STS 7, flow through cell and a Gamry potentiostat. The system was first characterized in vitro and then tested in a clinical study in 5 diabetic volunteers over 24h. An antithrombotic drug was used to minimise clotting of the MD membranes. Blood glucose was clamped to four target levels for 6 hours. Dialysate was analysed offline and online for glucose and ions and related applying a regression analysis.

**Results:** Measurement of glucose and conductivity could be established in vitro in a reliable and reproducible manner. In contrast, data of in vivo investigations showed a weak correlation for glucose signals obtained with the online sensor and no correlation for the conductivity measurement.

**Conclusion:** We showed that online glucose- and conductivity measurement can be established using the same sensor electrodes to enable the application of the IRT. Nevertheless, the system needs substantial improvement to be ready for in vivo use.

**Keywords:** Ionic Reference Technique, continuous blood glucose monitoring, clinical study, online

## ZUSAMMENFASSUNG

**Ziel:** Neue Insulinanaloge zur Behandlung von Diabetes-Patienten müssen in klinischen „Clamp“-Studien getestet werden, bevor sie auf den Markt kommen. Automatisierte „Clamp“-Geräte könnten die Kosten, die bei manuellen und daher arbeitsintensiven durchgeführten „Clamps“ entstehen, reduzieren. Als interessanter Ansatz hat sich die intravenöse Mikrodialyse (ivMD) zur kontinuierlichen Glukose-Überwachung (CGM) herauskristallisiert, jedoch ist ihre Anwendbarkeit aufgrund der Schwankungen in der Glukosewiederfindungsrate begrenzt. Es wurde in früheren Studien gezeigt, dass solche Schwankungen teilweise durch Verwendung der „Ionen-Referenz-Technologie“ (IRT) kompensiert werden können. Das Ziel dieser Arbeit war es herauszufinden, ob eine CGM basierend auf ivMD durch die Verwendung einer online Leitfähigkeitsmessung über die bestehenden Sensorelektroden und somit mittels Korrektur durch die IRT verbessert werden kann.

**Methoden:** Das CGM bestand aus einer CMA64 ivMD, Dexcom STS 7, Durchflusszelle und einem Gamry Potentiostaten. Das System wurde zuerst in vitro charakterisiert und anschließend in einer klinischen Studie an 5 freiwilligen Diabetespatienten über 24 Stunden getestet. Ein anti-thrombotisches Arzneimittel wurde zur Reduzierung der Blutgerinnung auf den Membranen verwendet. Der Blutzucker wurde für je 6 Stunden auf vier „Clamp“-Niveaus eingestellt. Die Dialysatproben wurden offline analysiert, um sie später mittels Regressionsanalyse mit den online gemessenen Glukose- und Ionenwerten zu vergleichen.

**Ergebnisse:** Die Messung von Glukose und Leitfähigkeit konnte in vitro in zuverlässiger und reproduzierbarer Weise gezeigt werden. Im Gegensatz dazu zeigten die Daten der in vivo Untersuchungen eine schwache Korrelation für Glukosesignale und keine Korrelation für Leitfähigkeitsmessung.

**Fazit:** Es konnte gezeigt werden, dass eine Online-Glukose- und Leitfähigkeitsmessung mittels der Elektroden eines Glukosesensors möglich ist, was wiederum die online Anwendung der IRT ermöglichen könnte. Dennoch muss das System verbessert werden, um ein CGM-System für die in vivo Anwendung erfolgreich zu implementieren.

# 1 INTRODUCTION

## 1.1 Background

Diabetes mellitus, briefly called diabetes, is a metabolic disease and associated with reduced life expectancy and diminished quality of life. Reasons are increased morbidity, caused by specific diabetes related microvascular complications and increased risk of macro vascular complications (ischaemic heart disease, stroke and peripheral vascular disease) [1]. In the year 2004 a total number of 366 million people with diabetes mellitus was predicted for 2030 [2]. Unexpectedly the number of patients increased faster, thus already in September 2012 the number has reached 347 million [3]. For the prediction it was assumed that risk factors such as overweight (BMI > 25 kg/m<sup>2</sup>) and obesity (BMI > 30 kg/m<sup>2</sup>) remain constant, which was not the case and thus diabetes becomes an increasing problem for society.

There are 2 types of diabetes:

**Type 1 (Insulin dependent diabetes mellitus - IDDM)** is an autoimmune disease leading to a lack of synthesis of the hormone insulin due a deficit of the islet cells caused by cell destruction. Reasons for this type are currently unknown and it is not preventable so far. Symptoms are over-average excretion of urine, loss in weight, thirst, permanent hunger, vision disorders and general fatigue.

**Type 2 (Non-Insulin dependent diabetes mellitus - NIDDM)** is based on a delayed or insufficient insulin secretion combined with abnormal insulin action in the peripheral target organs. 90% of all patients with diabetes suffer from type 2 diabetes and the reasons for this development are well known such as overweight, obesity and physical inactivity. Symptoms are similar to type 1, but often less pronounced, causing a long period until diabetes mellitus type 2 is diagnosed. Few years ago this type was only observed in adults, nowadays it is found also in children. [3][4]

Since the breakthrough discovery of insulin by Frederick Banting and Charles Best, patients suffering from diabetes are able to treat their disease with extracorporeal insulin doses to

adjust their glucose level [5]. Doses can be administered either manually subcutaneously or intramuscularly using pens, syringes or insulin pumps. In any case the carbohydrate supply, the level of physical training, exercise and the blood sugar level have to be considered to determine the insulin dosage. Health consequences caused by inadequate treatment of diabetes mellitus are associated with both types, whereby two short-term harmful cases can be distinguished:

- **Hypoglycaemia** is defined as the state when blood sugar levels are below 60 mg/dl. It results if too much insulin is administered or too little carbohydrates are consumed. Serious effects are unconsciousness, brain damage or even death caused by undersupply of glucose to the brain [6].

- **Hyperglycaemia** is defined as the state when blood sugar levels are above 140 mg/dl. It results if too little insulin is administered or too many carbohydrates are consumed. This is associated with long term damages of organs, blood vessels, eyes, the nervous system or kidneys [6].

The demand for better insulin and special types of insulin is still urgent because in 2002 blood sugar levels were not well controlled in 49 % of the financial indigent diabetic patients and also in 23 % of well-treated diabetes patients [7]. Insulin is nowadays available with different action profiles (e.g. long-, short-, intermediate- and rapid acting) to increase the quality of treatment. The pharmaceutical industry still launches new types of insulin which have to be approved by the health authorities. Effectiveness has to be tested in clinical trials using the glucose clamp technique as suggested by the European Medicines Agency [8]. This technique represents the golden standard to quantify the insulin secretion and resistance in humans [9].

Usually a glucose clamp is performed in the following manner: Plasma insulin is raised artificially by the injection of insulin either intravenously or subcutaneously. Periodic measurements of plasma glucose are the basis for the calculation of a glucose infusion to stabilize blood glucose at a certain target level, also called "clamp level". At the same time this glucose infusion avoids an instantaneous drop of blood glucose due to the administered insulin. The result of this golden standard technique is the glucose infusion rate (GIR), which

quantifies the glucose lowering effect in time as well as in amplitude of the administered insulin. [10][11]

Investigations using the glucose clamp technique can be performed either manually or automatically. Manual clamps are very expensive because of high workload and costs and at the same time the results are non-continuous. Additionally blood sugar levels have to be maintained within a very narrow range [6]. This causes a need for high precision of the obtained blood glucose measurements. To overcome these drawbacks a fully automated clamp device is needed as depicted in **Figure 1**.

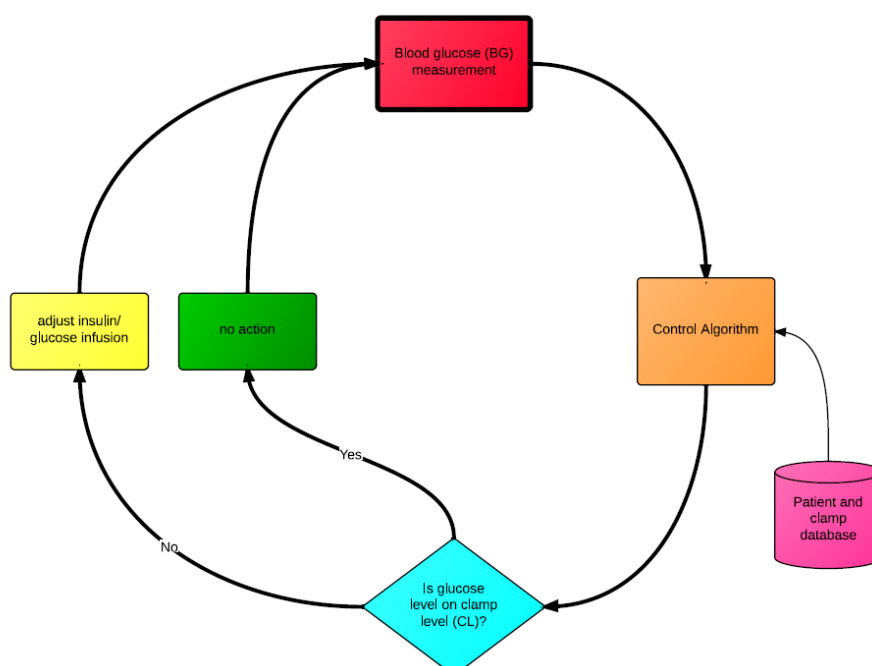


**Figure 1:** The principle of a fully automated continuous glucose clamp device: Blood glucose (BG) is the controlled variable. Using this value and other data stored in the patient- and clamp database (e.g. BMI, age, nutrition, clamp levels (CL)) the algorithm steers subsequent steps to adjust the control variables (glucose and insulin infusion) in time and amplitude.

The biggest challenges regarding the development of such an automated clamp device are the reliable continuous glucose measurements without blood loss and an accurate algorithm to calculate the dosage of the required substances (e.g. glucose, insulin). Existing automated clamp systems such as the Nikkiso STG-22, Glucostator or Biostator suffer from several problems:

- High loss of blood > 2.5 ml/h

- Unreliable measurement of glucose (variability > 5%)
- Untrustworthy algorithm
- Short recalibration intervals of < 30 min

Methods for glucose continuous monitoring known to treat type 1 diabetes measure in the interstitial fluid (ISF). This is not suitable for an automated continuous glucose measurement system because of the time delay between glucose concentration of blood and ISF [12] [13][14]. An alternative method without blood loss is the intravenous microdialysis (ivMD) technique introduced by Ungerstedt [15] which is depicted **Figure 2**.

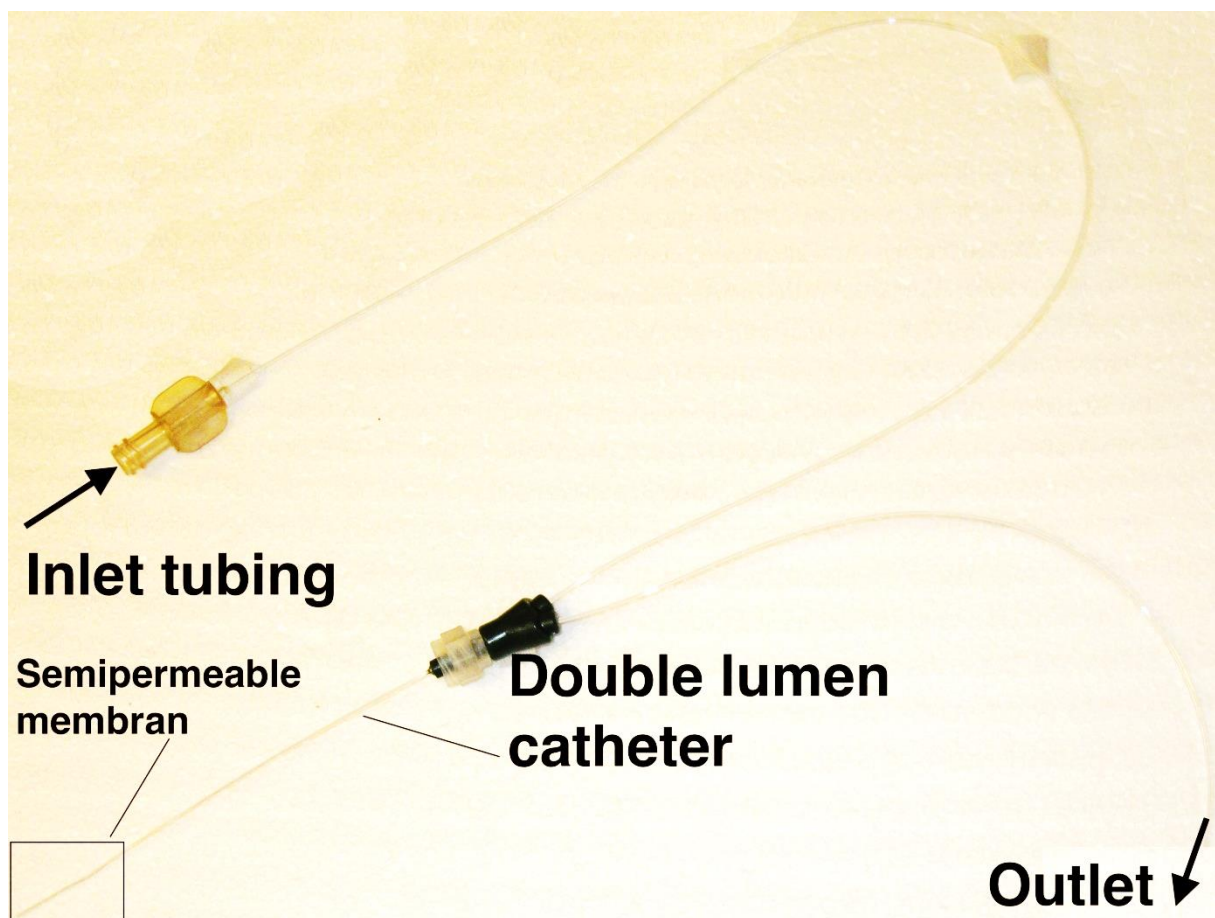


**Figure 2:** Setup of the intravenous microdialysis: The microdialysis probe: "Microeye" PME-011 microdialysis probe (Probe Scientific Ltd, UK) has a molecular mass cut off of approximately 10 kDalton and 20mm membrane length.

This method requires a microdialysis probe which is inserted into a vein using a standard catheter (e.g. Venflon). When such a probe is used, a liquid (perfusate) is pumped through

the probe and the collected liquid (dialysate) is enriched with glucose molecules which are able to pass the semipermeable membrane. The degree of equilibration (recovery) between blood and perfusate depends on the analyte's molecular mass and its charge, the surface area of the semipermeable membrane, temperature and the flow of the perfusate. Full equilibration between blood and perfusate is only possible if the flow rate is very low ( $< 1 \mu\text{l}/\text{min}$ ). In general flow rates of less than  $1 \mu\text{l}/\text{min}$  can be established, but the delay time until the dialysate reaches the glucose measurement system (glucose sensor) is unacceptably high.

Furthermore microdialysis probes inserted in the human body evoke an immune response, which can be seen for instance as fouling of bodily cells and proteins on the semipermeable membrane. These biological effects cause changes in the diffusion properties of the membrane, consequently less glucose is able to pass the semipermeable membrane and the recovery is decreasing. Glucose monitoring can be performed in a reliable manner when the recovery is held stable. Since this is not practicable corrections have to be done. Such corrections can be performed in using the "Ionic Reference Technique" (IRT) introduced by Schaupp et al [16][17]. Huber has shown in his diploma thesis [18], that this technique is promising and shows reproducible results for continuous blood glucose measurements. The Ionic Reference Technique is based on the fact that not just the analyte (glucose) but also other molecules, smaller or equal in molecular mass (e.g. lactate, ions) can pass the semipermeable membrane. The recovery of glucose is defined as the ratio between glucose found in dialysate and blood (Equation 1). The recovery of the ions is defined by the ratio between ions found in dialysate and blood (Equation 2).

$$Rec_{Gluc} = \frac{C_{GlucDia}}{C_{GlucBlood}} \quad \text{Equation 1}$$

$$Rec_{Ions} = \frac{C_{IonsDia}}{C_{IonsBlood}} \quad \text{Equation 2}$$

According to Equation 1 it is not feasible to calculate the glucose recovery because the glucose concentration in blood is an unknown parameter, but it is possible to calculate the

relative recovery of the ions assuming a constant ion concentration in blood. The electrical conductivity of a fluid is proportional to its overall ion concentration; therefore ion measurement of the dialysate can be replaced by measurement of the electrical conductivity. Assuming the electrical conductivity of blood to be equal to the conductivity of physiologic saline solution (0.9% NaCl) Equation 2 can be changed to Equation 3.

$$Rec_{Ions} = \frac{\textit{Conductivity of Dialysate}}{\textit{Conductivity of Blood}} \quad \textit{Equation 3}$$

There is a relationship between the recoveries of blood glucose and ions, which is discussed in the methods section (2.3). The use of the IRT to determine the blood glucose concentration requires a good correlation between these two recoveries. Changes of the permeability of the membrane have to be compensated with the IRT.

Therefore to establish a reliable continuous glucose measurement using ivMD, glucose and conductivity of the perfusate have to be measured in an accurate way.

## 1.2 Objectives

### Primary objective

The aim of this thesis was to proof whether the measurement of glucose and conductivity can be established in an accurate and reproducibly manner in vitro as well as in vivo using the electrodes of the Dexcom STS7 glucose sensor.

Therefore a continuous glucose monitoring unit comprising ivMD, glucose sensor for online glucose- and conductivity measurements allowing the application of the IRT should be tested in vitro and in vivo.

### Secondary objectives:

To achieve the primary objectives the subsequent tasks were performed:

- Flow cell design and assembly
- Characterization of the amperometric glucose sensor
  - Cyclic voltammetry
  - Calibration curves for different ion concentrations
- Experiments to determine optimal working parameters (e.g. frequency and amplitude) for the conductivity measurement using the existing electrodes of the glucose sensor
- Choice of the best parameter set regarding signal quality for the final system
- Characterization of the impedance behaviour of the sensor using different glucose- and ion concentrations
- In vitro evaluation of the glucose monitoring unit (ivMD, sensor, flow cell and potentiostat)
- Risk assessment, fabrication and safety test of final in vivo system
- In vivo evaluation in 5 diabetic patients
  - Establishment of a reproducible and stable flow
  - Evaluation of glucose- and ion recoveries
  - Evaluation of glucose sensor current and conductivity (e.g. filtering and regression analysis)

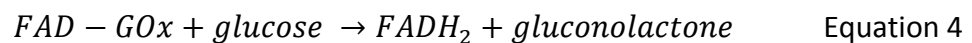
## 2 RESEARCH DESIGN, METHODS AND RESULTS

### 2.1 Glucose Oxidase Sensor – Dexcom STS7

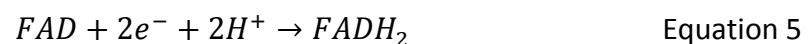
#### 2.1.1 Sensor Principles/ Biochemical Background

The used glucose sensor (Dexcom STS7, Dexcom, San Diego, USA) is based on an amperometric measurement principle, which is common for glucose measurement. A constant potential difference is applied between the sensor electrodes and a current proportional to the concentration of glucose can be measured. To convert this sensor current subsequently in a signal which is proportional to the blood glucose it must be at least one point calibrated.

In the case of an electrochemical sensor glucose is detected due to a catalytic oxidation, which is done by the enzyme glucose oxidase (Gox), see Equation 4 [19]

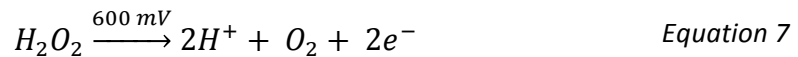
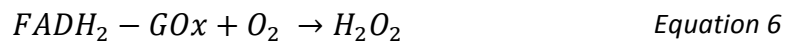


Oxidation of glucose involves an electron transfer from glucose to Flavin Adenine Dinucleotide (FAD) which is a co-factor of Gox. The Flavin of FAD undergoes the reversible reaction shown in Equation 5



Direct re-oxidation of  $FADH_2$  to produce a measurable current on an anodic electrode is slow because this co-factor is buried deep inside the enzyme. Therefore the enzyme electrodes need a tiny molecule that is able to oxidize the co-factor and is acting simultaneously as an electron shuttle to the electrode. Usually oxygen/hydrogen peroxide is used as a redox pair to perform this process. The redox pair is also called mediator.[19] [20]

These reactions are shown in Equation 6 and Equation 7.



In order to oxidize the mediator it is necessary to apply a potential between the working- (WE; electron producing) and counter electrode (CE; electron-consuming). This voltage is specific for the electrode material and the analyte, and represents the activation energy for the electrochemical reaction. [20]

By applying this potential to the working electrode the electrode becomes polarized, which results in a capacitive current. This causes a charge separation at the phase boundary interface (electrode surface, electrolyte) and thus an electrochemical double layer is formed. After the formation of the entire layer no capacitive current should occur anymore. Only when electroactive species are present, depolarization occurs and thus leads to a current flux. This current is generated by the electrochemical reaction of the analyte at the electrode surface and is called Faradic current. [21]

The working potential has to be in the range of the diffusion limiting regime and is determined by the redox potential of the mediator. In the diffusion limited range or also called "limiting diffusion current range" the total amount of incoming analyte is oxidized immediately, therefore the analyte concentration at the surface is practically zero. The Faradic current is driven by diffusion and is not caused by kinetics of the electrochemical reaction at the electrode. This means that the reaction is much faster than the renewal of the analyte caused by diffusion. So the concentration in the solution determines the concentration gradient and as a result the limiting current. This current is proportional to concentration variation of the analyte . [19][20]

### 2.1.2 Two and Three-Electrode Systems

By applying a certain potential difference between working- and counter electrode the specific reaction of the analyte which provides the measurable current signal occurs. This potential needs to be stable, because it determines the whole electrode reaction.

Additionally only a stable potential guarantees the occurrence of only faradic currents.

There are two common systems used in amperometric glucose measurement to provide a stable potential between sensor electrodes:

1.) **Two-electrode-system** which is used with the Dexcom glucose sensor consists out of a working and a pseudo reference electrode. With this assembly counter- and reference electrode are combined into a single electrode (counter/reference). In the Two-electrode-system Ag/AgCl is reduced at the counter/reference electrode and therefore care must be taken to provide enough AgCl for the whole lifetime of the sensor. Furthermore this assembly bears the disadvantage that a large current flux polarizes the counter or in this case also reference electrode which can cause an unstable potential at the electrochemical cell [20]. Also the Dexcom glucose sensor is using an Ag/AgCl counter/reference electrode. [19]

2.) **Three-electrode-system:** In contrast to the two-electrode system this system comprises a individual working, counter and reference electrode. The reference electrode is used to apply a defined voltage to the working electrode. This reference electrode is a high impedance electrode of second type. The reference electrode is used to apply and guarantee a defined and stable working potential. Using three electrodes allows a current flux through the counter electrode, thus the reference electrode is not loaded by this current flow and there will be no fluctuation of the working potential. [20][22]

### 2.1.3 Glucose Oxidase

Glucose oxidase belongs to a large group of catalysing enzymes and is an inexpensive and readily available enzyme. The electron acceptor (also called oxidant) is oxygen which

becomes the second substrate concerning the kinetic sequence. In any reaction, where oxygen is the acceptor for electrons,  $H_2O_2$  is an intermediate; refer also to Equation 7. Hydrogen peroxide is a cytotoxic molecule; therefore another molecule called catalase is necessary to remove the hydrogen peroxide as fast as it is produced. Anyhow a limited amount of  $H_2O_2$  always escapes and causes loss of glucose oxidase. This is the reason why the lifetime of Gox based glucose sensors is limited. This reaction is one out of many examples for an enzymatic cascade arrangement, in which the intermediate is the substrate for the next enzymatic reaction. [23]

Glucose oxidase is an enzyme which is produced by a range of fungal sources, mainly from *Aspergillus* and *Penicillium*. [24]

#### **2.1.4 Membrane**

Placing a membrane on top of the glucose sensor's working electrode offers lots of benefits[20]:

- 1.) A semipermeable membrane is only permeable for some substances (e.g. glucose) and at the same time impermeable for interfering substances.
- 2.) Moreover any semipermeable membrane represents a physical barrier to avoid growth of the time dependent diffusion layer. The downside of the coin is that with thicker membranes the reaction time increases.
- 3.) The membrane keeps the composition of the inner electrolyte between working electrode interface and membrane almost constant. Up to the diffusion limiting current, the current at the working electrode is a function of time, until a steady state is achieved, which is caused by a constant concentration gradient.

At that certain moment the electrochemical turnover is exactly the amount which can be delivered out of the bulk solution due to the concentration gradient. Usually those sensors require a constant incident flow which means a well stirred solution because the membrane is normally chosen as not very thick. Concentration gradients between membrane and the

bulk solution are quite high because the analyte concentration at the inner membrane interface is the same as the analyte concentration inside the bulk solution. Thus the depletion zone is located inside the membrane. In case of insufficiently stirred or unstirred bulk solution the depletion zone expands out of the membrane into the bulk solution. The consequence is a decreasing analyte gradient and furthermore a decreasing sensor current. This is the so called drift. This drift can be avoided by thicker membranes which cause inadequately long reaction time. So usually the trade-off is working under non-steady state conditions. [20]

The membrane of the Dexcom STS 7 glucose sensor consists of hydrophobic polyurethane and a hydrophilic polyurethane mixture. The hydrophobic part of the membrane provides oxygen flux and blocks glucose, whereas the hydrophilic polymer enables glucose flux. By varying the ratio between these two polymers the oxygen and glucose flux can be optimized. [19]

## **2.2 Flow Through Cell**

A glucose sensor is used for the measurement of glucose and ions. The two electrode sensor is usually used for CGM placed in the subcutaneous adipose tissue. As we were aiming to develop a device based on ivMD the sensor had to be placed in a flow through cell enabling the measurement of glucose and ions within the dialysate.

A 4 cm tube (S-50-HL; Saint-Gobain Performance Plastics Corporation, ID: = 0.8mm; OD: = 2.4mm), biocompatible according to ISO 10993 standards and also meeting the USP Class VI criteria, builds the core of the flow through cell. At a distance of 1 cm the tube was punctured using a needle (Sterican, BBRAUN, Melsungen, Germany, 0.6 – 60mm = 23G x 2 3/8”) and the sensor was inserted through the needle. Afterwards the needle was removed taking care that the sensor`s active area was not damaged and this section was afterwards sealed using an instant adhesive (Cyanolit, 732F, Panacol, Steinbach, Germany). Inflow and

outflow were realized using a polyamide tubing (PA 6228, 0.28 x 0.95 mm, Raumedic, Helmbrechts, Germany).

In order to minimize the influence of electrical fields, the sensor was operated within a plastic housing containing a Faraday cage. The flow cell was directly connected to the outlet-port of the ivMD probe and was affixed to the volunteers arm using a Velcro strip.

To minimize the risk of air bubbles being trapped within the flow cell it was streamed in the direction from the sensor inlet to its tip (**Figure 3a.**: from right to left). This assembly minimises the risk that air bubbles are able to coat the active area of the sensor membrane. Primarily air bubbles get trapped at the sensor inlet, which is a non-active area, thus the sensor signal will not be affected.

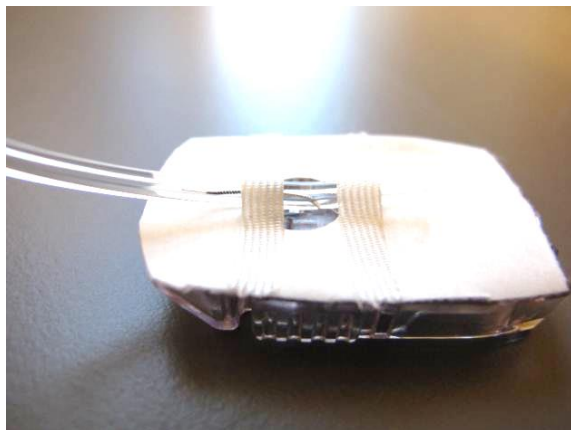
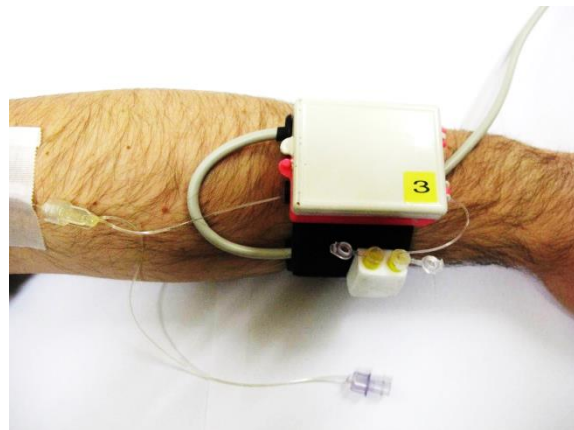


**Figure 3a.)** In-house made flow through cell inclusive Dexcom STS 7 sensor for intermittent glucose and conductivity measurement.



**b.)** Arrangement of ivMD probe CMA64, flow cell inclusive sensor and unit to sample dialysate.

## 2.3 Ionic Reference Technique

The Ionic Reference Technique (IRT) has been previously described [16]. Normally, the blood glucose concentration is the parameter of interest, whilst the glucose recovery is unknown as it changes over time due to varying flow rate and membrane permeability caused by movement, swelling or clot formation shortly after probe implantation. [25][26][27] The glucose recovery cannot be measured directly; however, the recovery of ions can be used to determine the glucose concentration in the blood. The sodium chloride concentration of

blood is assumed to be constant (100%) and the recovery of ions is assumed to be nearly directly proportional ( $k \triangleq$  proportionality factor) to the recovery of glucose and can be easily determined measuring the conductivity. Therefore the glucose concentration of blood can be calculated according to the following formula:

$$Gluc_{blood} = \frac{Gluc_{dialysate} \cdot Conductivity_{NaCl\ 0.9\%}}{Conductivity_{dialysate\ [\% \text{ of NaCl } 0.9\%]} \cdot \frac{1}{k}} \quad \text{Equation 8}$$

## 2.4 Analytical Methods

### 2.4.1 Offline Glucose Measurement – Super GL2

Supernatant from reference blood samples and dialysate samples were both analysed for glucose by using a bench-top glucose analyser (SUPER GL2, Dr. Müller Gerätebau GmbH, Freital, Germany). This device has a working range from 11 to 910 mg/dl when 20  $\mu$ l of the sample is pipetted into Glucocapil caps (Dr. Müller Gerätebau GmbH, Freital, Germany) prefilled with 1000  $\mu$ l buffer solution. Furthermore, concentrations of the antithrombotic drug used during the in vivo experiments for anti-coagulation purposes showed little influence on the measured glucose concentrations (CV < 4.8%).

### 2.4.2 Conductivity Measurement – TraceDec

A capacitively coupled contactless conductivity measuring device (TraceDec<sup>®</sup>, Innovative Sensor Technologies GmbH, Strasshof, Austria) was used for analysing the electrical conductivity [28]. Less than 5  $\mu$ l of the sample is withdrawn from a container with a peristaltic pump (Minipuls MP3, Gilson, Cedex, France) using a pump tubing and a fused silica capillary placed inside the sensor. Since the device does not measure absolute values (e.g. S/m), fluids of known conductivity, e.g. different saline solutions, have to be used for calibration. A nonlinear calibration curve with a polynomial fit function of 3<sup>rd</sup> order and coefficients of variation (CV) smaller than 2% (Min: 0.61 Max: 1.89%) were found. [18]

### 2.4.3 Glucose/ Conductivity Sensing – Gamry

A high precision potentiostat (Gamry Instruments, Series G™ 300, PA, USA) was used to perform the measurements of the amperometric current as well as the conductivity using the same electrodes of the Dexcom STS 7 glucose sensor.

#### 2.4.3.1 Chrono-amperometry

The Gamry's chrono-amperometric measurement protocol (package PHE200™) is used to enable diffusion-controlled electrochemical reactions like the glucose enzyme reaction of the Dexcom STS 7 glucose sensor. **Figure 4** shows a screen shot of the GUI. The Gamry's software package allows specifying sampling period and various potential settings.

To improve the quality of data the menu offers a “noise reject” sampling mode, where data points during the last 20% of the sample period are recorded at an increased sampling frequency of 60 kHz being afterwards averaged to a single data point. Unfortunately this feature is not available for the G300 potentiostat which was used during these investigations. The G300 potentiostat offers just the “fast” sampling mode which records just one data point per sample period without averaging. [29] As the Gamry potentiostat is supplied by a switching power supply running at 300 kHz every measurement procedure is coupled to this frequency. This fact provides the opportunity to suppress lots of disturbances which are coming from the same source as the power supply or from sources with inferences correlated with the switching perturbations. In contrast other disturbances (e.g. conducted through the cell supply cable) can affect the measured signal.

**Chronoamperometry**

Default Save Restore OK Cancel

Pstat  PCI4G300-51041  CH5

Test Identifier Chronoamperometry Scan ch1

Output File chrono\_param\_eval\_normal.DTA

Electrode Area 1

Notes... 

Pre-step Voltage (V) 0,6  vs Eref  vs Eoc

Pre-step Delay Time 0

Step 1 Voltage (V) 0,6  vs Eref  vs Eoc

Step 1 Time (s) 15000

Step 2 Voltage (V) 0,6  vs Eref  vs Eoc

Step 2 Time (s) 0

Sample Period (s) 10

Decimate  Off

I/E Range Mode  Auto  Fixed

Max Current (mA) 1

Limit I (mA/cm<sup>2</sup>) 1

IRComp  None  PF  CI

PF Corr. (ohm) 50

Equil. Time (s) 5

Init. Delay  Off Time(s) 300 Stab. (mV/s) 0,1

Conditioning  Off Time(s) 15 E(V) 0

Sampling Mode  Fast  Noise Reject  Surface

**Figure 4:** Screen shot of the Gamry software to configure the chrono-amperometric measurements.

### 2.4.3.2 Single Frequency Electrochemical Impedance Spectroscopy (EIS)

The Gamry's EIS measurement protocol (package EIS300™) allows determining the impedance of an electrochemical cell (glucose sensor) by applying a sine wave of a defined frequency and amplitude (AC signal). **Figure 5** shows a screen shot of the graphical user interface. Additionally an optional DC offset can be applied onto the cell. Gamry uses a novel single-sine EIS technique called sub-harmonic sampling [30].

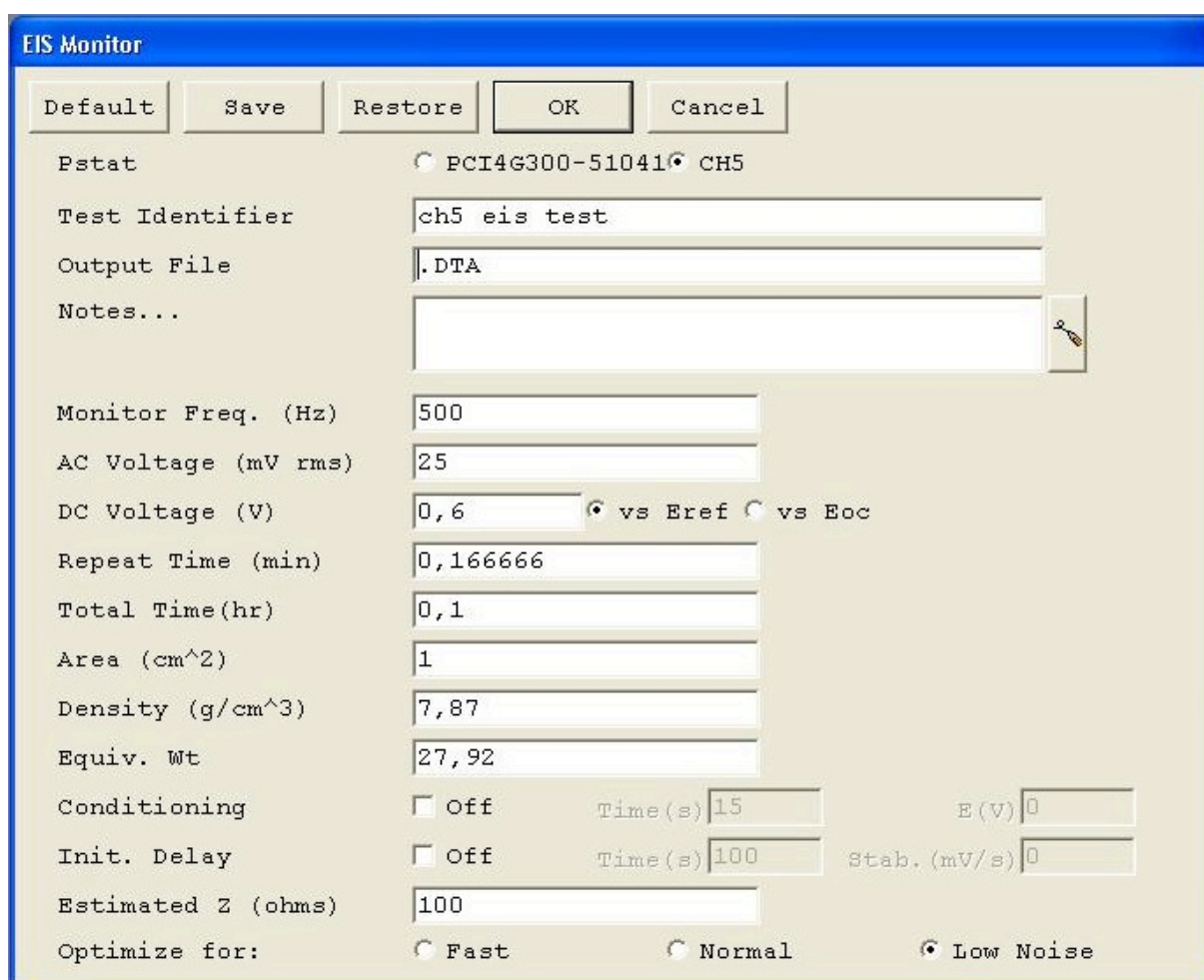


**Figure 5:** Screen shot of the Gamry software to configure the EIS measurements.

### 2.4.3.3 Sub-harmonic Sampling

Gamry uses sub-harmonic sampling to avoid costs caused by fast and thus expensive A/D converters and allows sampling at frequencies lower than the Nyquist frequency.

Therefore the AC waveform for EIS is generated using “Direct Digital Synthesis” (DDS), which represents the State of the Art procedure for AC waveform generation using an internal clock. Digital signal processing techniques used for DDS allow generating low-distortion, true sine wave excitations at the desired frequencies. The circuit design implemented by Gamry insures that the excitation waveform is accurately synchronized with the Potentiostat’s data acquisition. Sub-harmonic sampling is now used in the data acquisition, transforming high frequency AC waveforms into lower frequencies. The potentiostat’s A/D converter samples the excitation as well as the response at many points on different cycles of the waveform. Sub-harmonic sampling is feasible because the sampling position on the waveform is accurately controlled as the sampling frequency is an exact sub-harmonic of the excitation waveform. This procedure results in a sine wave which is lower in frequency than the excitation wave but amplitude and phase is preserved. [30]

#### ***2.4.3.4 Gamry’s Sequence Wizard***

The final approach for the glucose monitoring unit was measuring glucose and conductivity subsequently. This was done using Gamry’s Sequence Wizard which allows performing chrono-amperometry and “Single Frequency Electrochemical Impedance Spectroscopy” (EIS) subsequently. In order to combine them to various complex experiments Gamry offers the user an easy way to access the script source and to customize experiments. Beside these functions implemented by the different software packages provided by Gamry Instruments, other usual functions (e.g. loops) are included as predefined functions in the wizard. [31] To achieve a customized experiment the user can use Drag & Drop and save the whole sequence as a customized script. Furthermore it is even possible to run the new sequence directly from the program window, which is very convenient for quick tests.

The whole setup window can be seen in **Figure 6**.

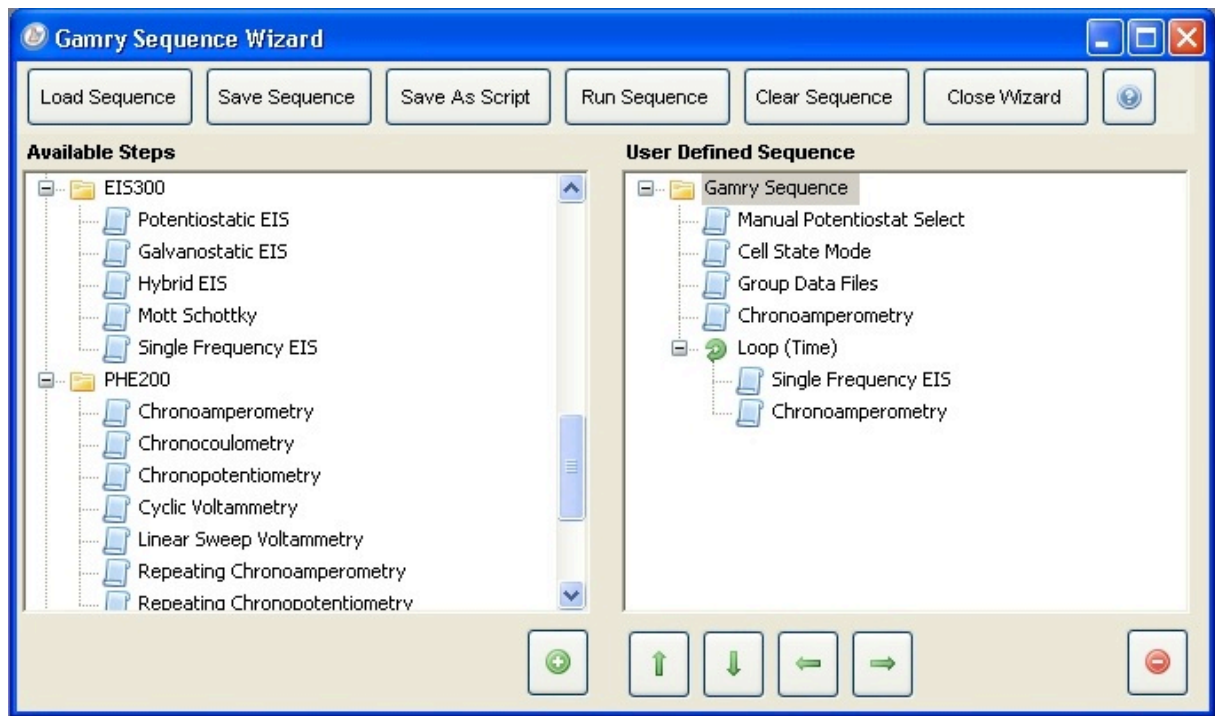


*Figure 6: Screen shot of the Gamry's sequence wizard.*

## 2.5 Data Acquisition and Analysis

Data were recorded in CRFs and Microsoft Excel spread sheets files and processed using MatLab (Mathworks, version: R2009b) [32].

### 2.5.1 Statistical Methods

The following statistical parameters were calculated taking into consideration the glucose concentration of the dialysate and the blood plasma as well as the sensor current:

- Coefficient of correlation and regression analysis I [33]
- Mean absolute relative difference (MARD) [34]
- Signal to Noise Ratio (SNR) [35]
- Variation coefficient (CV)[36]

To enable the calculation of these parameters blood glucose (single point values) and dialysate glucose values (single point values of 15 min samples) were compared with sensor values (also single point values) derived from the quasi continuous sensor currents and impedance measurements.

## **2.6 In Vitro Investigations**

### **2.6.1 Determination of the Polarization Potential using Cyclic Voltammetry**

#### **Primary Objective**

The aim of this investigation was to proof whether the polarization potential of 600 mV chosen by Dexcom is reasonable. To find the optimal working potential of the sensor a cyclic voltammetry was performed. Throughout this procedure a sensor is immersed in an unstirred solution and the potential was varied while measuring the related current. The potential was usually varied between a minimal and a maximal value and vice versa, causing diffusion controlled oxidation or reduction of the analyte. [20]

#### **Setup and Methods**

The glucose sensor was immersed into a matrix of phosphate buffer with a glucose concentration of 200 mg/dl and an ion concentration of 50% of physiological saline solution.

The sensor was operated in the cyclic voltammetry mode of the potentiostat. The polarization voltage was chosen to be between a minimum of 0 mV and a maximum of 800 mV. With a scan rate of 1mV/s two scans were performed.

## Results

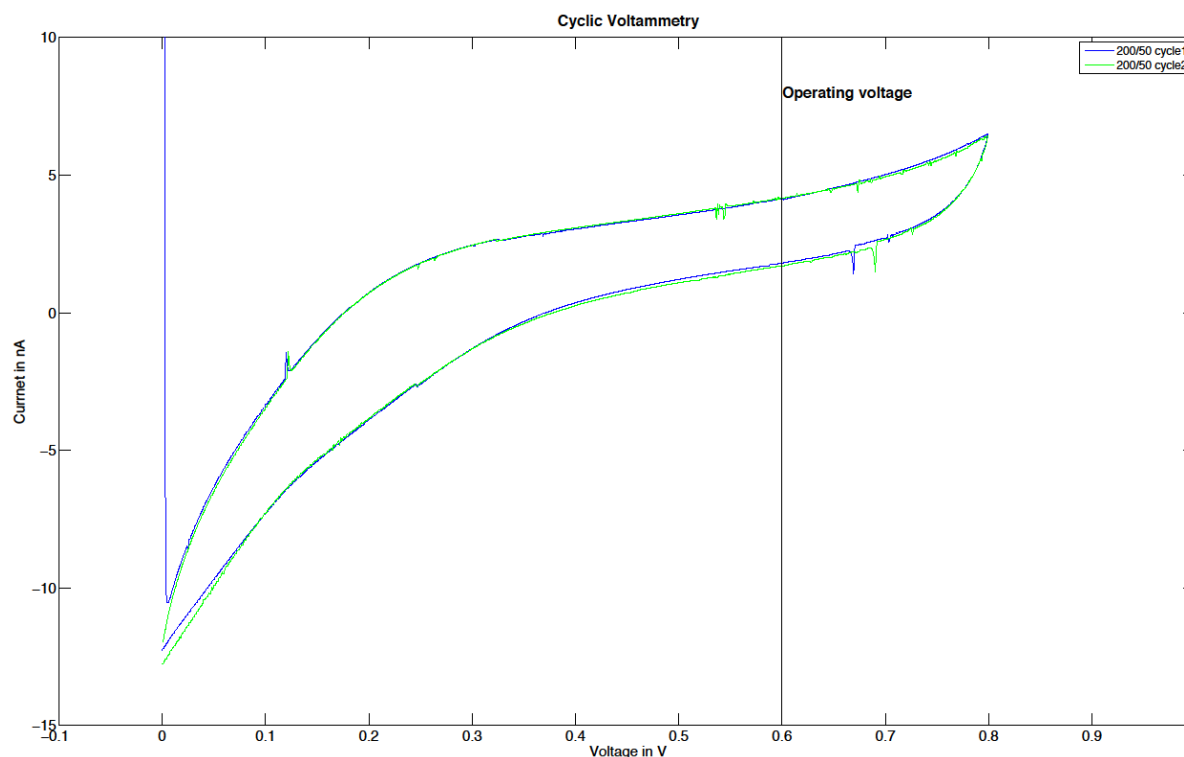


**Figure 7:** Cyclic voltammogram of the Dexcom STS 7.

**Figure 7** shows the cyclic voltammogram of the Dexcom STS 7 glucose sensor. Usually the optimal polarization voltage can be found at the beginning of the plateau phase (here 400 mV). This leads to a current proportional to the analyte concentration [37]. The potential of the Dexcom STS 7 is chosen to be 600 mV, which is located in the plateau phase, this is reasonable because the membrane of the Dexcom STS 7 offers the ability to prevent interactions caused by higher potentials.

### 2.6.2 Temperature Dependency

#### Primary Objective

The aim of this investigation was to determine whether the glucose sensor has a temperature dependency.

## Setup and Methods

The glucose sensor was immersed into a test matrix of 5% Mannitol with a glucose concentration of 100 mg/dl and an ion concentration of 50% of physiological saline solution.

A water bath was used to modulate the temperature of the test matrix. The sensor was run-in for 2 hours at 37°C. Afterwards the temperature was held constant at 42°C to allow the quantification of the sensor drift. Finally the heater was switched off and the sensor current was recorded until the water bath reached room temperature.

The sensor was operated intermittently chrono-amperometrically as well as in EIS mode. The potentiostat was operated in “Wizard” mode, where glucose was measured for 10 minutes followed by 5 minute measurement periods to quantify conductivity. The polarization voltage was chosen to be 600 mV and held constant throughout the whole experiment. Additionally an AC amplitude of 25 mV and a frequency of 500 Hz was superimposed to the DC – voltage so as to measure impedance.

Data were recorded via Gamry software, processed without filtering using MatLab. The drift of the glucose sensor was determined during the stable phase at 42°C. To calculate only the drift caused by the temperature, the drift of the stable phase was subtracted from the drift observed during the whole cool down phase.

## Results

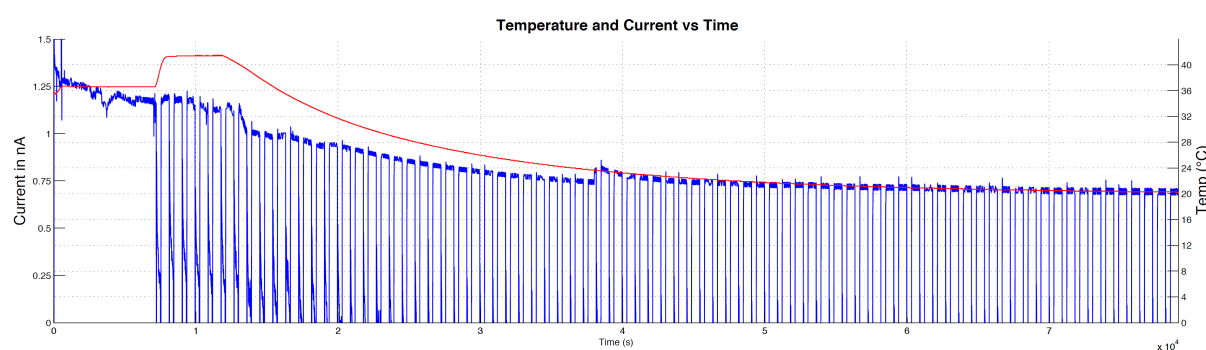


**Figure 8:** Temperature dependency of sensor current. On the first y-axis the sensor current (blue line) is plotted over time. On the second y-axis the temperature is plotted over time (red line).

The temperature dependency was calculated as 5.7 pA/°C or 0.8 %/°C for a glucose concentration of 100 mg/dl and 50% of physiological saline solution.

## 2.6.3 Simultaneous Measurement Approach

### 2.6.3.1 Estimation of the optimal Parameters

#### Primary Objective

The aim was to establish a reproducible, reliable and simultaneous glucose- and conductivity measurement.

Therefore the best combination of AC amplitude and frequency, to achieve a minimal coefficient of variation (CV) of the impedance and the glucose current, was investigated in a phosphate-buffered matrix. Furthermore to proof whether the sensor is still working after an application of a certain frequency, the chrono-amperometrically measured glucose current should not be influenced by simultaneous measurement phases.

#### Setup and Methods

The test matrix consisted of 50% phosphate buffer (equals 50 % ion concentration of physiological saline solution) spiked with glucose to a final concentration of 100 mg/dl. The sensor was directly immersed into the test matrix, no flow cell was used.

After a chrono-amperometrical run-in period of 2 hours the sensor was operated in EIS mode and sensor current as well as impedance were measured. To ensure that the glucose sensor was working properly, after each EIS measurement phase a chrono-amperometrical measurement phase was started to analyse the quality of the sensor signal. For a detailed measurement protocol refer to the **APPENDIX, Table 2**.

The polarization voltage was chosen to be 600 mV and held constant over the whole investigation. Additionally the AC amplitude was varied from 1 mV to 25 mV and the frequency was varied from 1 kHz to 10 kHz.

The potentiostat was operated in “Wizard” mode. Data were recorded via Gamry software, processed without filtering using MatLab.

## Results – Sensor current

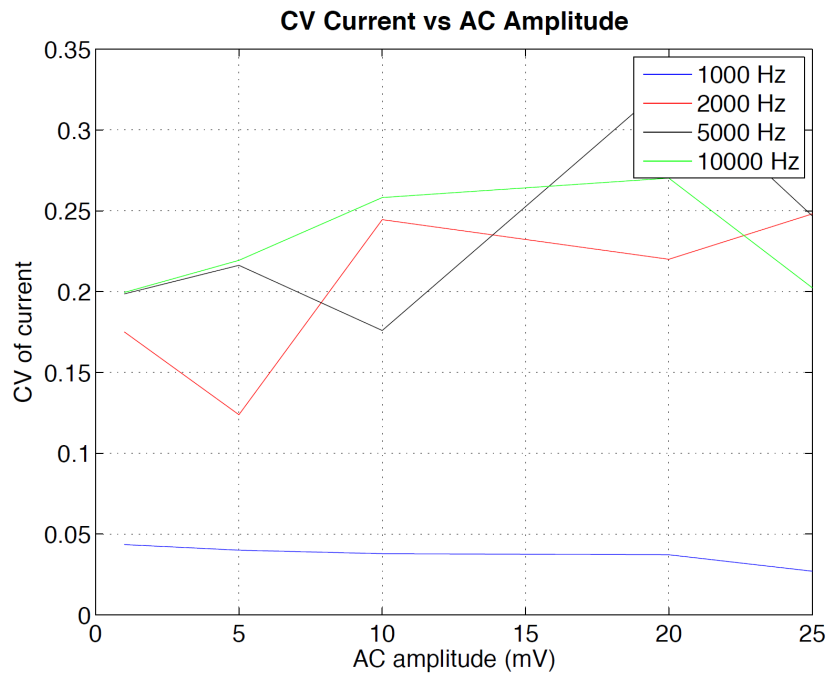


**Figure 9:** The coefficient of variation (CV) of the sensor current as a function of different AC amplitudes and frequencies.

**Figure 9** shows the calculated coefficient of variation (CV) of the sensor current for different AC amplitudes and frequencies. The amplitude does not influence the CV whereas the chosen frequency is crucial. Therefore for the further investigations a frequency of 1 kHz was chosen.

**Results – Impedance:**

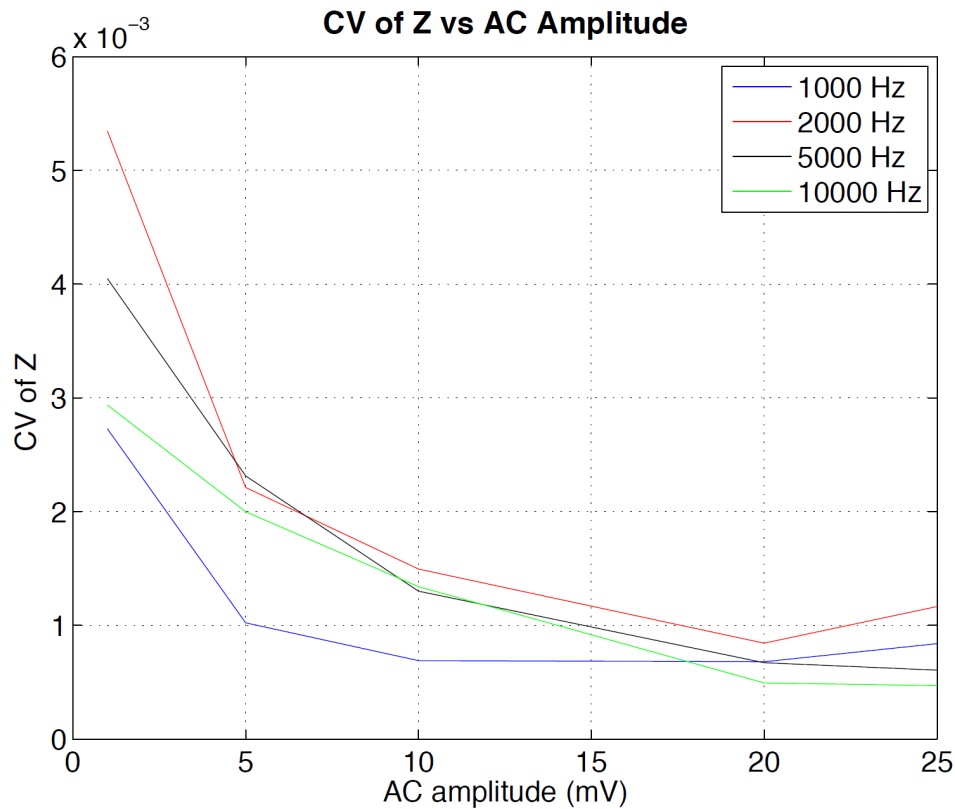


**Figure 10:** The coefficient of variation (CV) of the impedance as a function of different AC amplitudes and frequencies.

**Figure 10** shows the coefficient of variation (CV) of the impedance as a function of different AC amplitudes and frequencies. In general, CVs decrease with increasing AC amplitudes and decreasing frequencies. To achieve an acceptable CV the amplitude was chosen to be 5 mV and the frequency 1 kHz what is in line with the results observed in **Figure 9**.

### ***2.6.3.2 Simultaneous Measurement of Glucose and Conductivity using the Optimal Parameters***

#### **Primary Objective**

The aim was to prove if a simultaneous measurement of glucose and conductivity is possible. Therefore experiments were performed under buffered conditions in beakers as well as under un-buffered conditions using a flow through cell.

#### **Setup and Methods**

The test matrix consisted of phosphate buffer (buffered conditions) or 5% Mannitol (un-buffered conditions) spiked with glucose to final concentrations of 50, 100, 150, and 200 mg/dl and conductivities of 25, 50, 75 and 100% of that of physiological saline solution.

Under un-buffered conditions the sensor was directly immersed into the test matrix.

Under buffered conditions the test matrices were pumped through the flow cell at a flow rate of 5 $\mu$ l/min. To change the test matrices the pump was stopped to avoid air bubble problems. The sensor was operated in EIS mode. The polarization voltage was chosen to be 600 mV and held constant throughout the whole investigation. Additionally the AC amplitude of 5 mV and the frequency of 1000 Hz were chosen.

Data were recorded by Gamry software, processed without filtering using MatLab.

## Results

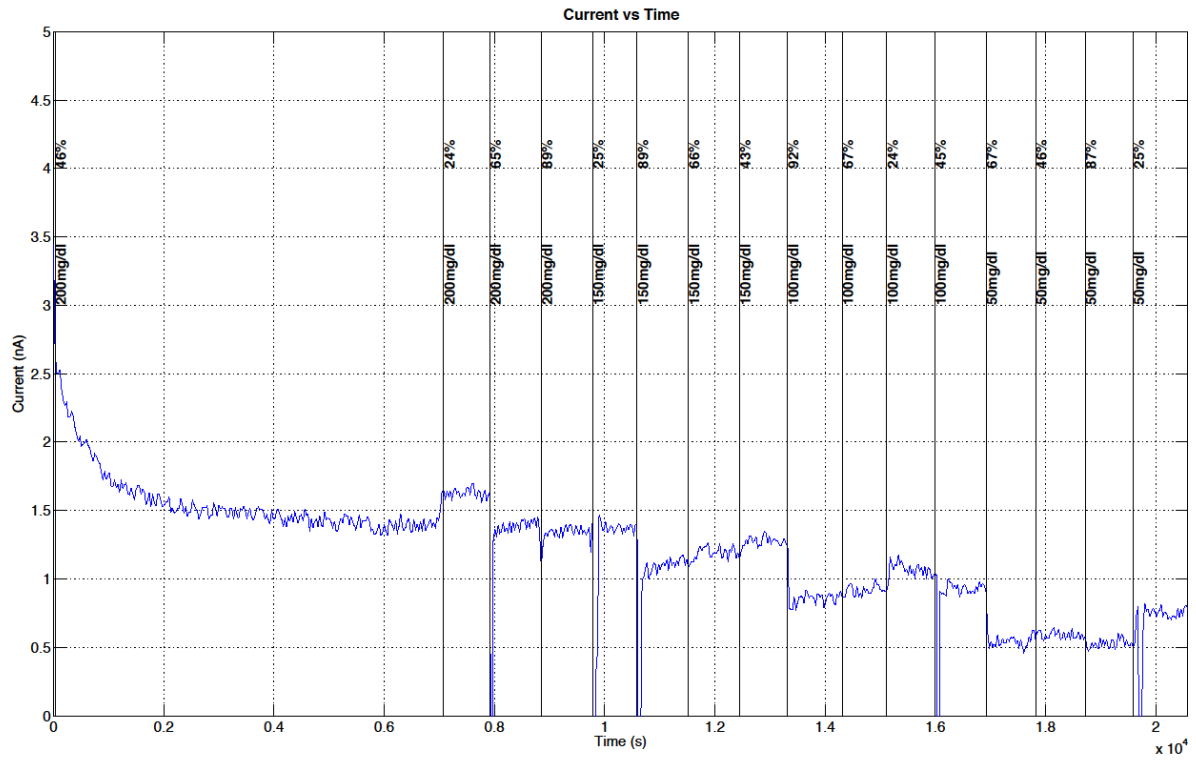


**Figure 11:** Glucose sensor current in EIS mode under buffered conditions

**Figure 11** shows the recorded sensor current under buffered conditions. It was in an expected range and high in SNR (SNR in worst case: 29.8 dB). This signal provides simultaneous glucose-and conductivity measurement.

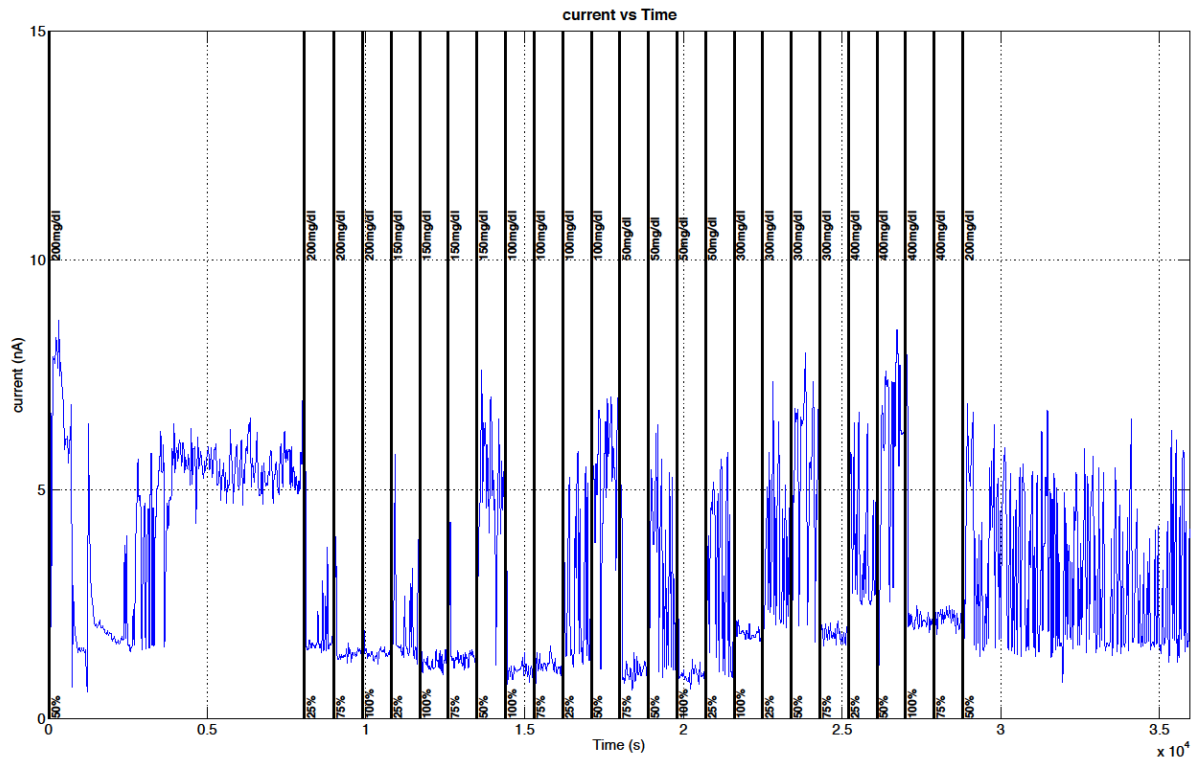


**Figure 12:** Glucose sensor current in EIS mode under un-buffered conditions using the flow through cell

**Figure 12** shows the recorded sensor current in an unexpected range (current > 7 nA) which was affected by noise with a minimum signal to noise ratio (SNR) of 5.8 dB. The simultaneous measurement mode could not provide a reliable glucose measurement while measuring conductivity simultaneously.

## 2.6.4 Intermittent Measurement Approach

### 2.6.4.1 Estimation of the Optimal Parameters

#### Primary Objective

The aim was to establish a reproducible, reliable and intermittent glucose- and conductivity measurement.

Therefore the best combination of AC amplitude and frequency, to achieve a minimal coefficient of variation (CV) of the impedance, was investigated. Furthermore to investigate whether this measurement approach is reliable or not, the chrono-amperometrically measured glucose current should not be influenced by the in between impedance measurement phases.

### **Setup and Methods**

The test matrix consisted of 5% Mannitol spiked with glucose to a final concentration of 500 mg/dl and a conductivity of 50% of physiological saline solution.

Liquids were pumped through the flow cell at a flow rate of 5 $\mu$ l/min. For changing the liquids the pump was stopped to avoid air bubble problems.

After a run-in period of 2 hours the sensor was operated in intermittent chrono-amperometric mode as well as in EIS mode. The polarization voltage was chosen to be 600 mV and held constant throughout the whole experiment. Additionally the AC amplitude was varied from 1mV to 25 mV and the frequency was varied from 100 Hz to 20 kHz. For a detailed measurement protocol refer to the **APPENDIX**, Table 3.

The potentiostat was operated in "Wizard" mode, where glucose was measured for 10 minutes followed by a measurement period of conductivity for 5 minutes.

Data were recorded via Gamry software, processed without filtering using MatLab.



## Results – Coefficient of variation (CV) of impedance Z as a function of AC amplitude and frequency

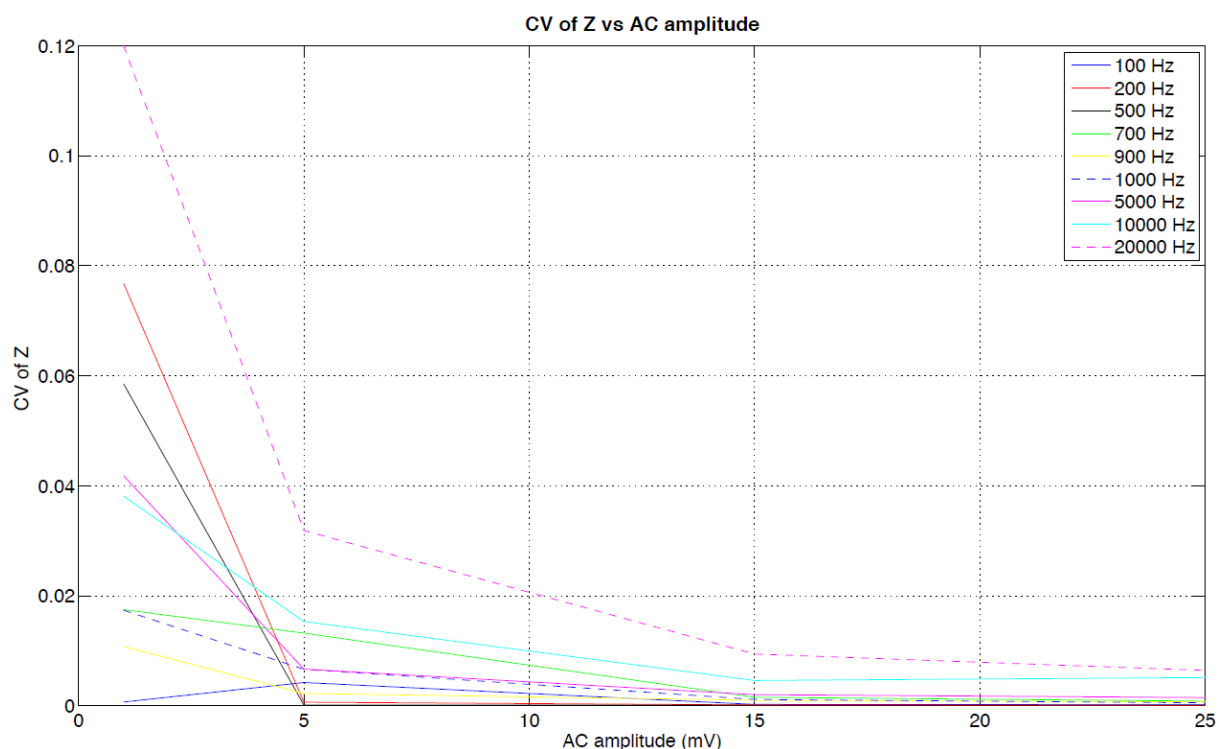


**Figure 14:** The coefficient of variation (CV) as a function of different AC amplitudes and frequencies.

**Figure 14** displays coefficient of variation (CV) as a function of different AC amplitudes and frequencies. In general, CVs decrease with increasing AC amplitude and decreasing frequencies. To achieve an acceptable CV the amplitude was chosen to be larger than 15 mV and the frequency lower than 5 kHz. During the in vivo investigations 25mV and 1 kHz was chosen. The time signal used for this analysis can be found in **APPENDIX, Figure 32**.

### 2.6.4.2 Intermittent Measurement of Glucose and Conductivity using the Optimal Parameters

As we were not able to establish a reproducible and reliable simultaneous glucose- and conductivity measurement it was obvious to measure the glucose and conductivity intermittently for 10 and 5 minutes each. The initial idea was to take these conductivity values to correct the glucose signal online during the 10 minutes measurement period.

## **Primary Objective**

The aim was to proof if intermittent measurement of glucose and conductivity is feasible. Furthermore the relationship in a matrix of known ion concentration (in % of physiological saline solution) and conductivity was investigated. Additionally the influence of the ion concentration on the glucose current was investigated.

## **Setup and Methods**

The test matrix consisted of 5% Mannitol spiked with glucose to final concentrations of 10, 50, 100, 150, 200 and 400 mg/dl and had conductivities of 10, 30, 50, 70 and 90% of that of physiological saline solution.

Liquids were pumped through the flow through cell at a flow rate of 5  $\mu$ l/min. For changing the liquids the pump was stopped to avoid air bubble problems.

After a run-in period of 2 hours the sensor was operated intermittently in chrono-amperometric as well as in EIS mode. The polarization voltage was chosen to be 600 mV and held constant over the whole investigation. Additionally the AC amplitude of 25 mV and the frequency of 500 Hz were chosen. The potentiostat was operated in "Wizard" mode, where glucose was measured for 10 minutes followed by a measurement period of conductivity for 5 minutes.

Data were recorded via Gamry software, processed without filtering using MatLab.

## Results

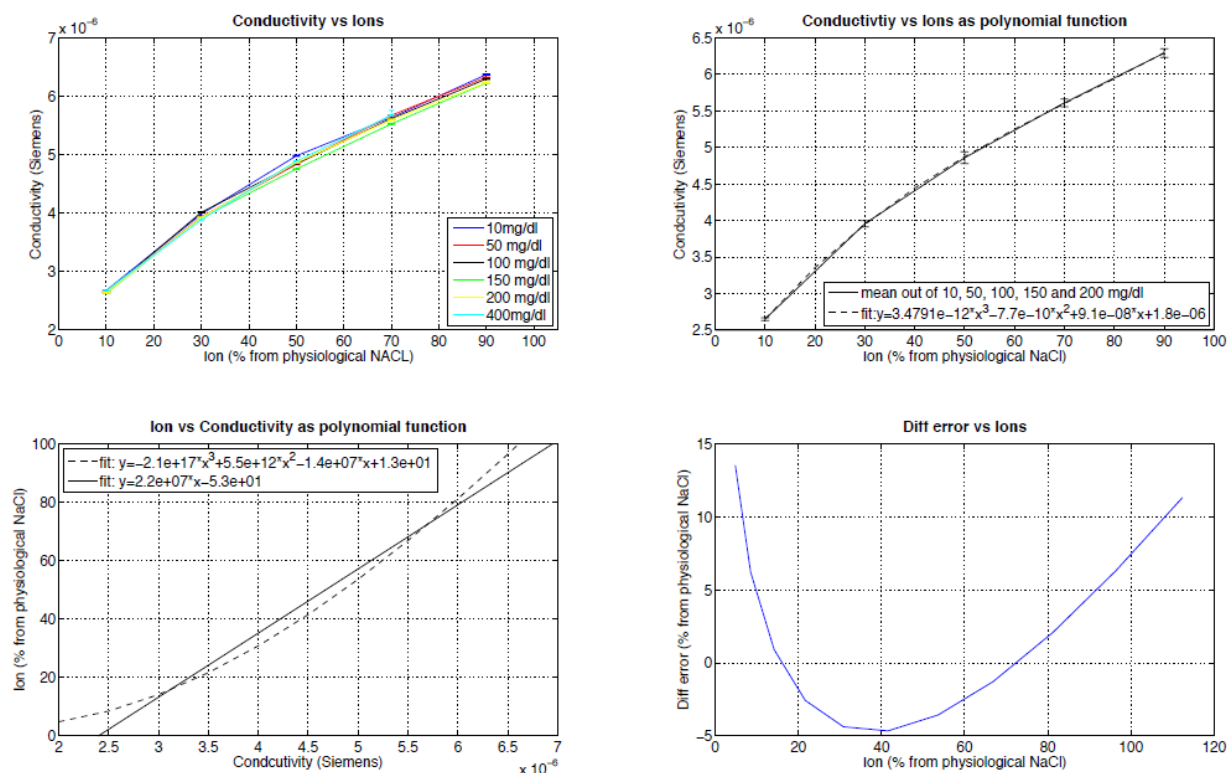


**Figure 15: Top left** shows the individual conductivities for different glucose concentrations (10, 50, 100, 150, 200 and 400 mg/dl) as function of the relative ion concentration in % of physiological saline solution (10, 30, 50, 70 and 90 %).

**Top right** shows the mean conductivity of all glucose concentrations as function of the relative ion concentration in % of physiological saline solution and the respective polynomial function of 3<sup>rd</sup> order.

**Bottom left** shows the relative ion concentration in % of physiological saline solution as a function of the conductivity and the respective linearized fit function.

**Bottom right** shows the differential error between linearized fit function and the polynomial function of 3<sup>rd</sup> order

**Figure 15 Top left:** Independently of the concentration of glucose present in the matrix a reproducible conductivity can be measured. This can be proven as all non-linear fitting functions are more or less congruent. These non-linear functions were then averaged (**top right**). Subsequently this non-linear function was inverted and linearized (**bottom left**). This function is essential if the measured conductivity should be calibrated to ion concentration in % of physiological saline solution. The bottom right graph shows the differential error that occurs if a linearized fit function is used instead of the original polynomial function of 3<sup>rd</sup> order for calibration. Due to the fact that the ion concentration expected to be found during the in vivo experiments will be between 20 and 70% the resulting error ranges from 0.9% (15% relative ion concentration) to -4.6% (50% relative ion concentration).

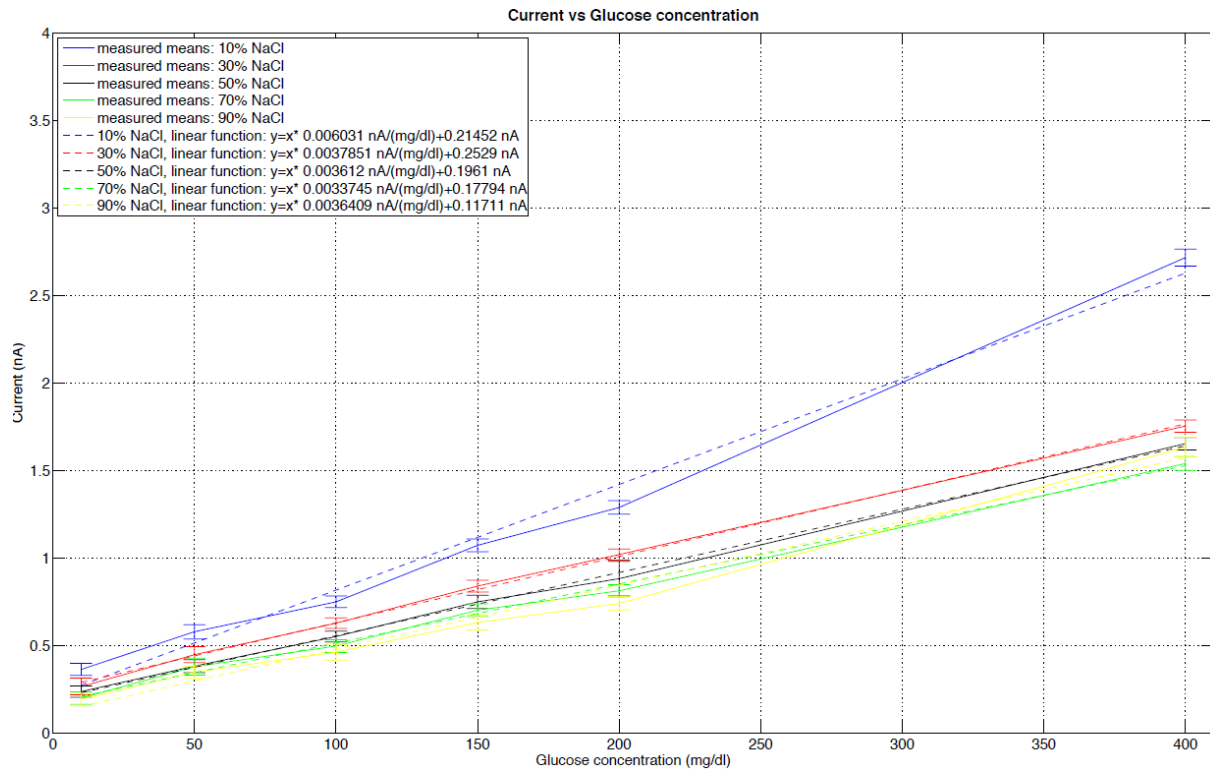


**Figure 16:** Relationship between glucose concentration and sensor current at different ion concentrations

**Figure 16** shows a linear relationship between glucose concentration and sensor current. Furthermore a dependency of the measured glucose current on the ion concentration could be found. With increasing ion concentration the sensor current is decreasing. Nevertheless for the ion concentration expected to be found during the in vivo experiments, which will be between 20 and 70%, the curves are more or less congruent meaning that there will be a negligible influence of different ion concentrations on the sensor current.

## 2.6.5 Test of the Final System inclusive ivMD

### Primary Objective

The aim of this investigation was to test the final system comprising of pump, ivMD, glucose sensor and flow through cell and sampling unit to be operated in vitro under defined conditions (temperature, polarization voltage, AC amplitude and AC frequency).

### Setup and Methods

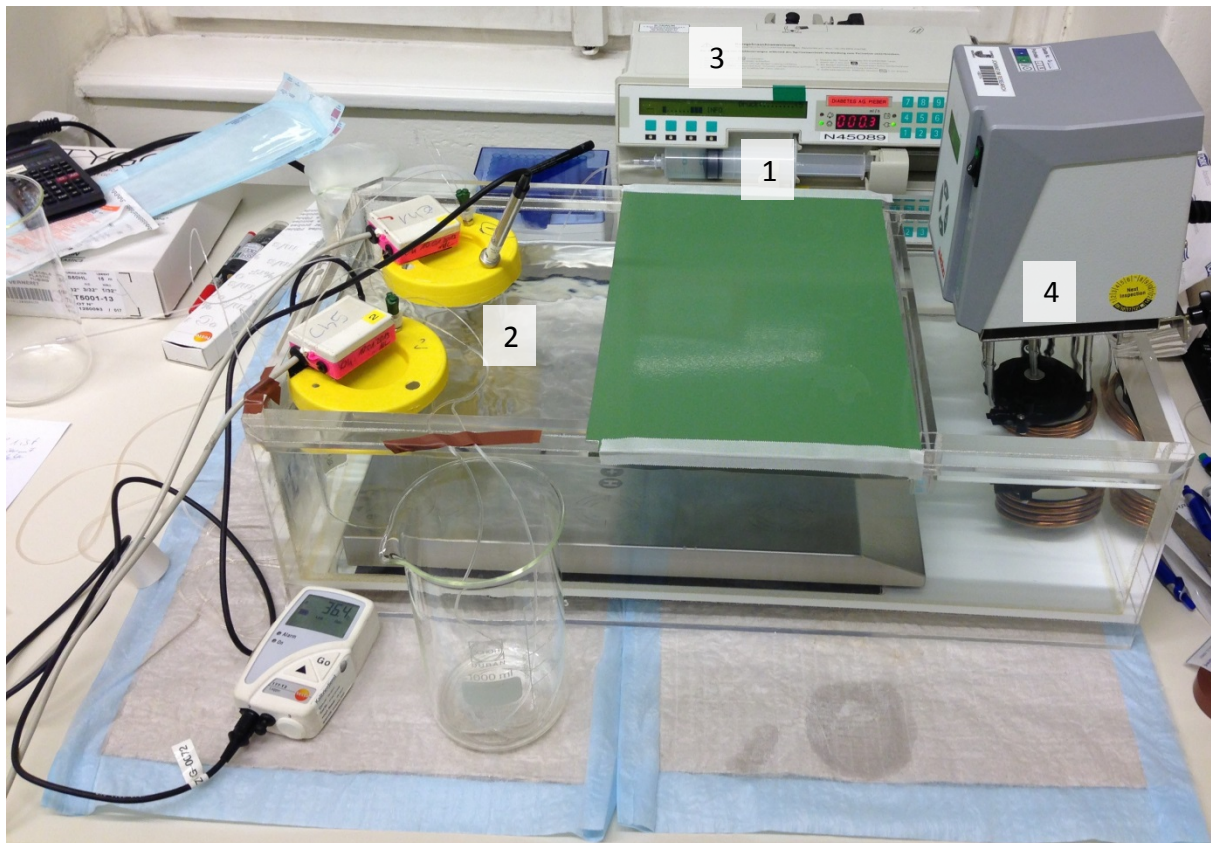


**Figure 17:** In vitro setup to test the final glucose monitoring unit.

**Figure 17** shows the in vitro setup to test the final system: Test matrices (2) of 5% Mannitol spiked with glucose to final concentrations of 30, 60 and 120 mg/dl with ion concentrations of 15 and 32% of physiological saline solution were tempered using a water bath (4).

Mannitol (5%) was used as perfusate (1) and pumped (3) through the MicroEye® microdialysis catheter (Probe Scientific Ltd, Coventry, UK) and the subsequent flow cell at a flow rate of 3.3  $\mu\text{l}/\text{min}$ . To avoid air bubbles the perfusate was degassed prior to the experiment applying under pressure [38].

After a run-in period of 2 hours the sensor was operated intermittently in chronoamperometric as well as in EIS mode. The polarization voltage was chosen to be 600 mV and held constant throughout the whole experiment. Additionally an AC amplitude of 25 mV and a frequency of 1000 Hz were chosen. The potentiostat was operated in “Wizard” mode, where glucose was measured for 10 minutes followed by a measurement period of conductivity for 5 minutes.

Data were recorded via Gamry software, processed without filtering using MatLab.

## Results

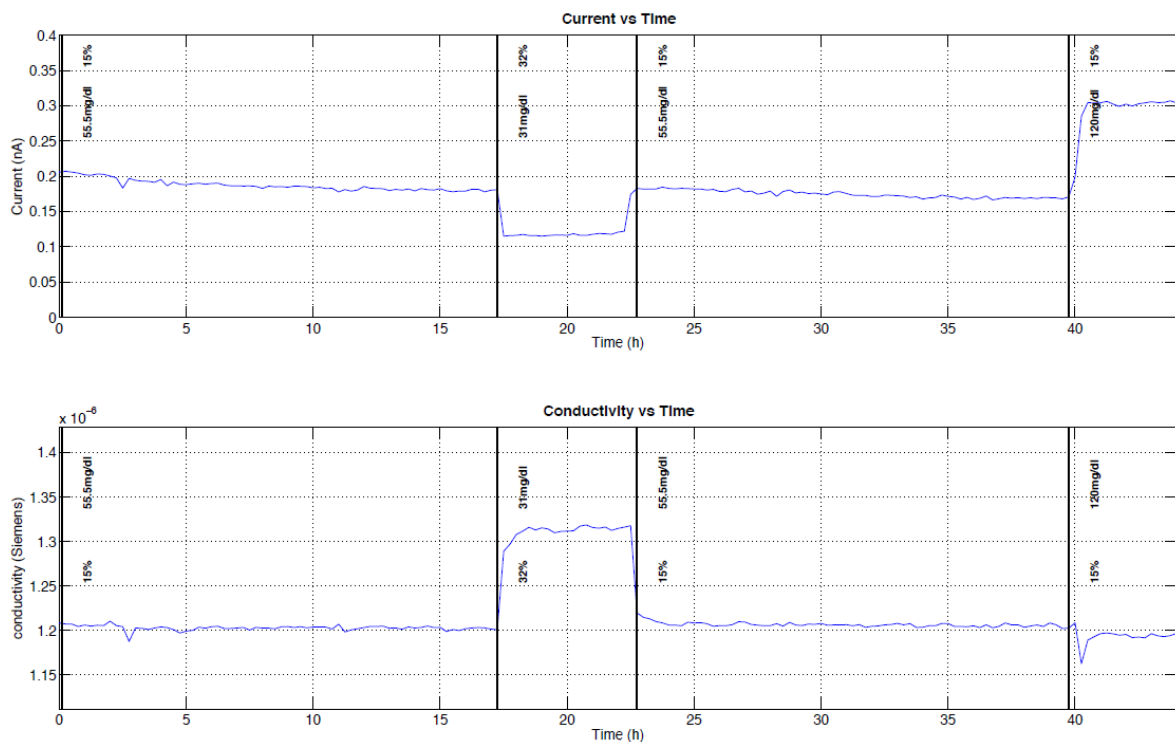


**Figure 18 top** shows the sensor current over time using the microdialysis probe in different beakers. **Bottom** shows the conductivity over time.

**Figure 18:** The graph at the **top** shows a reproducible and expected sensor current. The glucose signal shows a drift of  $4.26 \cdot 10^{-7}$  nA/s or 0.8 %/h. Test solutions containing 60 and 120 mg/dl and 15 % relative ion concentration caused different sensor currents of 0.19 and 0.31 nA for the same ion concentration.

**Bottom:** Conductivity can be measured reproducibly. The conductivity signal shows a relative small drift of 0.03 %/h. Test solutions containing 60 and 120 mg/dl and 15 % of ions caused the same conductivity level of  $1.2 \mu\text{S}$  independently of the glucose concentration, whereas a clear difference between test solutions containing 15 and 32 % relative ion concentration ( $1.2 \mu\text{S}$  vs.  $1.3 \mu\text{S}$ ) can be seen.

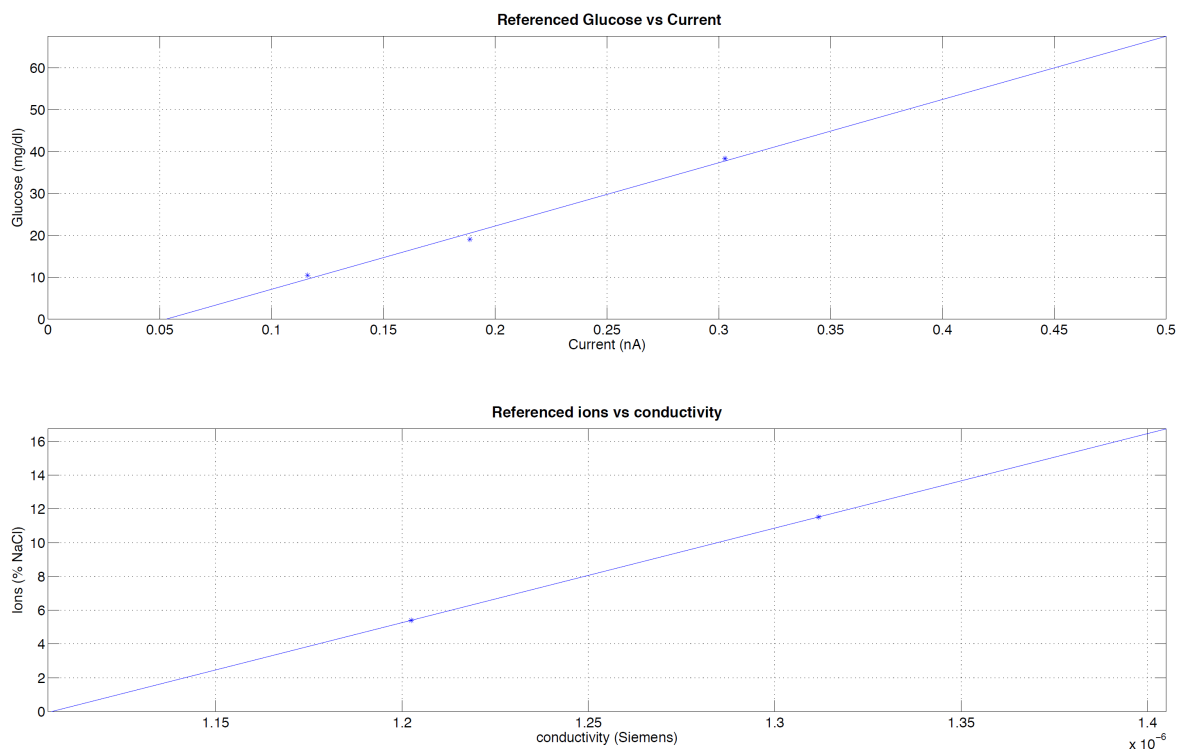


**Figure 19 top** shows the calibration curve for glucose considering the sensor current and the dialysate values referenced with the Super GL2.

**Bottom** shows the calibration curve for ions considering the sensor conductivity and the dialysate values referenced with the TraceDec.

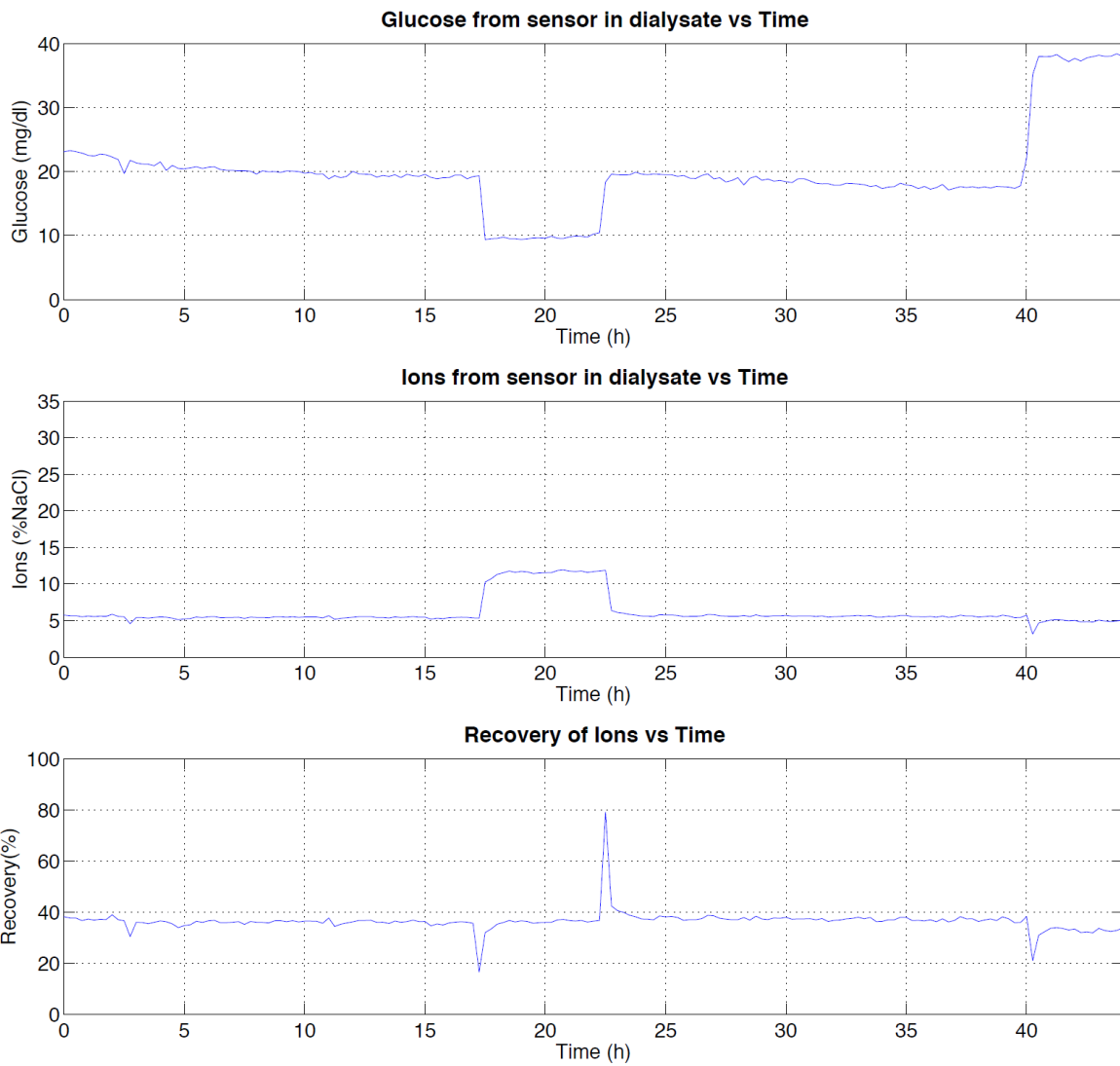


**Figure 20 top** shows the glucose over time derived from the sensor current shown in **Figure 18 top** which was calibrated using the calibration curve shown in **Figure 19 top**.

**Middle** shows the relative ion concentration over time derived from the sensor conductivity shown in **Figure 18 bottom** which was calibrated using the calibration curve shown in **Figure 19 bottom**.

**Bottom** shows the ions recovery over time calculated as ratio of ion concentrations of the dialysate and test matrices.

## Application of the IRT

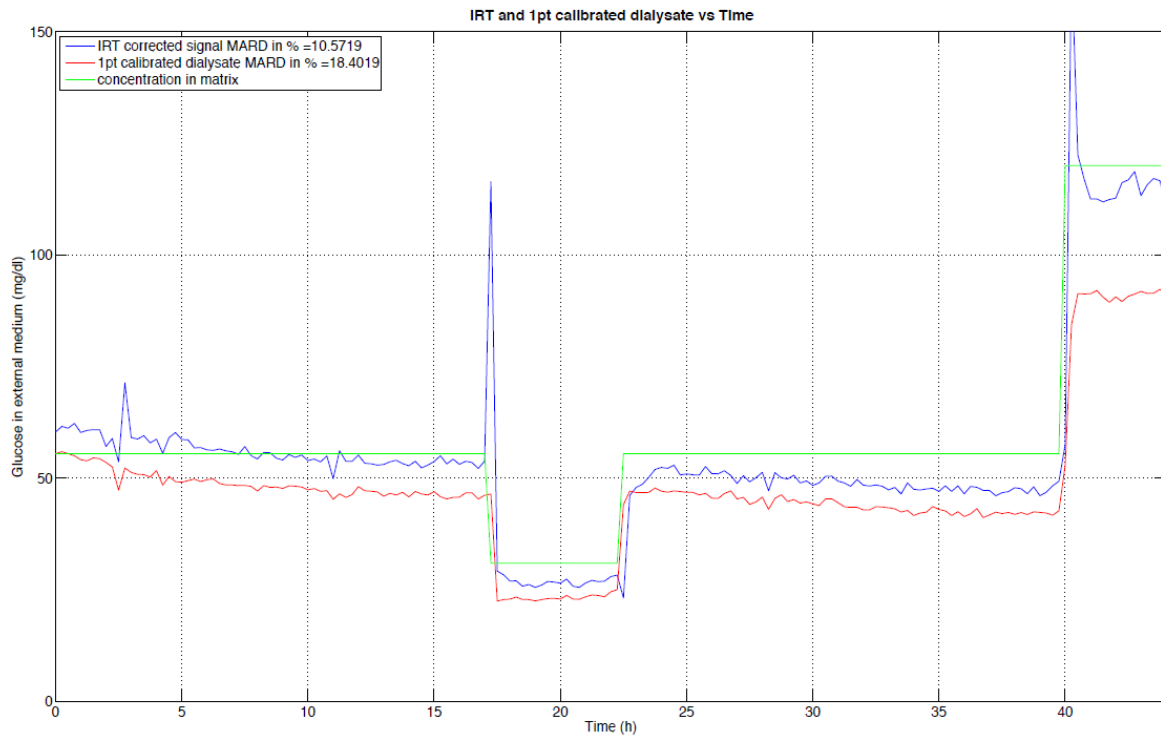


**Figure 21:** The green curve represents the glucose concentration in the test matrix referenced with the Super GL2. The red curve shows dialysate glucose measured with the glucose sensor which was afterwards 1pt calibrated using the concentration of the test matrix. The blue graph shows dialysate glucose measured with the glucose sensor which was afterwards corrected with the IRT taking into consideration the recovery of **Figure 20 bottom**.

The dialysate glucose profile was 1pt calibrated using the reference value of the first matrix. Both signals as well as the concentration in the matrix are plotted in **Figure 21**. By using 1pt calibration of the dialysate the result shows an MARD of 18.4 %. When the IRT is implemented the MARD decreases to 10.6 %. Considering these results an in vivo experiment of the monitoring unit was considered as feasible.

**Figure 21** shows clearly that the MARD can be reduced from 18.4 to 10.6 % if the IRT instead of a 1pt calibration is applied onto the data set. Based on these results it was obvious to test the final system during an in vivo investigation.

## 2.7 In Vivo Investigations

### 2.7.1 Primary Objective

The aim was to proof whether the measurement of glucose and conductivity can be established in an accurate and reproducible manner in vivo using the electrodes of the Dexcom STS7 glucose sensor.

### 2.7.2 Setup and Methods

#### 2.7.2.1 Location of Catheters

Microdialysis probes (CMA64, CMA Microdialysis AB, Solna, Sweden) with a membrane's molecular mass cut-off of 20 kDalton and a membrane length of 20mm were inserted into catheters (Introcan Safety 18G x 1 ¼", B. Braun, Melsungen, Germany) positioned at the distal position of the left or right arm. Proximal catheters were used for reference blood sampling and administration of the glucose infusion to clamp the subjects at predefined target blood glucose levels.

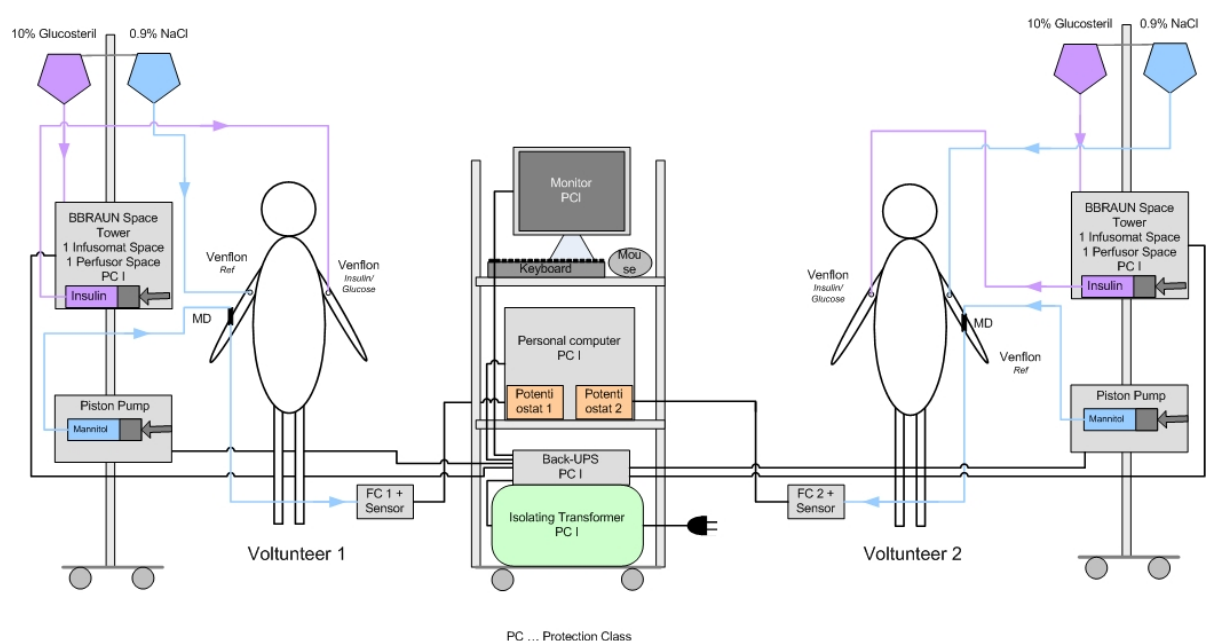


Figure 22: Setup of the glucose monitoring unit

### **2.7.2.2 Setup of the ivMD system**

The setup of the glucose monitoring unit is shown in **Figure 22**. Two volunteers can be investigated at the same time. Therefore an iso-osmotic and ion-free solution of 5% Mannitol was used as perfusate and pumped at a flow rate of 3.3  $\mu\text{l}/\text{min}$  through the ivMD probes using a bedside piston pump (Perfusor fm, B. Braun, Melsungen, Germany) and a 20 ml syringe (Plastipak, BD Medical, Heidelberg, Germany) as perfusate container. The syringe was connected to the ivMD probe with an extension line (E-87P, Codan, Lehnsan, Germany).

To minimize blood clotting at the probe's membrane 2.5mg of an anti-coagulant antithrombotic drug was added to the perfusate syringe which results in a concentration of 0.125mg/ml. Additionally the subjects received 2.5mg of an antithrombotic drug subcutaneously enabling systemic anti-coagulation. The glucose and ion enriched dialysate was collected through the outlet tubing into PCR vials for offline analysis. Furthermore the dialysate was analysed online for glucose and ions (conductivity) using a glucose sensor (STS-7 CGM, DexCom, San Diego, USA) which was placed in a custom built flow through cell. A potentiostat (G300) and software (Framework 5), both from (Gamry Instruments, Warminster, USA) were used to record the sensor data. For safety reasons the whole system was connected to the mains via an isolating transformer (Isolating Transformer, DeMeTec, Langgöns, Germany) and security of energy supply was guaranteed using an uninterruptible power supply (APC, Back Ups RS 1500, Rhode Island, USA). For detailed lists of the used devices refer to **APPENDIX**, Table 4, Table 5 and Table 6.

### **2.7.2.3 Risk Management Process**

All parts of the integrated sampling system were CE-certified except the flow cell, the potentiostat and the software. For these non-certified items a risk management according to ISO14971:2007 [39] was performed. Furthermore these risks were then analysed in a Fault Tree Analysis (FTA) according to ÖVE/ÖNORM EN 61025:2006 [40] and a Failure Mode and Effects Analysis (FMEA) according to ÖVE/ÖNORM EN31010:2009 [41]. Finally the system was classified according to IEC 60601-1 [42] and tested to ensure a safe application in humans. Two major hazards were identified for the glucose monitoring unit:

1. Electrical hazards
2. Biological hazards

As the biological hazards could not be avoided satisfactorily measures had to be taken to avoid any contamination of the patients allowing only single usage of the potentially contaminated products. Furthermore a backflow from the sensor to the body interface was prevented by the usage of a piston pump that allows only a positive flow. To avoid any backflow caused by handling the system, operators were well trained according to SOPs.

#### **2.7.2.4 Safety Check**

Thresholds for the safety check depend on the class of the device. Therefore the glucose monitoring unit was classified according to IEC 60601-1 and 93/42/EWG **APPENDIX IX** (medical device with an applied part of type BF).

During the analysis only the glucose monitoring unit without glucose and insulin infusion was considered and classified as an invasive, active device with measuring function and an application time of less than 30 days.

A sticker “zur klinischen Prüfung” was visibly attached to the device according to Norbert Leitgeb [43].

An electrical safety check was carried out to quantify the essential electrical safety parameters as PE resistance, load current, operating voltage, power consumption, earth-, enclosure-, patient- and patient auxiliary leakage currents using a safety tester (Unimet 1100ST, Bender GmbH & Co. KG, Grünberg, Germany). As test solution of 0.9% physiological saline solution was used. For a detailed schematic of the test setup refer to **Figure 23**.

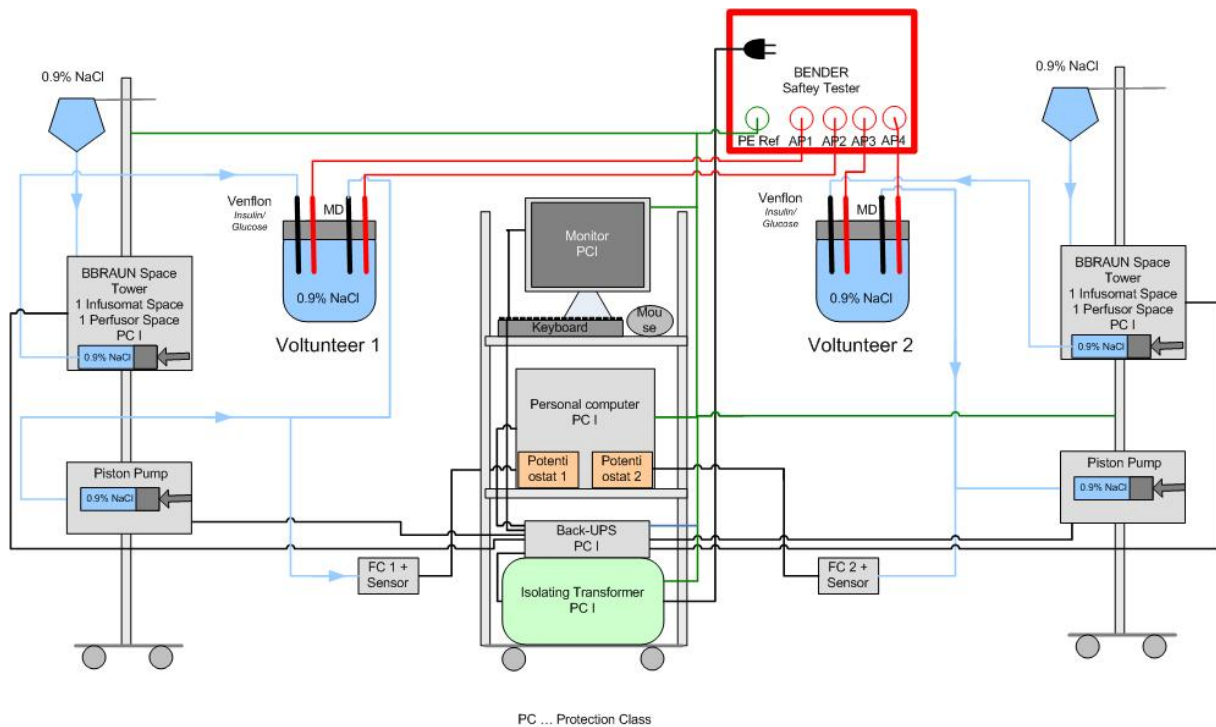


**Figure 23:** Setup of the glucose monitoring unit used to perform the safety test

## Results

All relevant electrical safety parameters as PE resistance, load current, operating voltage, power consumption, earth-, enclosure-, patient- and patient auxiliary leakage currents were below the thresholds defined by EN 60601-1 for BF devices (see **APPENDIX**, protocols depicted in **Figure 33**, **Figure 34**, **Figure 35** and **Figure 36**).

### 2.7.3 Clinical Study

#### 2.7.3.1 Protocol

A 24h open single-centre clinical feasibility study was conducted with 5 diabetic subjects. The study was performed at the Clinical Research Centre at the Medical University of Graz according to Good Clinical Practice (GCP) guidelines [44] and the Declaration of Helsinki [45]. Approval was obtained from the local ethics committee and the Austrian Agency for Health

and Food Safety (AGES). Before any trial-related activities were started a signed informed consent form was obtained from each subject.

Subjects arrived in the morning in fasting condition and received catheters for reference blood sampling, glucose infusion and ivMD systems. For the first 6 hours of the experiment, subjects were clamped to an eu-glycaemic level of around 90 mg/dl by adjusting glucose- and insulin infusion. After 6 hours, an intravenous glucose bolus of 20% Glucosteril, calculated according to the Dubois-method [46], was given to instantly reach a clamp level of 180 mg/dl. After administrating the bolus, the blood glucose was clamped to 180 mg/dl for 6 hours following by a level of 130 mg/dl for further 6 hours. Over the last 6 hours, the subjects were clamped to the same euglycaemic level as at the beginning of the experiment (around 90 mg/dl). Within the last half hour of the experiment subjects received a breakfast. Finally, ivMD probes plus catheters were simultaneously removed.

### ***2.7.3.2 Subjects***

In total, 5 ivMD systems were implanted and tested in diabetic subjects (5males/ 0 females; age: 44.5 +/- 8.5 years; BMI: 22.8 +/- 4.2 kg/m<sup>2</sup>) who fulfilled the inclusion and exclusion criteria which can be found in the screening information protocol. No ivMD probe needed to be removed or renewed during the study.

Data sets of the subjects (028, 031 and 032) showed an acceptable data quality and could be therefore further analysed. The Dexcom sensor of subject 029 showed an insensitive conductivity signal and data of subject 030 could only be partly recorded as the system was not reconnected after a volunteer had a toilet break.

### ***2.7.3.3 Blood Sampling Procedure***

Reference blood samples (51pprox.. 200 µl) were withdrawn every 15 minutes from the reference catheter. These samples were centrifuged, and the supernatant plasma was collected for offline glucose analysis using the Super GL2.

### 2.7.3.4 Dialysate Sampling Procedure

The dialysate was collected in PCR tubes for 15 minutes. Thus, dialysate samples reflect the average glucose and ion concentrations over the sampling period. Over the 24 hours a maximum of 96 dialysate samples per system were collected and analysed offline for weight, glucose and ion concentrations.

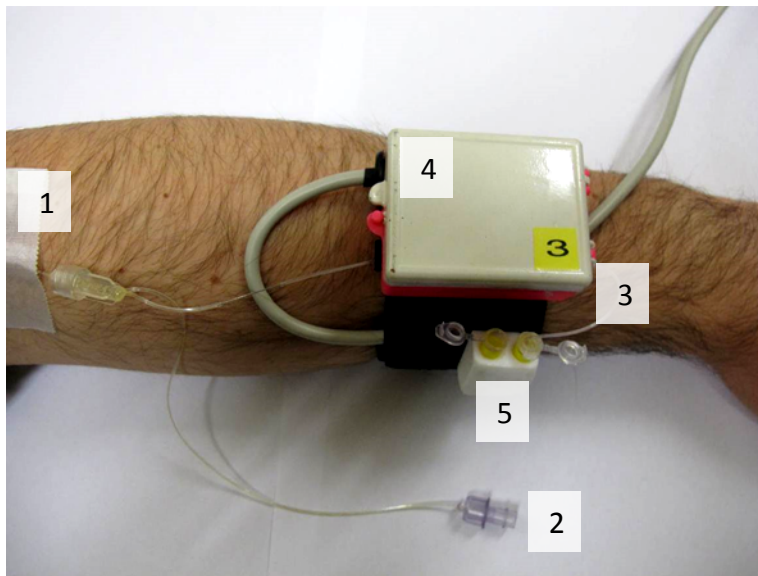


**Figure 24:** Volunteer's arm with body interface (1) with inlet and outlet port (2, 3). The sensor and flow through cell were located in the grey box (4) shielded with a copper foil to build a Faraday cage and to suppress interferences caused by any electric fields. PCR tubes to collect the dialysate sample are shown in (5).

### 2.7.4 Flow

#### Primary Objective

The aim of this investigation was to proof whether the ivMD, glucose sensor plus flow through cell and sampling unit can be operated under controlled conditions.

## Setup and Methods

Due to the lack of a CE-certified and sterile online flow sensor for in vivo use the flow rate was indirectly determined by weighing the dialysate samples over a 15 minute sample interval with a laboratory scale. With the assumption of a dialysate density of 1g/ml the flow-rates were calculated.

## Results

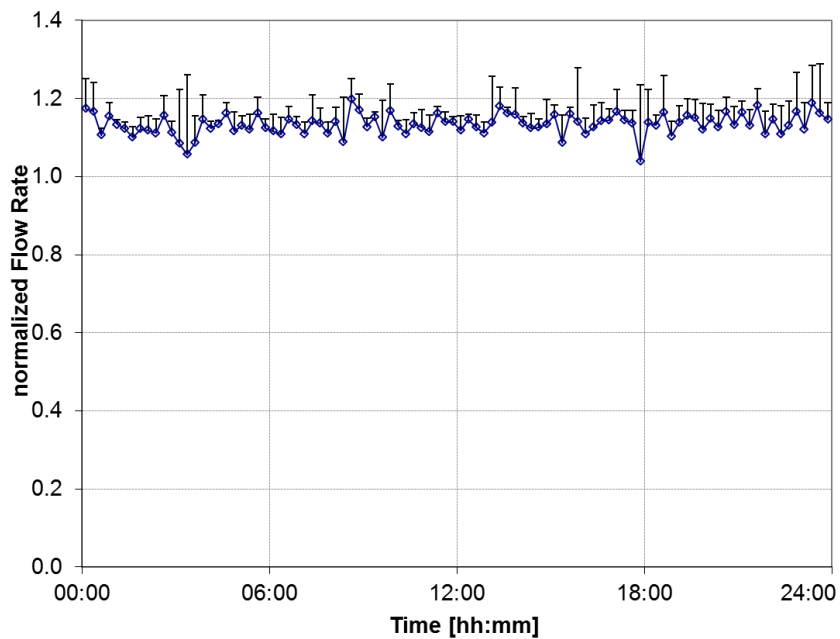


**Figure 25:** Normalized flow rate of ivMD system

**Figure 25** shows the mean values of the normalized flow rate (blue diamonds and blue solid line). The normalized flow rate in [%] was calculated as the ratio of measured flow rate [ $\mu\text{l}/\text{min}$ ] and nominal flow rate [ $\mu\text{l}/\text{min}$ ] multiplied with a factor of 100. The mean standard deviations of all 5 tested systems are depicted as black bars. The flow rate was found to be relatively stable over 24 h with values of  $113 \pm 5\%$  even if the glucose sensor and dialysate sampling unit were connected to the outlet port of the body interface. It can be observed that the flow was stable over 24 hours.

## 2.7.5 Recovery

### Primary Objective

The aim was to proof whether the basis for the Ionic Reference Technique is fulfilled.

### Setup and Methods

Glucose and ion recoveries measured by the reference methods Super GL2 (glucose) and TraceDec (conductivity) were plotted over time.

### Results

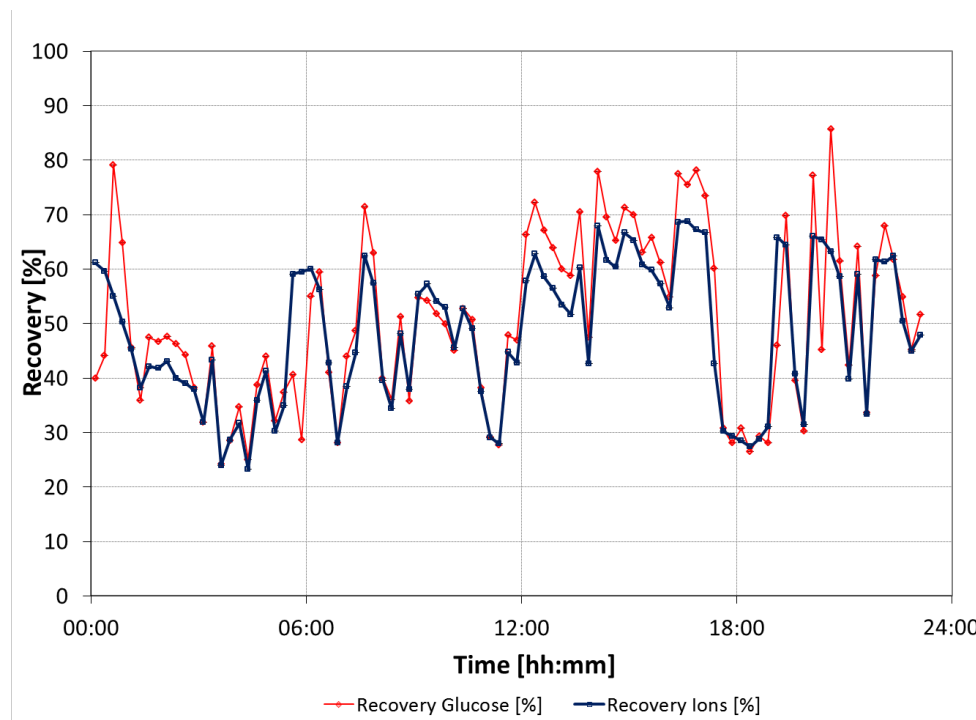


**Figure 26:** Individual glucose and ion recovery over time for subject 030 based on measurements of Super GL2 and TraceDec. Red triangles represent the glucose recovery whereas blue squares represent the ion recovery.

**Figure 26** shows the Individual glucose and ion recovery over time for subject 030. It can be observed that the recoveries show congruence over 24h and vary between 30% and 80%. Furthermore glucose and ion recoveries correlate what indicates that an application of the Ionic Reference Technique is feasible. For the remaining subjects such a correlation was rather found until time point 13:00 whereas afterwards glucose and ion recoveries showed an increasing divergence. This can also be seen in

Figure 27 where the Mean glucose- and ion recoveries over time of all subjects are shown.

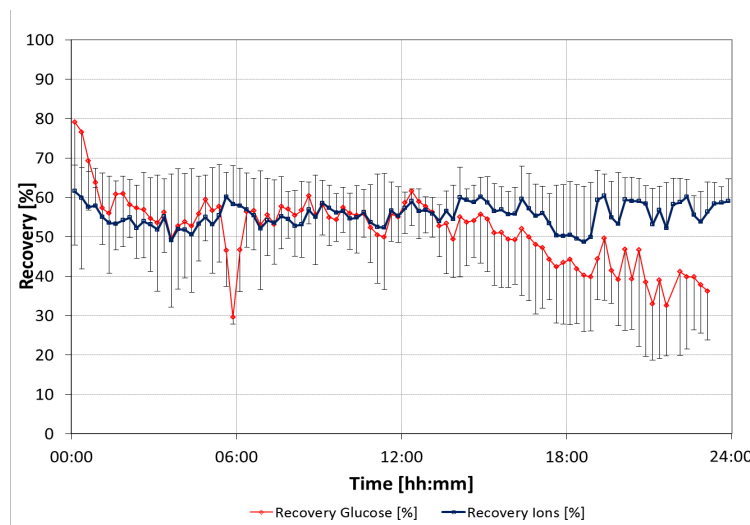


**Figure 27:** Mean glucose- and ion recovery over time for subject 028 – 032 based on measurements of Super GL2 and TraceDec. Red triangles represent the glucose recovery whereas blue squares represent the ion recovery. Standard deviations are expressed as red and blue bars.

Figure 27 shows the mean glucose- and ion recovery over time for subject 027 – 031. It can be observed that the mean recoveries show a good correlation only until hour 13:00. From hour 13:00 onwards the recovery for glucose and ions start to diverge for unknown reason. Huge spikes of the glucose recovery (e.g. hour 6:00) can be explained by the fact that the recovery was calculated by comparing spot measurements of the blood glucose with values of the time-integrated dialysate samples (collected for 15 minutes in a single PCR tube). These phases have to be considered extremely carefully for further analysis.

### 2.7.6 Filtering of Sensor Current

#### Primary Objective

The aim was to improve the data quality of the glucose sensor signals for further analysis.

## Setup and Methods

Since the impedance measurement was free of artefacts there was no need to filter the raw signal.

Due to the fact that glucose sensor currents became much noisier than in the in vitro investigations, when the glucose monitoring unit was connected to a human being, digital filtering is necessary to remove disturbing spikes from the signal. A causal (prospective), digital Butterworth filter of 3<sup>rd</sup> order was used as signal processing filter. A FFT-analysis led to the choice of a normalized cut-off frequency of 0.04, which was then applied onto the glucose data (**Figure 28**).

## Results

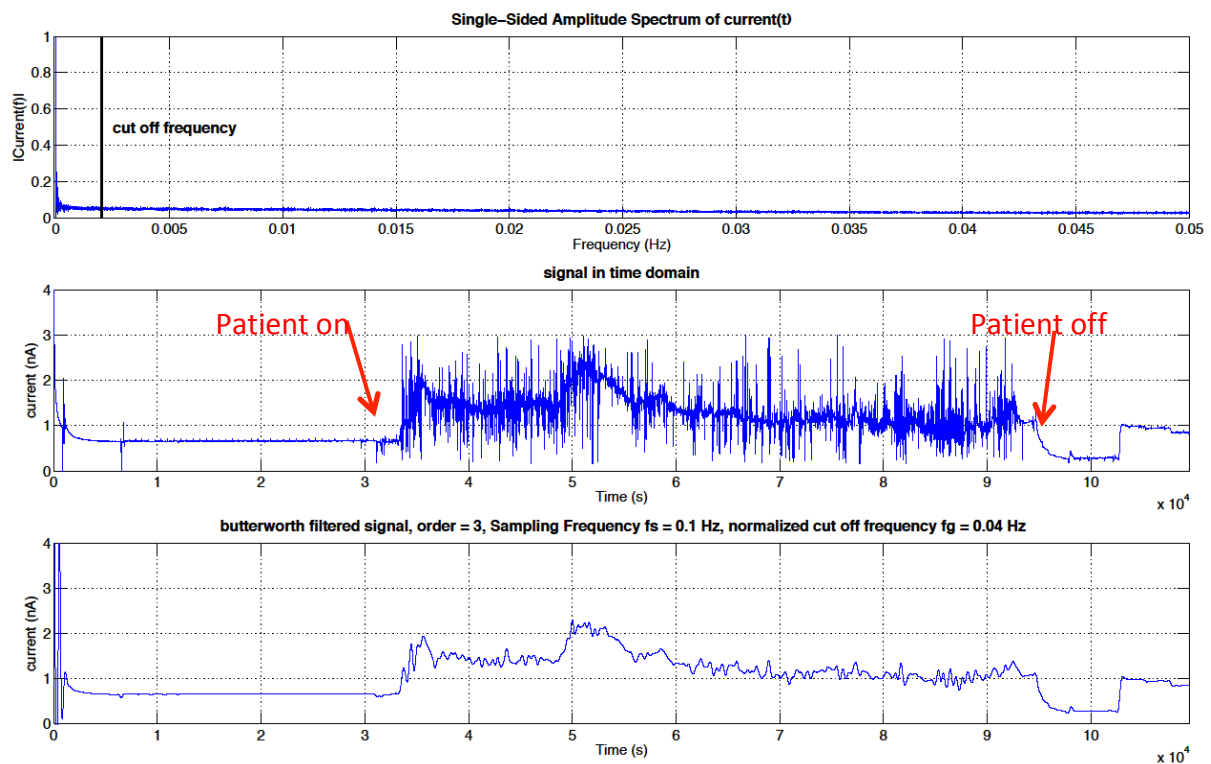


**Figure 28 top** shows the single sided amplitude spectrum of the current signal in the frequency domain and the used cut off frequency.

**Middle** shows the measured and unfiltered current in time domain.

**Bottom** shows the current in time domain after applying the Butterworth filter realized the Matlab "filtfilt" function (Zero-phase digital filtering).

**In Figure 28 (middle):** The glucose current showed a good signal to noise ratio (SNR) of 29.3 dB until time point 31000 s. After connecting the glucose monitoring unit to the volunteer the noise level was significantly increasing and thus the SNR was only 9.4 dB. Also after the removal of the system from the patient the system was working as expected again. To minimize the noise of the sensor current a Butterworth filter of 3<sup>rd</sup> order was applied. The used Matlab function “filtfilt” filters the sensor signal backwards and thus avoids an additional delay. The final result can be seen in the **bottom plot of Figure 28**. The current is less noisy and can be used for further processing.

### **2.7.7 Regression Analysis of Glucose Data**

#### **Primary Objective**

The aim was to find out whether the glucose measurement using the glucose sensor worked by taking into consideration the correlation coefficient as criterion.

#### **Setup and Methods**

A regression analysis was performed. Correlation coefficients were estimated between the glucose current, measured by the glucose sensor (new method) and the blood glucose measured by the Super GL2 (reference method).

## Results

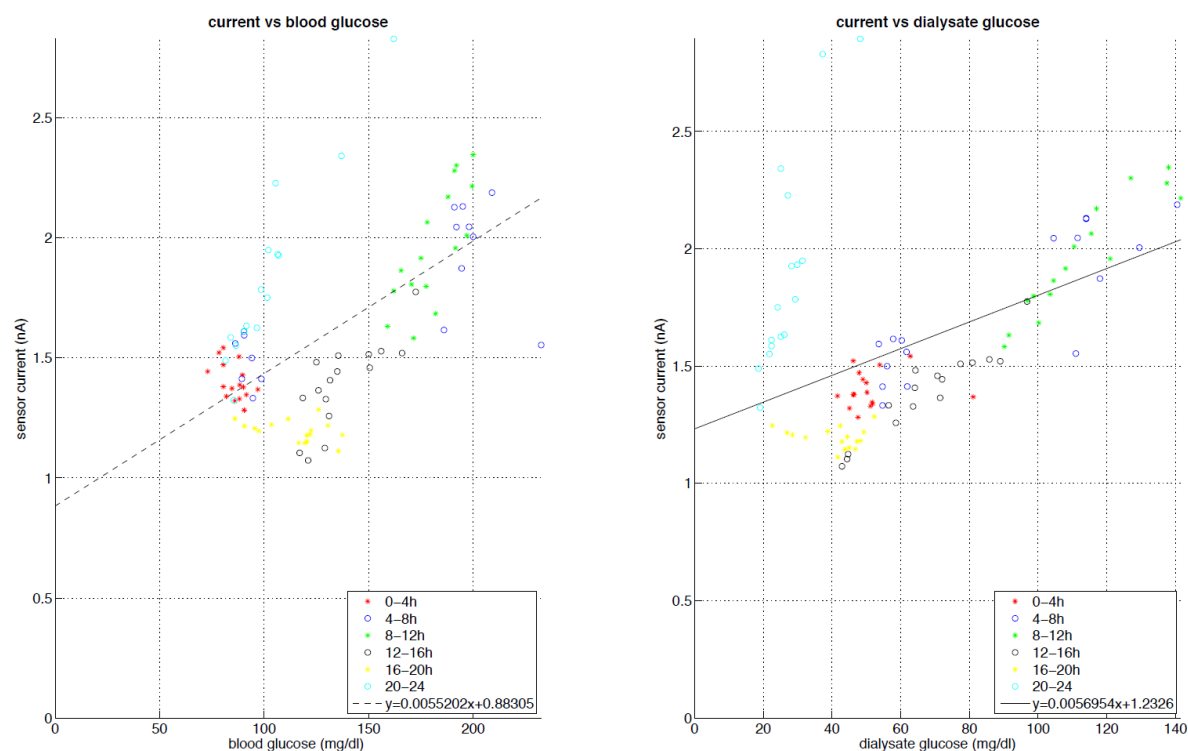


**Figure 29:** Regression analysis/ calibration curve of the glucose signal derived from Super GL2 vs. glucose sensor. **Left:** blood glucose vs. sensor current. **Right:** dialysate glucose vs. sensor current.

**Figure 29** shows the regression analysis/ calibration curve for glucose data determined during the in vivo investigations when subject 028 was connected to the glucose monitoring unit. For blood glucose the intercept was 0.88 nA and the correlation coefficient 0.6. For dialysate glucose the intercept was 1.23 nA and the correlation coefficient 0.49. Data were furthermore subdivided during the analysis into subgroups based on the time when they were recorded (red data points were recorded from hour 0:00 to 4:00, dark blue from 4:00 to 8:00; green from 8:00 to 12:00; black from 12:00 to 16:00; yellow from 16:00 to 20:00 and cyan from 20:00 to 24:00). For both graphs the slope changes for all subgroups over time. This analysis reveals that the sensor current can neither be calibrated to blood glucose values nor to dialysate glucose values using just one calibration factor. Changes in sensor dynamics make frequent recalibrations necessary.

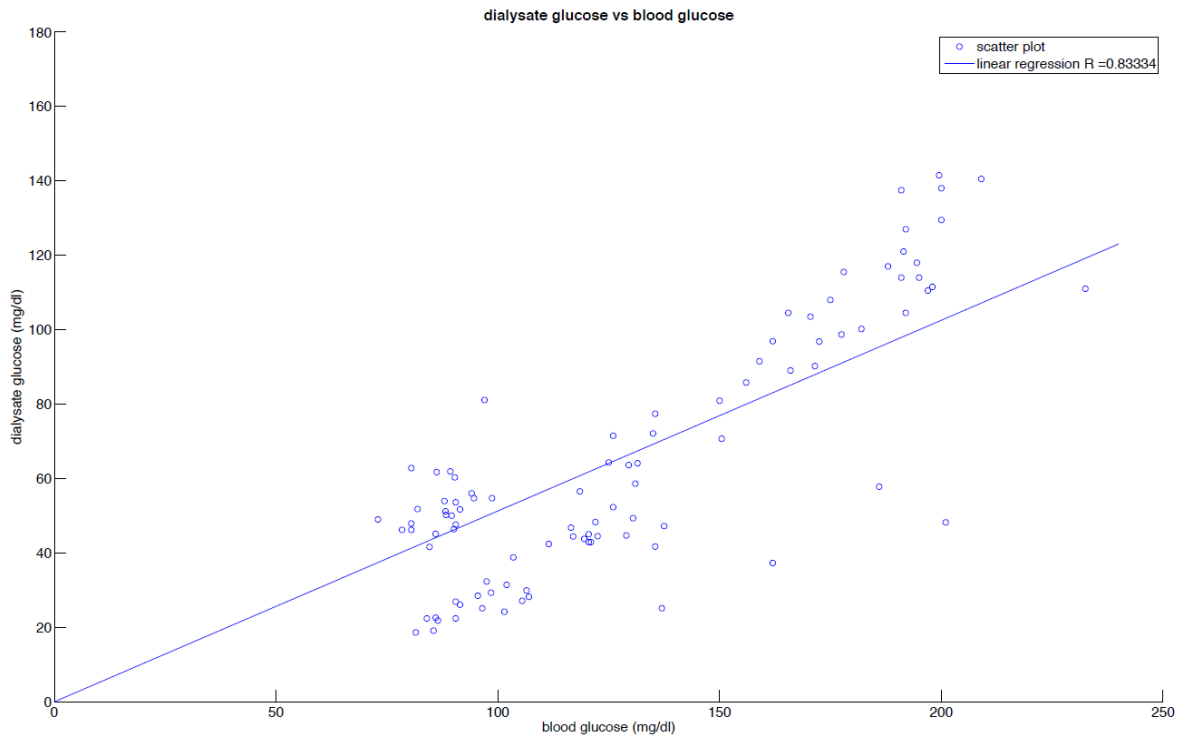


**Figure 30:** Shows the regression analysis of blood- and dialysate glucose referenced on the Super GL2, whereby the intercept was constricted to be zero.

**Figure 30** shows that the microdialysis was working as expected. A correlation coefficient of  $R = 0.83$  was found for the in vivo setup of subject 028. The correlation coefficient between sensor current and blood glucose (**Figure 29, left**) as well as sensor current and dialysate glucose (**Figure 29, right**) were comparatively poor. Regression analysis for the subjects 032 (**Figure 37, Figure 39**) and 031 (**Figure 38, Figure 40**) can be found in the **APPENDIX**. For a detailed overview of the results for subject 028, 031 and 032 refer to

**Table 1** which shows similar results:

	Subject number		
Correlation coefficient between	028	031	032
Blood glucose (Super GL2) vs. dialysate glucose (Super GL2)	0.83	0.86	0.79
Blood glucose (Super GL2) vs. sensor current of dialysate	0.60	0.27	0.54
Dialysate glucose (Super GL2) vs. sensor current of dialysate	0.49	0.50	0.74

*Table 1: Summary of the correlation coefficients.*

### 2.7.8 Analysis of Conductivity Data

#### Primary Objective

The aim was to find out if the in vivo conductivity measurement using sensor electrodes worked by taking into consideration the correlation coefficient as criterion.

#### Setup and Methods

Similar to the analysis of the glucose data a regression analysis was performed. Correlation coefficients were estimated between the conductivity, measured by the glucose sensor (new method) and the ion concentration measured by the TraceDec (reference method).

Impedance data, measured by the sensor, showed a very strong drift in comparison to the results obtained during the in vitro investigations. Hence drift compensation was performed according to the following procedure: Before and after the volunteers were connected to the glucose monitoring unit the sensor was exposed to a reference fluid of 100 mg/dl glucose and an ion concentration of 50% of physiological saline solution. The Impedance drift over time was then calculated as a ratio of  $\Delta Z/\Delta t$ . This linear correction factor (Ohm/s) for  $Z$ ,  $Z_{\text{real}}$  and  $Z_{\text{imag}}$  was then applied onto the data set, respectively. The regression analysis was then performed again using the drift corrected data set.

## Results

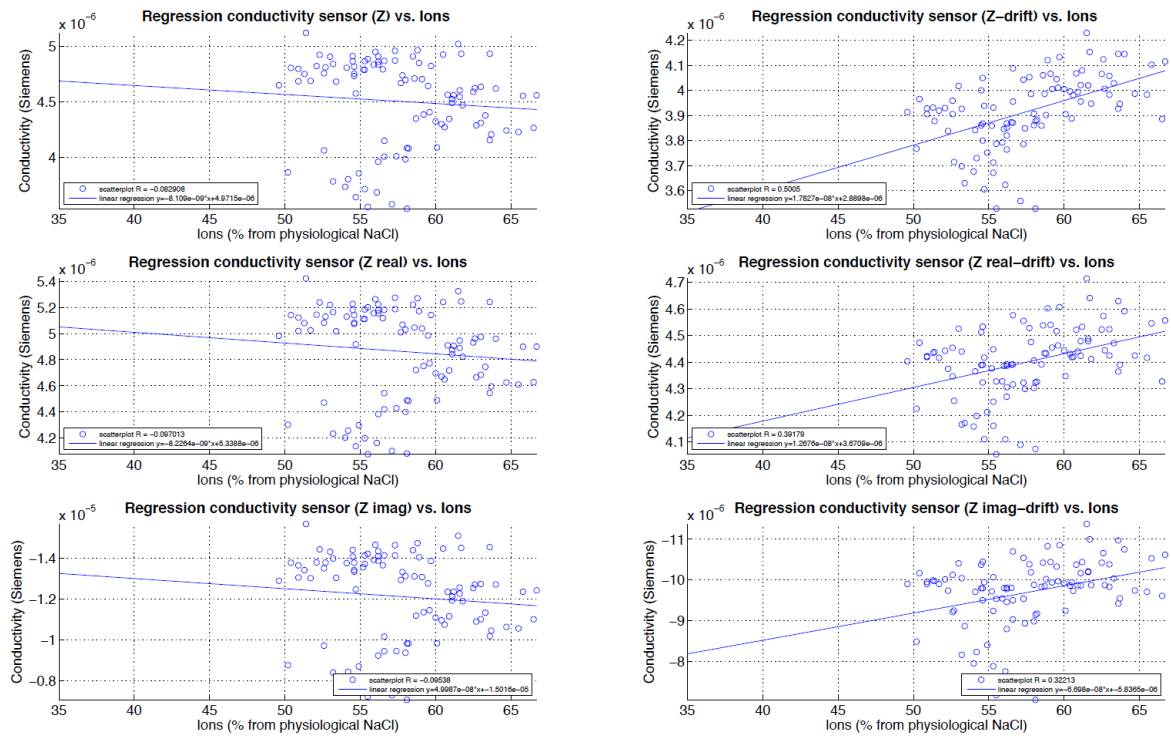


**Figure 31:** Regression analysis of the conductivity signal derived from TraceDec vs. conductivity measured by the glucose sensor (Z,  $Z_{real}$ ,  $Z_{imag}$ ) of subject 028. **Top row:** Regression analysis using conductivity based on Z. **Middle row:** Regression analysis using conductivity based on  $Z_{REAL}$ . **Bottom row:** Regression analysis using conductivity based on  $Z_{IMAG}$ . **Left column:** Regression analysis without drift compensation. **Right column:** Regression analysis with drift compensation.

Figure 31 shows the regression analysis/ calibration curve for conductivity data determined during the in vivo investigations when subject 028 was connected to the glucose monitoring unit. Negative correlations were found no matter what impedance parameter (Z,  $Z_{real}$ ,  $Z_{imag}$ ) was used for analysis. A negative correlation, no matter if drift compensated or not, was achieved for subjects 031 and 032 (refer to **APPENDIX, Figure 41 and** ). For subject 028 the drift compensation caused at least a positive correlation with  $R = 0.5005$ , what can still be rated as a very weak correlation.

### 3 DISCUSSION

The main outcome of Andreas Huber's diploma thesis in 2012 [18] was that the application of the Ionic Reference Technique (IRT) significantly improves glucose measurements based on dialysate samples withdrawn using the intra venous micro dialysis (ivMD). Changing membrane characteristics can be partly compensated by the IRT taking into consideration a glucose related signal of the dialysate (e.g. ion concentration). Therefore he performed a study using offline measurement of glucose and ions in the dialysate. One of his major findings was the high degree of correlation between glucose- and ion recoveries. This builds the basis to calculate suitable blood glucose level considering glucose- and ion concentrations of the dialysate during a glucose clamp. Hannah Greiner evaluated in subsequent investigations the performance of an online glucose sensor in the dialysate outflow of the ivMD. It was concluded that an accurate glucose sensor with a large measurement range would lead to good results [38]. Therefore the Dexcom STS 7 sensor was chosen as its glucose measurement range covers concentrations from 40 to 400 mg/dl.

Combining the results of Andreas Huber and Hannah Greiner stimulated the further development of an online glucose monitoring unit based on ivMD. The only missing item towards an online glucose monitoring unit was to quantify the glucose- and ion concentration of the dialysate continuously. The ion concentration is strongly related to the electrical conductivity of the dialysate [4]. Thus the measurement of the electrical conductivity enables the determination of the requested ion concentrations. When implementing such an online glucose monitoring unit a glucose sensor is needed anyway. Thus impedance measurement across the electrodes of the sensor is an elegant approach to determine the ion concentration of the dialysate. If successful, this could be a solution for permanent measurement of the ion concentration in the dialysate without causing additional costs. Hence the primary objective of this thesis was to proof whether a conductivity measurement using the glucose sensor's electrodes is feasible. Results of these investigations are discussed below:

A cyclic voltammetry revealed that the sensor can be operated at 400 mV (refer to **Figure 7**). The manufacturer in contrast recommends a potential of 600 mV which leads to a certain safety margin. At a potential of 600 mV, fluctuations in the polarization potential do not evoke capacitive currents which occur at lower polarization voltages. Applying a higher potential than necessary requires a well-designed membrane around the working electrode, which is realized in the Dexcom sensor. This membrane is strongly selective for glucose and oxygen and thus avoids the interactions with other electroactive species.

As every enzyme based glucose sensor also the Dexcom STS 7 shows a temperature dependency. A strong temperature coefficient between 28 and 42° C of 5.8 pA/°C was found (refer to **Figure 8**). Due to the lack of a temperature sensor on the tip of the glucose sensor we were unable to implement compensation. During in vitro investigations temperature was logged and had no noteworthy fluctuations, what made compensation unnecessary.

We did not succeed in implementing the first choice “simultaneous measurement approach”. Using the prior determined optimal parameter set of 1 kHz and 5 mV showed non reproducible results (refer to **Figure 11** and **Figure 12**). In some cases the glucose signal was adversely affected by the simultaneous conductivity measurements. An explanation might be the inter sensor variation due to the insufficiently reproducible production of such glucose sensors. It can be speculated that the “simultaneous measurement approach” would possibly work if a three electrode glucose sensor with a better regulated polarization potential was used.

Therefore a second “intermittent measurement approach” was investigated showing promising results. The time intervals for glucose- and conductivity measurement were chosen to be 10 and 5 min, respectively. This timing fits also with the 15 minutes blood sampling intervals of the clamp studies. The optimal parameter set was estimated in a similar way as for the “simultaneous measurement approach” (refer to **Figure 13** and **Figure 14**). The focus was put on the signal to noise ratio (SNR) of the conductivity and not on the SNR of glucose current during the phases of conductivity measurement.

Applying this parameter set to the sensor while being exposed to different glucose- and ion concentrations enabled full characterization of the sensor (refer to **Figure 15** and **Figure 16**). The investigation showed that lower ion concentrations cause higher sensor currents.

Saturation effects were observed above ion concentrations of 25% of physiologic saline solution. Partially this can be explained by migration of ions to the working and counter electrode, respectively. This causes a current flow against the current produced by the glucose. The more ions are found in the solution the higher the counter flow is. Therefore it was concluded, that a minimum ion concentration of 25 % is necessary to perform reliable glucose measurements. This can be easily realized using lower flow rates causing higher recoveries.

During the same experiment the relationship between conductivity and different ion concentrations was investigated. The recorded impedance was fitted with a polynomial function of 3<sup>rd</sup> order which is very similar to a reciprocal function. As the conductance is the reciprocal value of the impedance, linearization is reasonable. Linearization was performed on the data set and compared with the 3<sup>rd</sup> order polynomial function. This comparison resulted in a maximum differential error of about 5% of physiologic saline solution, considering the interesting range from 20 % to 90 % of physiologic saline solution. Therefore linearization is feasible and does not cause unacceptable errors. The obvious advantage of such a linearization is the possibility to enable a one point calibration, whereas polynomial functions need multiple point calibration. The later approach would lead to increased costs as well as increased personnel expenditure when operating such a glucose monitoring unit or clamp device, respectively.

As the Dexcom sensor was originally designed to be operated in the subcutaneous adipose tissue for our investigations a flow through cell (refer to **Figure 3**) was necessary to enable the measurement of dialysate derived from the ivMD. Therefore a flow through cell was designed. The flow direction was chosen from the sensor's inlet to its tip. During in vitro and in vivo experiments no air bubbles on the sensor's active area were observed. Nevertheless the manufacturing process of the flow through cell is not standardized. This fact should be considered during future development steps.

The whole system was tested under in vivo conditions (refer to **Figure 17**). To obtain high recoveries the flow of 3.3  $\mu\text{l}/\text{min}$  was chosen. The system was operated around two days (>45h) showing no significant drift or noise. While the sensor was exposed to different glucose- and ion concentrations both signals, glucose current and conductivity, showed

clear, constant and expected levels (refer to **Figure 18**). As concentrations of dialysate as well as test matrix were known, it was possible to apply the IRT onto the data obtained during this experiment. When the IRT was applied the MARD was 10.6% whereas the MARD of the 1pt calibrated dialysate was only 18.4% (refer to **Figure 21**). With this encouraging result it was decided to test the system in vivo.

This final system was then evaluated concerning risks. All relevant hazards could be eliminated or even decreased to an acceptable risk level. By using an isolating transformer the system passed successfully the electrical safety check for type BF.

During the in vivo experiment the flow was proven to be almost constant, building the basis for a well working ivMD (refer to **Figure 25**).

However, good correlation between the mean glucose- and ion recoveries could only be observed until time point 13:00. Afterwards the recoveries differed for unknown reasons (refer to

**Figure 27**). This result stays in contrast with the results found by Andreas Huber [18] where a good correlation was observed throughout the whole 24 hours.

The glucose current signal obtained during the clinical study was very noisy when the patient was connected to the glucose monitoring unit. In contrast, sensor currents recorded during in vitro investigations were almost noiseless. But the signal quality could be significantly improved applying a Butterworth filter of 3<sup>rd</sup> order with a relative cut off frequency of 0.04 together with the Matlab function `filtfilt` (refer to **Figure 28**).

Data obtained in the clinical study showed a weak correlation between the current of the glucose sensor and the blood glucose values referenced with the Super GL 2 (refer to **Figure 29**). An explanation might be the changing dynamic and sensitivity of the glucose sensor caused by the noise in the glucose signal.

Even the conductivity data obtained during the clinical study did not show the desired correlation allowing the estimation of any dialysate ion concentration (refer to **Figure 31**). Additionally in contrast to the signals observed during in vitro investigations, a strong drift

was identified. After linear drift compensation had been applied to the data, the correlation improved, but remained negative in most cases.

Furthermore the following fact should be kept in mind when looking at the in vivo data: Dialysate was collected in probe containers for 15 minutes representing time-integrated glucose and conductivity concentrations. These values were then compared to 10 and 5 minutes averaged measurements for glucose and conductivity, respectively. Thus changes during the sampling process are not always fully reflected by the sensor signal which results in a decreased correlation coefficient.

After the clinical study the sensor was disconnected from the volunteer and exposed to known test matrices. An interesting fact is that the glucose- as well as the conductivity measurement worked then again in the expected manner.

## 4 CONCLUSION AND OUTLOOK

In this thesis a new system was tested which renders possible the measurement of glucose and electrical conductivity over the same sensor electrodes to build the basis for a glucose monitoring unit or clamp device. This method can be used to implement the Ionic Reference Technique with existing glucose sensors which could facilitate robust and reliable glucose monitoring for a glucose clamp device.

The first choice approach to measure glucose and conductivity in parallel failed and led to irreproducible results.

The second approach was successfully tested and allows to measure glucose and conductivity subsequently for 10 and 5 minutes each. Investigations showed that a good correlation between conductivity and ion concentrations was found in vitro. The almost linear relationship builds the basis to apply the Ionic Reference Technique. This enables the compensation of changing membrane characteristics of the ivMD and thus allows quantification of blood glucose by applying a 1pt calibration.

This system was afterwards tested in a clinical study in 5 volunteers over 24 hours.

Throughout this study ivMD was operated at a flow rate of 3.3  $\mu\text{l}/\text{min}$  established by clinical piston pumps. As known from previous experiments such low flow rates cause high recoveries of about 60 to 80 %. With these recoveries the Dexcom sensor with a measurement range from 40 to 400 mg/dl can be used without adaptations to allow the quantification of blood glucose in human in a range from 60 to 300 mg/dl. Therefore the glucose sensor was used without modifications and only a suitable flow through cell had to be designed and tested. Results showed that this flow through cell remains free of air bubbles, thus the recorded signals were not influenced.

Unfortunately, after attaching the system to the volunteer immediately unacceptable levels of noise occurred. Thus sensor data had to be filtered in any case. Additionally the In vivo conductivity measurements showed a huge drift. This fact makes the linearization approach

inapplicable. Due to negative results no further investigations towards the in vivo implementation of the IRT were performed.

Compared to Andreas Huber's data we did find a correlation between glucose- and ion recoveries only until time point 13:00 (except for subject 030) during the clinical study. The only difference between Andreas Huber's and our work was the lower flow rate. An explanation might be that bodily components partly block the membrane leading to the result that ions could still better pass over the membrane than glucose molecules. Further investigations have to be performed to discover the reasons for this finding.

The following improvements should be taken into consideration for further development of this particular glucose monitoring unit:

- Investigations should be performed with a three electrode glucose sensor which probably enables a parallel measurement of glucose and ions.
- A reliable and accurate model of the sensor cell has to be designed to estimate the bulk resistance.
- An alternative potentiostat for clinical use should be found and tested under in vivo like conditions achieving less drift and better SNR.
- The conductivity signal can be used to detect air bubbles

## 5 ACKNOWLEDGMENTS

This thesis would not have been possible in the same way without the support of many people whom I want to express my thanks:

*Dipl.-Ing. Dr.techn. Lukas Schaupp*, for the supervision of my work, his optimism and motivation and his unique way,

*Dipl.-Ing. Dr.techn. Roland Schaller-Ammann* for being a good friend, his invaluable experience in microfluidics and in performing *in vivo* studies,

*Dipl.-Ing. Dr. Martin Hajsek* for providing the Gamry potentiostat,

*Dipl.-Ing. Andreas Huber* for doing an extraordinarily good work which laid the fundament for this diploma thesis and

*Ao.Univ.-Prof. Dipl.-Ing. Dr.techn. Hermann Scharfetter* for evaluating my thesis and for his open ear.

Furthermore, I would like to thank all of the following people that made an incident-free, high-quality clinical trial possible and who provided me with advice and support whenever needed:

*Andrea Berghofer, Barbara Binder, Martina Brunner, Sigrid Deller, Werner Doll, Martin Gaksch, Janka Gerdova, Madlen Hernach, Harald Kojzar, Stefan Korsatko, Thomas Pieber, Joachim Friedl, Sarah Raudner, Werner Regittnig, Mathias Tschaikner, and all student assistants* who contributed to the study.

Moreover, I would like to thank all 5 *volunteers* for participating.

And last but not least, I would like to thank my family, especially my parents *Cristina*, my father *Franz* and my brother *Martin*.

## 6 REFERENCES

- [1] WHO, "Definition and Diagnosis of Diabetes Mellitus and intermediate Hyperglycaemia," 2006.
- [2] H. Yang, Q. Wang, and W. F. Elmquist, "The design and validation of a novel intravenous microdialysis probe: application to fluconazole pharmacokinetics in the freely-moving rat model.," *Pharmaceutical Research*, vol. 14, no. 10, pp. 1455-60, Oct. 1997.
- [3] <http://www.who.int/mediacentre/factsheets/fs312/en/>, "Media centre Diabetes Fact sheet NR 312," *Fact sheet NR 312*, 2012. [Online]. Available: <http://www.who.int/mediacentre/factsheets/fs312/en/>. [Accessed: 03-Feb-2013].
- [4] H. Kontschieder, "Glukose-Messung," University of Technology, Graz, 1992.
- [5] F. G. Banting, C. H. Best, J. B. Collip, W. R. Campbell, and a Fletcher, "Pancreatic extracts in the treatment of diabetes mellitus: preliminary report. 1922.," *CMAJ : Canadian Medical Association Journal = journal de l'Association medicale canadienne*, vol. 145, no. 10, pp. 1281-6, Nov. 1991.
- [6] C. . Zalpour, *Anatomie Physiologie*, 1<sup>st</sup> ed. Urban&Fischer, 2002.
- [7] A. Heller and B. Feldman, "Electrochemistry in diabetes management.," *Accounts of Chemical Research*, vol. 43, no. 7, pp. 963-73, Jul. 2010.
- [8] The European Agency for the Evaluation of Medicinal Products, "Note for guidance on clinical investigation of medicinal products in the treatment for diabetes.," 2002.
- [9] M. Hompesch and K. Rave, "An analysis of how to measure glucose during glucose clamps: are glucose meters ready for research?," *Journal of Diabetes Science and Technology*, vol. 2, no. 5, pp. 896-8, Sep. 2008.
- [10] L. Von Wartburg, "What's a glucose clamp, Anyway?" [Online]. Available: <http://www.diabeteshealth.com/read/2007/11/06/5500/whats-a-glucose-clamp->. [Accessed: 24-Jan-2013].
- [11] R. A. DeFronzo, J. D. Tobin, and R. Andres, "Glucose clamp technique: a method for quantifying insulin secretion and resistance.," *The American Journal of Physiology*, vol. 237, no. 3, pp. E214-23, Sep. 1979.
- [12] D. B. Keenan, J. J. Mastrototaro, G. Voskanyan, and G. M. Steil, "Delays in minimally invasive continuous glucose monitoring devices: a review of current technology.," *Journal of Diabetes Science and Technology*, vol. 3, no. 5, pp. 1207-14, Sep. 2009.

- [13] E. Kulcu, J. A. Tamada, G. Reach, R. O. Potts, and M. J. Lesho, "Physiological differences between interstitial glucose and blood glucose measured in human subjects.," *Diabetes Care*, vol. 26, no. 8, pp. 2405-9, Aug. 2003.
- [14] J. N. Roe and B. R. Smoller, "Bloodless glucose measurements.," *Critical Reviews in Therapeutic Drug Carrier Systems*, vol. 15, no. 3, pp. 199-241, Jan. 1998.
- [15] U. Ungerstedt, "Microdialysis--principles and applications for studies in animals and man.," *Journal of Internal Medicine*, vol. 230, no. 4, pp. 365-73, Oct. 1991.
- [16] L. Schaupp and T. Pieber, "Verfahren zur Messung von Konzentrationen in lebenden Organismen mittels Mikrodialyse und Vorrichtung zur Durchführung dieses Verfahrens," U.S. Patent AT 412 0602004.
- [17] L. Schaupp and T. Pieber, "Method for measuring the concentration of substances in living organisms using microdialysis and a device for carrying out said method," U.S. Patent 7,022,0712006.
- [18] A. Huber, "Continuous Blood Glucose Monitoring in Humans combining Intravenous Microdialysis and Ionic Reference Technique," Technical University Graz, 2012.
- [19] G. McGarraugh, "The chemistry of commercial continuous glucose monitors.," *Diabetes Technology & Therapeutics*, vol. 11 Suppl 1, no. 1, pp. S17-24, Jun. 2009.
- [20] K. Cammann, *Instrumentelle Analytische Chemie: Verfahren, Anwendungen und Qualitaetssicherung*. Spektrum, Akad. Verlag, 2000.
- [21] E. Hering and G. Schönfelder, *Sensoren in Wissenschaft und Technik*. Wiesbaden: Vieweg + Teubner Verlag, 2012.
- [22] P. Gründler, *Chemische Sensoren Eine Einführung für Naturwissenschaftler und Ingenieure*. Berlin: Springer, 2004.
- [23] J. Janata, *Principles of Chemical Sensors*. Springer, 2010.
- [24] J. Raba and H. a. Mottola, "Glucose Oxidase as an Analytical Reagent," *Critical Reviews in Analytical Chemistry*, vol. 25, no. 1, pp. 1-42, Sep. 1995.
- [25] Z. Chen and R. W. Steger, "Plasma microdialysis. A technique for continuous plasma sampling in freely moving rats.," *Journal of Pharmacological and Toxicological Methods*, vol. 29, no. 2, pp. 111-8, Apr. 1993.
- [26] R. K. Verbeeck, "Blood microdialysis in pharmacokinetic and drug metabolism studies.," *Advanced Drug Delivery Reviews*, vol. 45, no. 2-3, pp. 217-28, Dec. 2000.
- [27] H. Yang, Q. Wang, and W. F. Elmquist, "The design and validation of a novel intravenous microdialysis probe: application to fluconazole pharmacokinetics in the

- freely-moving rat model.," *Pharmaceutical Research*, vol. 14, no. 10, pp. 1455-60, Oct. 1997.
- [28] "www.istech.at," *TraceDec® Contactless Conductivity Detector*. .
- [29] "PHE200 Physical Electrochemistry Software - Application Note," 2000.
- [30] "Electrochemical Impedance Spectroscopy Software - Application Note."
- [31] "Gamry 's Sequence Wizard – An easy way to create complex test sequences - Application Note."
- [32] "Matlab." Mathworks, 2009.
- [33] Köhler, Schachtel, and Voleske, *Biostatistik*, 2<sup>nd</sup> ed. Springer, 1995.
- [34] I. M. E. Wentholt, A. A. M. Hart, J. B. L. Hoekstra, and J. H. Devries, "How to assess and compare the accuracy of continuous glucose monitors?," *Diabetes Technology & Therapeutics*, vol. 10, no. 2, pp. 57-68, Apr. 2008.
- [35] A. V Oppenheim, *Digital Signal Processing*. .
- [36] C. Brown, *Coefficient of Variation*. Springer, 1998, pp. 155-157.
- [37] P. T. Kissinger and W. R. Heineman, "Cyclic Voltammetry," *Journal of Chemical Education*, vol. 60, no. 9, p. 702, 1983.
- [38] H. Greiner, "Development of a continuous glucose monitoring system for humans combining intravenous microdialysis, glucose sensors and ionic reference technique," 2013.
- [39] *ISO 14971 Second Edition; Medical Devices - Application of risk management to medical devices*. International Organization for Standardisation, 2007.
- [40] *ÖVE/ÖNORM EN61025:2006; Fehlzustandsbaumanalyse*. Österreichischer Verband für Elektrotechnik, 2007.
- [41] *ÖVE/ÖNORM EN3100:2009; Risikomanagement - Verfahren zur Risikobeurteilung*. Österreichischer Verband für Elektrotechnik, 2010.
- [42] *IEC 60601-1*. Genève, Switzerland: International Electrotechnical Commission, 2002.
- [43] N. Leitgeb, *Sicherheit von Medizingeräten*. Wien: Springer, 2010.
- [44] "ICH Topic E6(R1) Guideline for Good Clinical Practice," 1996. [Online]. Available: [http://www.ich.org/fileadmin/Public\\_Web\\_Site/ICH\\_Products/Guidelines/Efficacy/E6\\_R1/Step4/E6\\_R1\\_\\_Guideline.pdf](http://www.ich.org/fileadmin/Public_Web_Site/ICH_Products/Guidelines/Efficacy/E6_R1/Step4/E6_R1__Guideline.pdf). [Accessed: 25-May-2013].

- [45] "World Medical Association - Declaration of Helsinki," Sep-2001. [Online]. Available: <http://www.wma.net/en/30publications/10policies/b3/17c.pdf>. [Accessed: 25-May-2013].
- [46] D. Dubois and E. F. Dubois, "A formula to estimate the approximate surface area if height and weight be known;," *Archives of Internal Medicine*, no. 17, pp. 863-871, 1916.

## 7 APPENDIX

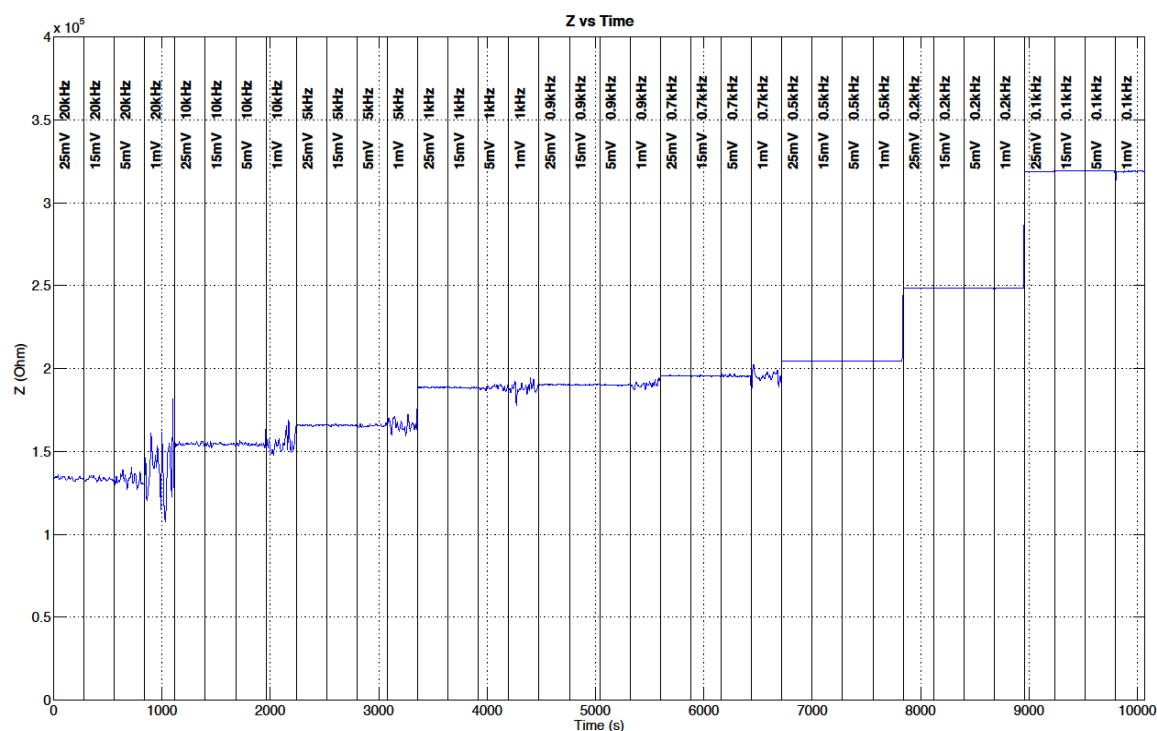
Step NR	Duration in s	Frequency in kHz	AC amplitude in mV	DC amplitude in mV	Mode
1	7200	0	0	600	Chronoamperometry
2	1200	1	25	600	EIS
3	1200	0	0	600	Chronoamperometry
4	1200	1	20	600	EIS
5	1200	0	0	600	Chronoamperometry
6	1200	1	10	600	EIS
7	1200	0	0	600	Chronoamperometry
8	1200	1	5	600	EIS
9	1200	0	0	600	Chronoamperometry
10	1200	1	1	600	EIS
11	1200	0	0	600	Chronoamperometry
12	1200	2	25	600	EIS
13	1200	0	0	600	Chronoamperometry
14	1200	2	20	600	EIS
15	1200	0	0	600	Chronoamperometry
16	1200	2	10	600	EIS
17	1200	0	0	600	Chronoamperometry
18	1200	2	5	600	EIS
19	1200	0	0	600	Chronoamperometry
20	1200	2	1	600	EIS
21	1200	0	0	600	Chronoamperometry
22	1200	5	25	600	EIS
23	1200	0	0	600	Chronoamperometry
24	1200	5	20	600	EIS
25	1200	0	0	600	Chronoamperometry
26	1200	5	10	600	EIS
27	1200	0	0	600	Chronoamperometry
28	1200	5	5	600	EIS
29	1200	0	0	600	Chronoamperometry
30	1200	5	1	600	EIS
31	1200	0	0	600	Chronoamperometry
32	1200	10	25	600	EIS
33	1200	0	0	600	Chronoamperometry
34	1200	10	20	600	EIS
35	1200	0	0	600	Chronoamperometry
36	1200	10	10	600	EIS
37	1200	0	0	600	Chronoamperometry
38	1200	10	5	600	EIS
39	1200	0	0	600	Chronoamperometry
40	1200	10	1	600	EIS
41	7200	0	0	600	Chronoamperometry

Table 2: Measurement protocol for the determination of the optimal parameters using simultaneous measurement mode

Step NR	Duration in s	Frequency in Hz	AC amplitude in mV	DC amplitude in mV	Mode
1	7200	0	0	600	Chronoamperometry
2	600	0	0	600	Chronoamperometry
3	300	20000	25	600	EIS
4	600	0	0	600	Chronoamperometry
5	300	20000	15	600	EIS
6	600	0	0	600	Chronoamperometry
7	300	20000	5	600	EIS
8	600	0	0	600	Chronoamperometry
9	300	20000	1	600	EIS
10	600	0	0	600	Chronoamperometry
11	300	10000	25	600	EIS
12	600	0	0	600	Chronoamperometry
13	300	10000	15	600	EIS
14	600	0	0	600	Chronoamperometry
15	300	10000	5	600	EIS
16	600	0	0	600	Chronoamperometry
17	300	10000	1	600	EIS
18	600	0	0	600	Chronoamperometry
19	300	5000	25	600	EIS
20	600	0	0	600	Chronoamperometry
21	300	5000	15	600	EIS
22	600	0	0	600	Chronoamperometry
23	300	5000	5	600	EIS
24	600	0	0	600	Chronoamperometry
25	300	5000	1	600	EIS
26	600	0	0	600	Chronoamperometry
27	300	1000	25	600	EIS
28	600	0	0	600	Chronoamperometry
29	300	1000	15	600	EIS
30	600	0	0	600	Chronoamperometry
31	300	1000	5	600	EIS
32	600	0	0	600	Chronoamperometry
33	300	1000	1	600	EIS
34	600	0	0	600	Chronoamperometry
35	300	900	25	600	EIS
36	600	0	0	600	Chronoamperometry
37	300	900	15	600	EIS
38	600	0	0	600	Chronoamperometry
39	300	900	5	600	EIS
40	600	0	0	600	Chronoamperometry
41	300	900	1	600	EIS
42	600	0	0	600	Chronoamperometry
43	300	700	25	600	EIS
44	600	0	0	600	Chronoamperometry
45	300	700	15	600	EIS
46	600	0	0	600	Chronoamperometry
47	300	700	5	600	EIS
48	600	0	0	600	Chronoamperometry
49	300	700	1	600	EIS
50	600	0	0	600	Chronoamperometry
51	300	500	25	600	EIS

52	600	0	0	600	Chronoamperometry
53	300	500	15	600	EIS
54	600	0	0	600	Chronoamperometry
55	300	500	5	600	EIS
56	600	0	0	600	Chronoamperometry
57	300	500	1	600	EIS
58	600	0	0	600	Chronoamperometry
59	300	200	25	600	EIS
60	600	0	0	600	Chronoamperometry
61	300	200	15	600	EIS
62	600	0	0	600	Chronoamperometry
63	300	200	5	600	EIS
64	600	0	0	600	Chronoamperometry
65	300	200	1	600	EIS
66	600	0	0	600	Chronoamperometry
67	300	100	25	600	EIS
68	600	0	0	600	Chronoamperometry
69	300	100	15	600	EIS
70	600	0	0	600	Chronoamperometry
71	300	100	5	600	EIS
72	600	0	0	600	Chronoamperometry
73	300	100	1	600	EIS
74	600	0	0	600	Chronoamperometry

**Table 3:** Measurement protocol for the determination of the optimal parameters using intermittent measurement mode.



**Figure 32:** Impedance vs. time to estimate the best parameter setup in intermittent measurement mode.

<b>SYSTEM 1 (yellow) for diabetic volunteers</b>					
<b>Device/Solution</b>	<b>Manufacturer</b>	<b>Ref. Nr.</b>	<b>Lot Nr.</b>	<b>Exp. Date</b>	<b>Comment</b>
<b>Space Tower</b>	BBRAUN	8713145	18566	n.a.	n.a.
<b>Infusomat Space</b>	BBRAUN	8713050	83073	n.a.	For glucose infusion
<b>Perfusor Space</b>	BBRAUN	8713030	96033	n.a.	For insulin infusion
<b>Perfusor fm</b>	BBRAUN	8713820	57917	n.a.	N49309
<b>Valve Operated Y-Connector</b>	IMPROMEDIFO RM GmbH	MF1532	MU001	2017-03	n.a.
<b>Extension Set E87-P</b>	CODAN	71.4310	F76635-1	2014-02	150cm, d=0.9/2.0mm, vol=1.15ml
<b>Glucose Sensor</b>	Dexcom	STS 7	5020794	2012-03-21	n.a.
<b>Syringe – Perfusate Container</b>	Plastipak	BD/ 300629	1103284	2016-02	n.a.
<b>Body Interface</b>	CMA	CMA/ 648010521	T22526	2013-11	n.a.
<b>ULF-Infusion Stand</b>	Böhm Medical	INFUSIO U-51806	n.a.	n.a.	n.a.
<b>ULF-Sterile Material Basket</b>	Böhm Medical	U-51463	n.a.	n.a.	30 x 20 x 10cm
<b>ULF-Stainless Steel Bowl</b>	Böhm Medical	U-51403	n.a.	n.a.	n.a.
<b>ULF-Handhold</b>	Böhm Medical	Vario U-51000	n.a.	n.a.	n.a.

**Table 4:** List of devices of system 1 (yellow) for use in diabetic volunteers

<b>SYSTEM 2 (green) for volunteers</b>					
<b>Device/Solution</b>	<b>Manufacturer</b>	<b>Ref. Nr.</b>	<b>Lot Nr.</b>	<b>Exp. Date</b>	<b>Comment</b>
<b>Space Tower</b>	BBRAUN	8713145	17558	n.a.	n.a.
<b>Infusion Space</b>	BBRAUN	8713050	90914	n.a.	For glucose infusion
<b>Perfusor Space</b>	BBRAUN	8713030	92207	n.a.	For insulin infusion
<b>Perfusor fm</b>	BBRAUN	8713820	43178	n.a.	N45089
<b>Valve Operated Y-Connector</b>	IMPROMEDIFO RM GmbH	MF1532	MU001	2017-03	n.a.
<b>Extension Set E87-P</b>	CODAN	71.4310	F76635-1	2014-02	150cm, d=0.9/2.0m m, vol=1.15ml
<b>Glucose Sensor</b>	Dexcom	STS 7	5020794	2012-03-21	n.a.
<b>Syringe – Perfusate container</b>	Plastipak	BD/300629	1103284	2016-02	n.a.
<b>Body interface</b>	CMA	CMA/ 648010521	T22526	2013-11	n.a.
<b>ULF-Infusion Stand</b>	Böhm Medical	INFUSIO U- 51806	n.a.	n.a.	n.a.
<b>ULF-Sterile Material Basket</b>	Böhm Medical	U-51463	n.a.	n.a.	30 x 20 x 10cm
<b>ULF-Stainless Steel Bowl</b>	Böhm Medical	U-51403	n.a.	n.a.	n.a.
<b>ULF-Handhold</b>	Böhm Medical	Vario U-51000	n.a.	n.a.	n.a.

*Table 5: List of devices of system 2 (green) for use in diabetic volunteers*

<b>MEASUREMENT SYSTEM for diabetic volunteers</b>					
<b>Device/Solution</b>	<b>Manufacturer</b>	<b>Ref. Nr.</b>	<b>Lot Nr.</b>	<b>Exp. Date</b>	<b>Comment</b>
<b>Isolating Transformer 1</b>	DeMeTec	IPS-1400R3-8K	54116320	n.a.	G-0054
<b>Uninterruptible Power Supply</b>	APC	Back Ups RS 1500	BB0549042187	n.a.	G-0026
<b>Monitor</b>	Samsung - SyncMaster570S TFT	RN15LSMPS /EDC	n.a	n.a.	
<b>Keyboard</b>	Keysonic – Rubber Keyboard	EA2888-62976468	n.a.	n.a.	Water proof
<b>Mouse</b>	Fujitsu Siemens	LNA14706626			
<b>PC</b>	Fujitsu Siemens	YBES087530			JR.-Nr.: 36722
<b>Potentiostat 1</b>	Gamry	5103949021			
<b>Potentiostat 2</b>	Gamry	5106049041			
<b>Data Cable for Gamry</b>	Gamry	985-00038E1			Nr. 1
<b>Data Cable for Gamry</b>	Gamry	985-00038E1			Nr. 4
<b>Medical Cart</b>	Haeberle	Swingo			
<b>Safety Tester BENDER</b>	BENTRON	Unimet 1100ST	0401001206	n.a.	G-0035

**Table 6:** List of devices of measurement system for use in diabetic volunteers



Bender GmbH&Co.KG  
Prüfprotokoll

**Gerätedaten**

Geräte-ID	130314-eu-clamp-1	Leitungslänge [m]	-
Typ/Modell	60601/I /BF/4	Nennleistung [kW]	-
Hersteller	-	Prüfablauf	Automatisch
Werk.Nr.	-	Anwendungsteil	Typ BF
Gerätebezeichnung	-	Pat.-Anschlüsse	4
Prüfnorm	IEC 60601-1:1988+A1:1991+A2:1995	Gebäude	-
Geräteart	Allgemein	Abteilung	-
Schutzklasse	SK I	Raum	-
Nennspannung [V]	230	Kommentar	-

MessNr.	Messung	Grenzwert	Messwert	Einheit	Bestanden
3	Schutzleiterwiderstand feste Leitung	0.200	0.122	Ohm	Ja
83	PE-Messtrom		25.5	A	1
80	Laststrom		0.938	A	1
81	Betriebsspannung		227	V	1
82	Leistungsaufnahme		0.214	kVA	1
7	Erdableitstrom NC	0.500	0.101	mA	Ja
11	Erdableitstrom SFC AP geerdet	1.000	0.101	mA	Ja
12	Erdableitstrom NC FE geerdet	0.500	0.101	mA	Ja
223	Patientenableitstrom NC DC	0.010	0.002	mA	Ja
225	Patientenableitstrom SFC DC PE offen	0.050	0.001	mA	Ja
229	Patientenableitstrom NC DC FE geerdet	0.010	0.002	mA	Ja
230	Patientenableitstrom SFC DC FE geerdet PE offen	0.050	0.001	mA	Ja
235	Patientenhilfsstrom NC DC	0.010	0.001	mA	Ja
237	Patientenhilfsstrom SFC DC PE offen	0.050	0.008	mA	Ja
241	Patientenhilfsstrom NC DC FE geerdet	0.010	0.001	mA	Ja
242	Patientenhilfsstrom SFC DC PE offen FE geerdet	0.050	0.008	mA	Ja
323	Patientenableitstrom NC AC	0.100	< 0.001	mA	Ja
325	Patientenableitstrom SFC AC PE offen	0.500	0.071	mA	Ja
329	Patientenableitstrom NC AC FE geerdet	0.100	< 0.001	mA	Ja
330	Patientenableitstrom SFC AC FE geerdet PE offen	0.500	0.071	mA	Ja
335	Patientenhilfsstrom NC AC	0.100	< 0.001	mA	Ja
337	Patientenhilfsstrom SFC AC PE offen	0.500	0.001	mA	Ja
341	Patientenhilfsstrom NC AC FE geerdet	0.100	< 0.001	mA	Ja
342	Patientenhilfsstrom SFC AC PE offen FE geerdet	0.500	0.001	mA	Ja
8	Erdableitstrom NC ph. rev.	0.500	0.022	mA	Ja
224	Patientenableitstrom NC DC ph. rev.	0.010	0.002	mA	Ja
226	Patientenableitstrom SFC DC PE offen ph. rev.	0.050	0.001	mA	Ja
236	Patientenhilfsstrom NC DC ph. rev.	0.010	0.001	mA	Ja
238	Patientenhilfsstrom SFC DC PE offen ph. rev.	0.050	0.002	mA	Ja
324	Patientenableitstrom NC AC ph. rev.	0.100	< 0.001	mA	Ja
326	Patientenableitstrom SFC AC PE offen ph. rev.	0.500	0.013	mA	Ja
336	Patientenhilfsstrom NC AC ph. rev.	0.100	< 0.001	mA	Ja
338	Patientenhilfsstrom SFC AC PE offen ph. rev.	0.500	< 0.001	mA	Ja
9	Erdableitstrom SFC Netzl. offen	1.000	0.112	mA	Ja
13	Erdableitstrom SFC AP+FE geerdet Netzl. offen	1.000	0.106	mA	Ja
227	Patientenableitstrom SFC DC Netzl. offen	0.050	0.002	mA	Ja
239	Patientenhilfsstrom SFC DC Netzl. offen	0.050	0.001	mA	Ja
327	Patientenableitstrom SFC AC Netzl. offen	0.500	< 0.001	mA	Ja
339	Patientenhilfsstrom SFC AC Netzl. offen	0.500	< 0.001	mA	Ja
10	Erdableitstrom SFC Netzl. offen ph. rev.	1.000	0.117	mA	Ja
228	Patientenableitstrom SFC DC Netzl. offen ph. rev.	0.050	0.002	mA	Ja
240	Patientenhilfsstrom SFC DC Netzl. offen ph. rev.	0.050	0.001	mA	Ja

MessNr.	Messung	Grenzwert	Messwert	Einheit	Bestanden
328	Patientenableitstrom SFC AC Netzl. offen ph. rev.	0.500	< 0.001	mA	Ja
340	Patientenhilfsstrom SFC AC Netzl. offen ph. rev.	0.500	< 0.001	mA	Ja

<b>Prüfergebnis</b>		<b>&gt;&gt; Bestanden &lt;&lt;</b>	
Prüfdatum	: 14.03.2013		
Prüfername	: Hernach		
 <b>Unterschrift</b>			
Seite	2/2	Ser.Nr.:	0401001206
UNIMET®	1000/1100ST	V7.70	Druckdatum: 14.03.2013

**Figure 33** Safety Check Report for the system in the chrono-amperometric measurement mode without patient - to - patient connection

### Gerätedaten

Geräte-ID	130314-EU-CLAMP-2	Leitungslänge [m]	-
Typ/Modell	60601/I /BF/4	Nennleistung [kW]	-
Hersteller	-	Prüfablauf	Automatisch
Werk.Nr.	-	Anwendungsteil	Typ BF
Gerätebezeichnung	-	Pat.-Anschlüsse	4
Prüfnorm	IEC 60601-1:1988+A1:1991+A2:1995	Gebäude	-
Geräteart	Allgemein	Abteilung	-
Schutzklasse	SK I	Raum	-
Nennspannung [V]	230	Kommentar	-

MessNr.	Messung	Grenzwert	Messwert	Einheit	Bestanden
---------	---------	-----------	----------	---------	-----------

3	Schutzleiterwiderstand feste Leitung	0.200	0.122	Ohm	Ja
83	PE-Messtrom		25.5	A	1
80	Laststrom		1.022	A	1
81	Betriebsspannung		226	V	1
82	Leistungsaufnahme		0.230	kVA	1
7	Erdableitstrom NC	0.500	0.101	mA	Ja
11	Erdableitstrom SFC AP geerdet	1.000	0.101	mA	Ja
12	Erdableitstrom NC FE geerdet	0.500	0.101	mA	Ja
223	Patientenableitstrom NC DC	0.010	0.002	mA	Ja
225	Patientenableitstrom SFC DC PE offen	0.050	0.001	mA	Ja
229	Patientenableitstrom NC DC FE geerdet	0.010	0.001	mA	Ja
230	Patientenableitstrom SFC DC FE geerdet PE offen	0.050	0.001	mA	Ja
235	Patientenhilfsstrom NC DC	0.010	< 0.001	mA	Ja
237	Patientenhilfsstrom SFC DC PE offen	0.050	0.008	mA	Ja
241	Patientenhilfsstrom NC DC FE geerdet	0.010	< 0.001	mA	Ja
242	Patientenhilfsstrom SFC DC PE offen FE geerdet	0.050	0.008	mA	Ja
323	Patientenableitstrom NC AC	0.100	< 0.001	mA	Ja
325	Patientenableitstrom SFC AC PE offen	0.500	0.071	mA	Ja
329	Patientenableitstrom NC AC FE geerdet	0.100	< 0.001	mA	Ja
330	Patientenableitstrom SFC AC FE geerdet PE offen	0.500	0.072	mA	Ja
335	Patientenhilfsstrom NC AC	0.100	< 0.001	mA	Ja
337	Patientenhilfsstrom SFC AC PE offen	0.500	0.001	mA	Ja
341	Patientenhilfsstrom NC AC FE geerdet	0.100	< 0.001	mA	Ja
342	Patientenhilfsstrom SFC AC PE offen FE geerdet	0.500	0.001	mA	Ja
8	Erdableitstrom NC ph. rev.	0.500	0.021	mA	Ja
224	Patientenableitstrom NC DC ph. rev.	0.010	0.001	mA	Ja
226	Patientenableitstrom SFC DC PE offen ph. rev.	0.050	0.001	mA	Ja
236	Patientenhilfsstrom NC DC ph. rev.	0.010	< 0.001	mA	Ja
238	Patientenhilfsstrom SFC DC PE offen ph. rev.	0.050	0.001	mA	Ja
324	Patientenableitstrom NC AC ph. rev.	0.100	< 0.001	mA	Ja
326	Patientenableitstrom SFC AC PE offen ph. rev.	0.500	0.012	mA	Ja
336	Patientenhilfsstrom NC AC ph. rev.	0.100	< 0.001	mA	Ja
338	Patientenhilfsstrom SFC AC PE offen ph. rev.	0.500	< 0.001	mA	Ja
9	Erdableitstrom SFC Netzl. offen	1.000	0.114	mA	Ja
13	Erdableitstrom SFC AP+FE geerdet Netzl. offen	1.000	0.107	mA	Ja
227	Patientenableitstrom SFC DC Netzl. offen	0.050	0.002	mA	Ja
239	Patientenhilfsstrom SFC DC Netzl. offen	0.050	0.001	mA	Ja
327	Patientenableitstrom SFC AC Netzl. offen	0.500	< 0.001	mA	Ja
339	Patientenhilfsstrom SFC AC Netzl. offen	0.500	< 0.001	mA	Ja
10	Erdableitstrom SFC Netzl. offen ph. rev.	1.000	0.123	mA	Ja
228	Patientenableitstrom SFC DC Netzl. offen ph. rev.	0.050	0.002	mA	Ja
240	Patientenhilfsstrom SFC DC Netzl. offen ph. rev.	0.050	0.001	mA	Ja

MessNr.	Messung	Grenzwert	Messwert	Einheit	Bestanden
328	Patientenableitstrom SFC AC Netzl. offen ph. rev.	0.500	< 0.001	mA	Ja
340	Patientenhilfsstrom SFC AC Netzl. offen ph. rev.	0.500	< 0.001	mA	Ja

<b>Prüfergebnis</b>		<b>&gt;&gt; Bestanden &lt;&lt;</b>	
<b>Prüfdatum</b>	: 14.03.2013		
<b>Prüfername</b>	: Hernach	_____	
		<b>Unterschrift</b>	
Seite 2/2	Ser.Nr.: 0401001206	UNIMET@1000/1100ST	V7.70 Druckdatum: 14.03.2013

**Figure 34:** Safety check report for the system in the chrono-amperometric measurement mode with patient - to - patient connection



### Gerätedaten

Geräte-ID	130314-EU-CLAMP-3	Leitungslänge [m]	-
Typ/Modell	60601/I /BF/4	Nennleistung [kW]	-
Hersteller	-	Prüfablauf	Automatisch
Werk.Nr.	-	Anwendungsteil	Typ BF
Gerätebezeichnung	-	Pat.-Anschlüsse	4
Prüfnorm	IEC 60601-1:1988+A1:1991+A2:1995	Gebäude	-
Geräteart	Allgemein	Abteilung	-
Schutzklasse	SK I	Raum	-
Nennspannung [V]	230	Kommentar	-

MessNr.	Messung	Grenzwert	Messwert	Einheit	Bestanden
3	Schutzleiterwiderstand feste Leitung	0.200	0.122	Ohm	Ja
83	PE-Messtrom		25.5	A	1
80	Laststrom		0.975	A	1
81	Betriebsspannung		227	V	1
82	Leistungsaufnahme		0.225	kVA	1
7	Erdableitstrom NC	0.500	0.101	mA	Ja
11	Erdableitstrom SFC AP geerdet	1.000	0.101	mA	Ja
12	Erdableitstrom NC FE geerdet	0.500	0.101	mA	Ja
223	Patientenableitstrom NC DC	0.010	0.001	mA	Ja
225	Patientenableitstrom SFC DC PE offen	0.050	0.001	mA	Ja
229	Patientenableitstrom NC DC FE geerdet	0.010	0.001	mA	Ja
230	Patientenableitstrom SFC DC FE geerdet PE offen	0.050	< 0.001	mA	Ja
235	Patientenhilfsstrom NC DC	0.010	0.001	mA	Ja
237	Patientenhilfsstrom SFC DC PE offen	0.050	0.008	mA	Ja
241	Patientenhilfsstrom NC DC FE geerdet	0.010	0.001	mA	Ja
242	Patientenhilfsstrom SFC DC PE offen FE geerdet	0.050	0.008	mA	Ja
323	Patientenableitstrom NC AC	0.100	< 0.001	mA	Ja
325	Patientenableitstrom SFC AC PE offen	0.500	0.072	mA	Ja
329	Patientenableitstrom NC AC FE geerdet	0.100	< 0.001	mA	Ja
330	Patientenableitstrom SFC AC FE geerdet PE offen	0.500	0.072	mA	Ja
335	Patientenhilfsstrom NC AC	0.100	< 0.001	mA	Ja
337	Patientenhilfsstrom SFC AC PE offen	0.500	0.001	mA	Ja
341	Patientenhilfsstrom NC AC FE geerdet	0.100	< 0.001	mA	Ja
342	Patientenhilfsstrom SFC AC PE offen FE geerdet	0.500	0.001	mA	Ja
8	Erdableitstrom NC ph. rev.	0.500	0.021	mA	Ja
224	Patientenableitstrom NC DC ph. rev.	0.010	0.002	mA	Ja
226	Patientenableitstrom SFC DC PE offen ph. rev.	0.050	0.001	mA	Ja
236	Patientenhilfsstrom NC DC ph. rev.	0.010	< 0.001	mA	Ja
238	Patientenhilfsstrom SFC DC PE offen ph. rev.	0.050	0.001	mA	Ja
324	Patientenableitstrom NC AC ph. rev.	0.100	< 0.001	mA	Ja
326	Patientenableitstrom SFC AC PE offen ph. rev.	0.500	0.013	mA	Ja
336	Patientenhilfsstrom NC AC ph. rev.	0.100	< 0.001	mA	Ja
338	Patientenhilfsstrom SFC AC PE offen ph. rev.	0.500	< 0.001	mA	Ja
9	Erdableitstrom SFC Netzl. offen	1.000	0.108	mA	Ja
13	Erdableitstrom SFC AP+FE geerdet Netzl. offen	1.000	0.105	mA	Ja
227	Patientenableitstrom SFC DC Netzl. offen	0.050	0.002	mA	Ja
239	Patientenhilfsstrom SFC DC Netzl. offen	0.050	0.001	mA	Ja
327	Patientenableitstrom SFC AC Netzl. offen	0.500	< 0.001	mA	Ja
339	Patientenhilfsstrom SFC AC Netzl. offen	0.500	< 0.001	mA	Ja
10	Erdableitstrom SFC Netzl. offen ph. rev.	1.000	0.106	mA	Ja
228	Patientenableitstrom SFC DC Netzl. offen ph. rev.	0.050	0.002	mA	Ja
240	Patientenhilfsstrom SFC DC Netzl. offen ph. rev.	0.050	0.001	mA	Ja

MessNr.	Messung	Grenzwert	Messwert	Einheit	Bestanden
328	Patientenableitstrom SFC AC Netzl. offen ph. rev.	0.500	< 0.001	mA	Ja
340	Patientenhilfsstrom SFC AC Netzl. offen ph. rev.	0.500	< 0.001	mA	Ja
<b>Prüfergebnis</b> >> <b>Bestanden</b> <<					
Prüfdatum : 14.03.2013					
Prüfername : Hernach _____					
<b>Unterschrift</b>					
Seite 2/2	Ser.Nr.: 0401001206	UNIMET®1000/1100ST	V7.70	Druckdatum: 14.03.2013	

Figure 35: Safety check report for the system in the EIS measurement mode without patient - to - patient connection

### Gerätedaten

Geräte-ID	130414-EU-CLAMP-4	Leitungslänge [m]	-
Typ/Modell	60601/I /BF/4	Nennleistung [kW]	-
Hersteller	-	Prüfablauf	Automatisch
Werk.Nr.	-	Anwendungsteil	Typ BF
Gerätebezeichnung	-	Pat.-Anschlüsse	4
Prüfnorm	IEC 60601-1:1988+A1:1991+A2:1995	Gebäude	-
Geräteart	Allgemein	Abteilung	-
Schutzklasse	SK I	Raum	-
Nennspannung [V]	230	Kommentar	-

MessNr.	Messung	Grenzwert	Messwert	Einheit	Bestanden
3	Schutzleiterwiderstand feste Leitung	0.200	0.122	Ohm	Ja
83	PE-Messtrom		25.5	A	1
80	Laststrom		1.006	A	1
81	Betriebsspannung		227	V	1
82	Leistungsaufnahme		0.232	kVA	1
7	Erdableitstrom NC	0.500	0.100	mA	Ja
11	Erdableitstrom SFC AP geerdet	1.000	0.101	mA	Ja
12	Erdableitstrom NC FE geerdet	0.500	0.101	mA	Ja
223	Patientenableitstrom NC DC	0.010	0.001	mA	Ja
225	Patientenableitstrom SFC DC PE offen	0.050	0.001	mA	Ja
229	Patientenableitstrom NC DC FE geerdet	0.010	0.002	mA	Ja
230	Patientenableitstrom SFC DC FE geerdet PE offen	0.050	0.001	mA	Ja
235	Patientenhilfsstrom NC DC	0.010	< 0.001	mA	Ja
237	Patientenhilfsstrom SFC DC PE offen	0.050	0.008	mA	Ja
241	Patientenhilfsstrom NC DC FE geerdet	0.010	< 0.001	mA	Ja
242	Patientenhilfsstrom SFC DC PE offen FE geerdet	0.050	0.008	mA	Ja
323	Patientenableitstrom NC AC	0.100	< 0.001	mA	Ja
325	Patientenableitstrom SFC AC PE offen	0.500	0.072	mA	Ja
329	Patientenableitstrom NC AC FE geerdet	0.100	< 0.001	mA	Ja
330	Patientenableitstrom SFC AC FE geerdet PE offen	0.500	0.072	mA	Ja
335	Patientenhilfsstrom NC AC	0.100	< 0.001	mA	Ja
337	Patientenhilfsstrom SFC AC PE offen	0.500	0.001	mA	Ja
341	Patientenhilfsstrom NC AC FE geerdet	0.100	< 0.001	mA	Ja
342	Patientenhilfsstrom SFC AC PE offen FE geerdet	0.500	0.001	mA	Ja
8	Erdableitstrom NC ph. rev.	0.500	0.021	mA	Ja
224	Patientenableitstrom NC DC ph. rev.	0.010	0.002	mA	Ja
226	Patientenableitstrom SFC DC PE offen ph. rev.	0.050	0.001	mA	Ja
236	Patientenhilfsstrom NC DC ph. rev.	0.010	< 0.001	mA	Ja
238	Patientenhilfsstrom SFC DC PE offen ph. rev.	0.050	0.001	mA	Ja
324	Patientenableitstrom NC AC ph. rev.	0.100	< 0.001	mA	Ja
326	Patientenableitstrom SFC AC PE offen ph. rev.	0.500	0.013	mA	Ja
336	Patientenhilfsstrom NC AC ph. rev.	0.100	< 0.001	mA	Ja
338	Patientenhilfsstrom SFC AC PE offen ph. rev.	0.500	< 0.001	mA	Ja
9	Erdableitstrom SFC Netzl. offen	1.000	0.108	mA	Ja
13	Erdableitstrom SFC AP+FE geerdet Netzl. offen	1.000	0.110	mA	Ja
227	Patientenableitstrom SFC DC Netzl. offen	0.050	0.002	mA	Ja
239	Patientenhilfsstrom SFC DC Netzl. offen	0.050	0.001	mA	Ja
327	Patientenableitstrom SFC AC Netzl. offen	0.500	< 0.001	mA	Ja
339	Patientenhilfsstrom SFC AC Netzl. offen	0.500	< 0.001	mA	Ja
10	Erdableitstrom SFC Netzl. offen ph. rev.	1.000	0.119	mA	Ja
228	Patientenableitstrom SFC DC Netzl. offen ph. rev.	0.050	0.002	mA	Ja
240	Patientenhilfsstrom SFC DC Netzl. offen ph. rev.	0.050	0.001	mA	Ja

MessNr.	Messung	Grenzwert	Messwert	Einheit	Bestanden
328	Patientenableitstrom SFC AC Netzl. offen ph. rev.	0.500	< 0.001	mA	Ja
340	Patientenhilfsstrom SFC AC Netzl. offen ph. rev.	0.500	< 0.001	mA	Ja
<b>Prüfergebnis &gt;&gt; Bestanden &lt;&lt;</b>					
Prüfdatum : 14.03.2013					
Prüfername : Hernach _____					
<b>Unterschrift</b>					
Seite 2/2	Ser.Nr.: 0401001206	UNIMET®1000/1100ST	V7.70	Druckdatum:	14.03.2013

Figure 36: Safety check report for the system in the EIS measurement mode with patient - to - patient connection

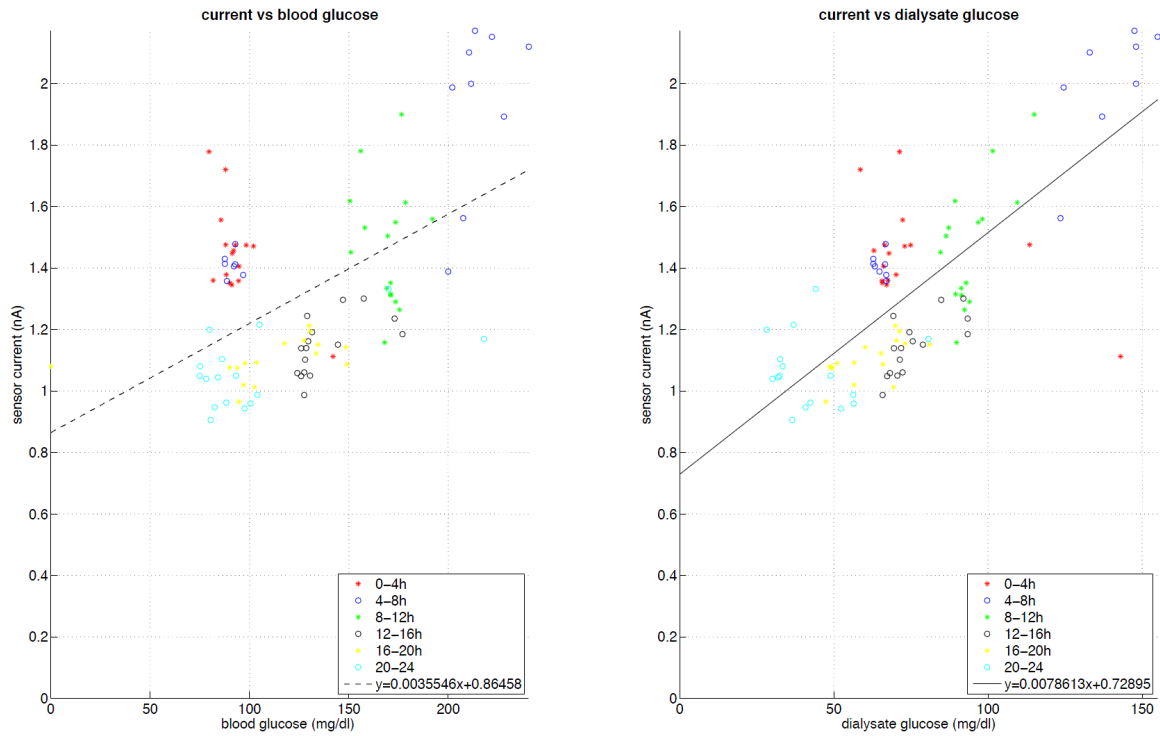


**Figure 37:** Regression analysis/ calibration curve for subject 032 of the glucose signal derived from Super GL2 vs. glucose sensor. **Left:** blood glucose vs. sensor current. **Right:** dialysate glucose vs. sensor current.

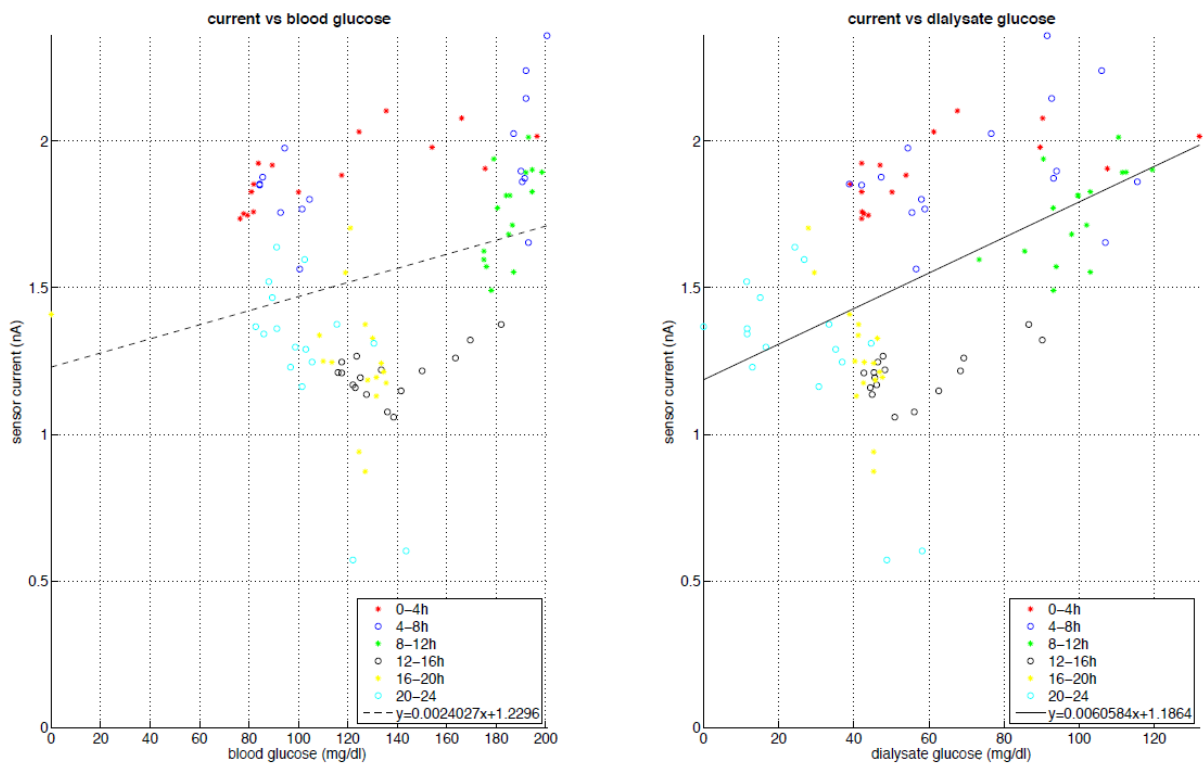


**Figure 38:** Regression analysis/ calibration curve for subject 031 of the glucose signal derived from Super GL2 vs. glucose sensor. **Left:** blood glucose vs. sensor current. **Right:** dialysate glucose vs. sensor current.

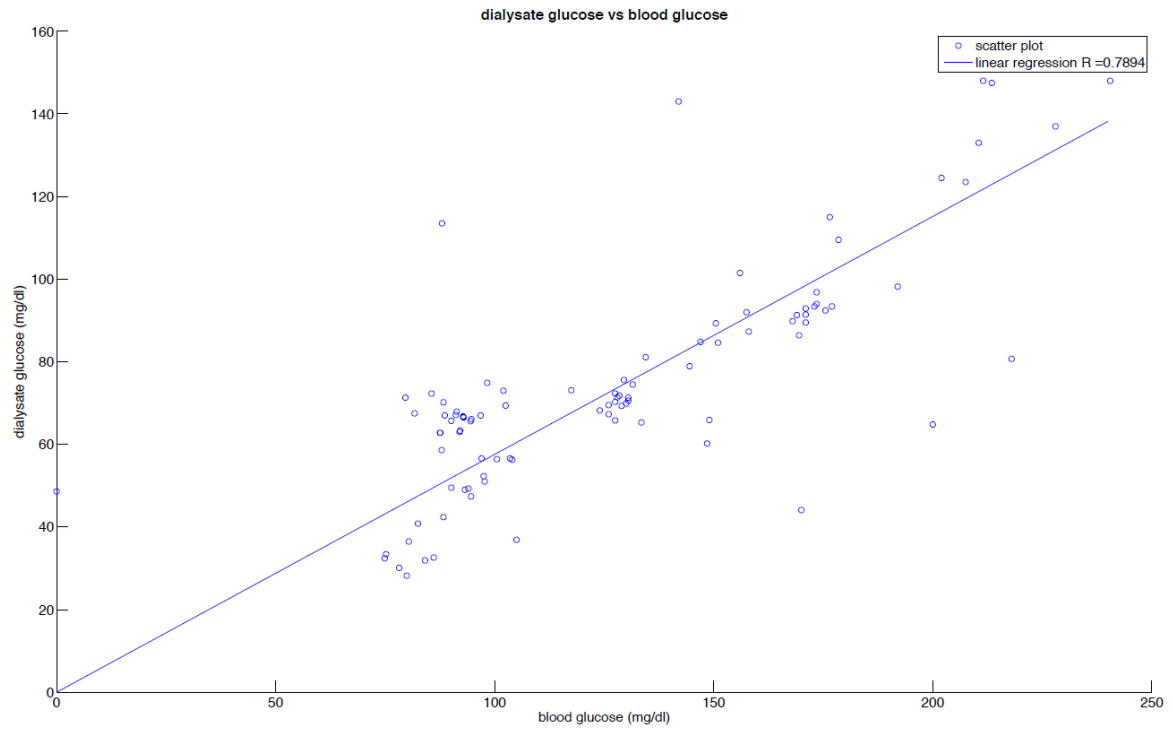


**Figure 39:** Dialysate glucose plotted against the blood glucose (blue dots) as well as the linear regression for subject 032.

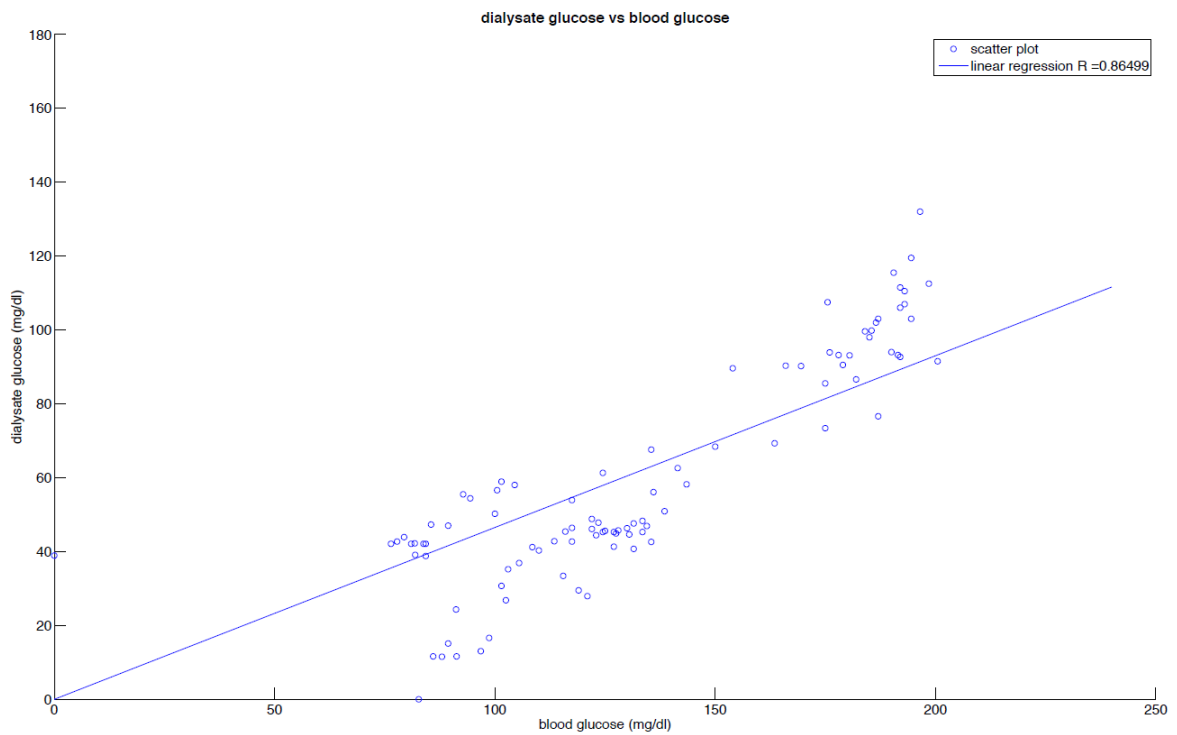


**Figure 40:** Dialysate glucose plotted against the blood glucose (blue dots) as well as the linear regression for subject 031.

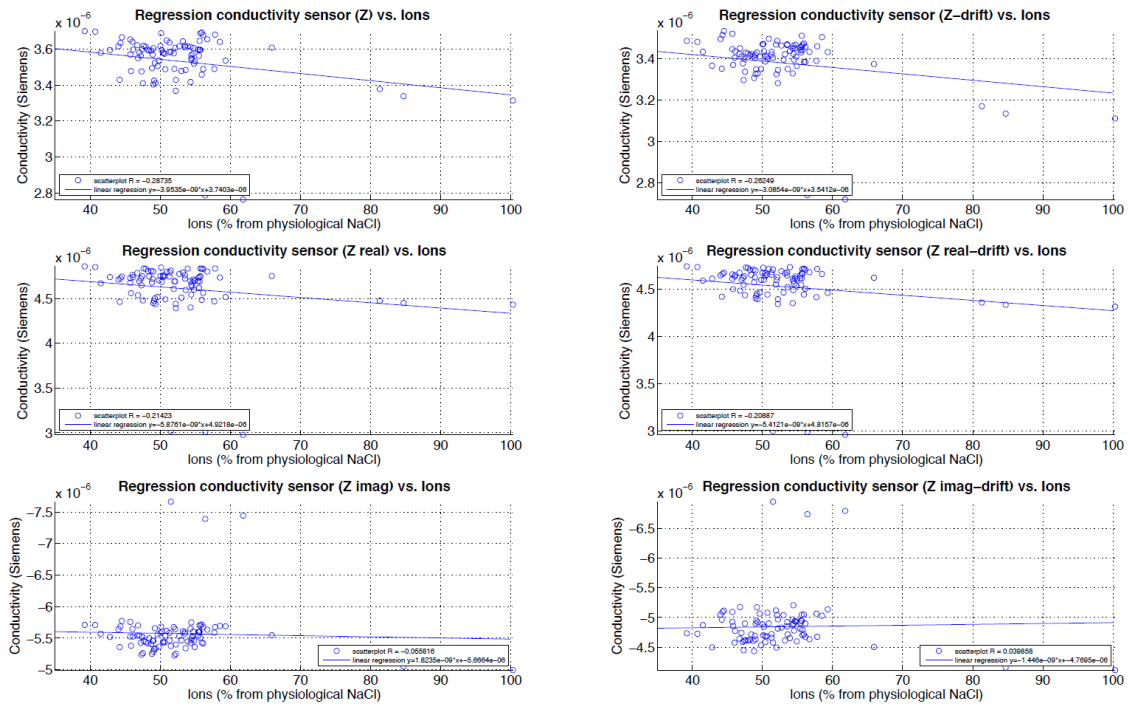


**Figure 41:** Regression analysis of the conductivity signal derived from TraceDec vs. conductivity measured by the glucose sensor ( $Z$ ,  $Z_{real}$ ,  $Z_{imag}$ ) of subject 31. **Top row:** Regression analysis using conductivity derived from  $Z$ . **Middle row:** Regression analysis using conductivity derived from  $Z_{REAL}$ . **Bottom row:** Regression analysis using conductivity derived from  $Z_{IMAG}$ . **Left column:** Regression analysis without drift compensation. **Right column:** Regression analysis with drift compensation.

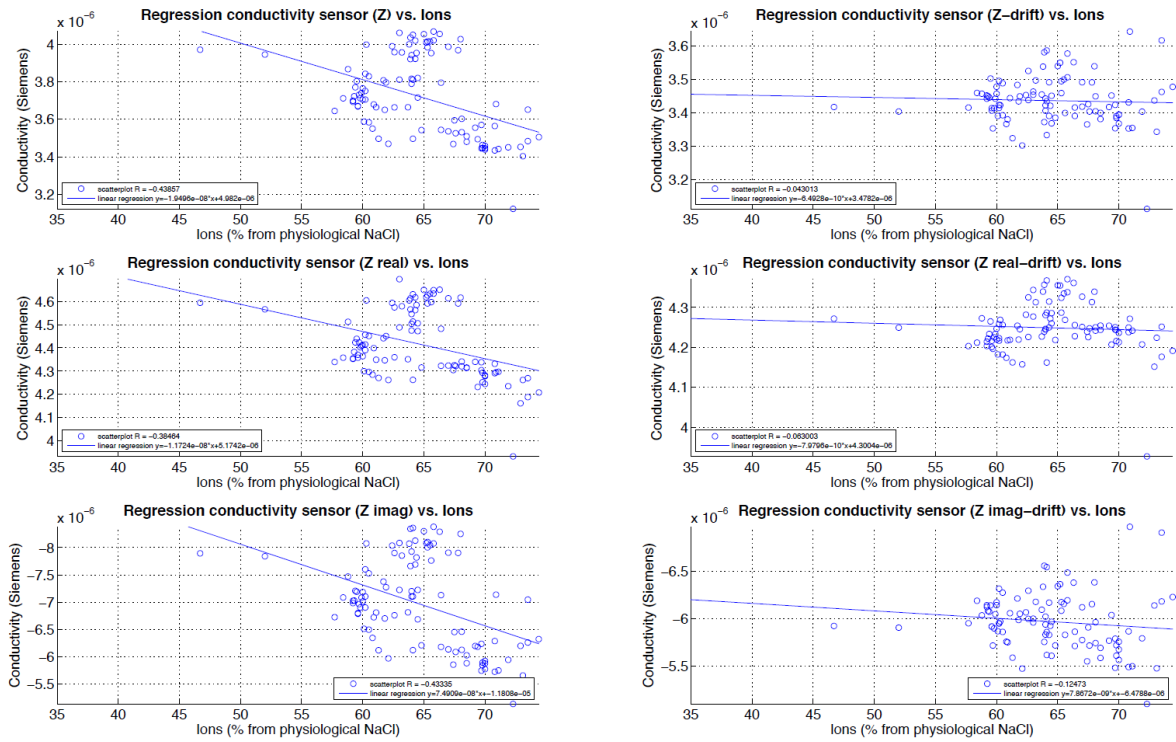


**Figure 42:** Regression analysis of the conductivity signal derived from TraceDec vs. conductivity measured by the glucose sensor (Z,  $Z_{real}$ ,  $Z_{imag}$ ) of subject 032. **Top row:** Regression analysis using conductivity derived from Z. **Middle row:** Regression analysis using conductivity derived from  $Z_{real}$ . **Bottom row:** Regression analysis using conductivity derived from  $Z_{imag}$ . **Left column:** Regression analysis without drift compensation. **Right column:** Regression analysis with drift compensation.